Biochemical analysis of the basic helix-loop-helix transcription factor Olig2

Het onderzoek beschreven in dit proefschrift is uitgevoerd aan de afdeling Cancer Biology van het Dana Farber Cancer Institute / Harvard Medical School te Boston, Verenigde Staten.

stophersentumoren, Roche Nederland, Panasonic en ChipSoft droegen bij aan de drukkosten voor dit proefschrift.

Vormgeving: Kat Ran Press, Cambridge, Verenigde Staten

BIOCHEMICAL ANALYSIS OF BASIC HELIX-LOOP-HELIX TRANSCRIPTION FACTOR OLIG2

De rol van transcriptiefactor Olig2
in gezonde hersenen en kwaadaardige hersentumoren

met een samenvatting in het Nederlands

Proefschrift ter verkrijging van de graad
van doctor aan de Universiteit Utrecht
op gezag van de rector magnificus,
prof. dr. G.J. van der Zwaan, ingevolge het
besluit van het college voor promoties,
in het openbaar te verdedigen op
donderdag 6 februari 2014 des middags
te 12.45 uur

DOOR **Dimphna Helena Maria Meijer**
GEBOREN OP 2 OKTOBER 1983 TE VOORSCHOTEN

Promotoren: Prof. dr. E.P.J.G. Cuppen & Prof. dr. C.D. Stiles

Contents

General introduction

A molecular guide for central nervous system development

During evolution of the vertebrate central nervous system (CNS), a rapid expansion of the cerebral cortex enabled human-specific behavior (Kaas, 2005). From a simplified point of view, the cerebral cortex can be seen as a network of multiple neural cell types and two principle cell types (astrocytes and oligodendrocytes) that are together termed glia or macroglia. A major question in vertebrate neurobiology is how neurons and glial cells arise from smaller subsets of multipotent neural progenitor cells.

The genetically accessible organism *Drosophila melanogaster* has provided insight for the specification of neurons from progenitor cells (Jan and Jan, 1990). Specifically, formation of *Drosophila* neurons is orchestrated to a large extent by proteins belonging to the basic helix-loop-helix (bHLH) transcription factor family. Pro-neural bHLH transcription factors (for example, *achaete-scute*, *atonal* and *daughterless*) oppose anti-neural bHLH transcription factors (*hairy*, *enhancer of split*, *extramacrochaetae*) to generate the correct number of neurons, at the right time and in the right place. Vertebrate orthologues of the *Drosophila* bHLH transcription factors have been well conserved in structure and function. For example, the mammalian *achaete-scute* homologues Mash1 and Mash2 function as pro-neural genes in the developing murine (CNS). Also, the mammalian *hairy/enhancer of split* homologue (*Hes)* is an anti-neural gene (Kageyama and Nakanishi, 1997; Lee, 1997; Parras et al., 2004).

In contrast with the *Drosophila* CNS, the vast majority of cells in the vertebrate CNS are glia, rather than neurons. Invertebrate and vertebrate glia differ in formation, form and function. With respect to formation, neurons and glia are specified simultaneously in *Drosophila*, whereas they are specified sequentially in vertebrate embryos. With regard to function, *Drosophila* axons are not enwrapped in myelin. Accordingly, there is no *Drosophila* equivalent of oligodendrocytes, the myelinating cell of the vertebrate CNS. The *Drosophila* CNS does contain cells referred to as astrocytes. However, *Drosophila* astrocytes are

functionally distinct from their vertebrate counterparts. For example, *Drosophila* astrocytes are the actual anatomical basis of the blood-brain barrier in flies. In contrast, the vertebrate blood-brain barrier is composed of endothelial cells.

The functional divergence of vertebrate glia is reflected in the genetics of glial development. To this point in time, forward genetic screens in genetically accessible model organisms, such as *Drosophila,* have been generally uninformative with respect to formation of vertebrate astrocytes and oligodendrocytes. Rather, insight into the specification of vertebrate glia has come by analyzing the spatial and temporal expression patterns of individual transcription factors (Fu et al., 2009; Gray et al., 2004; Stolt et al., 2003; Stolt et al., 2002). Using this strategy, the bHLH transcription factors Olig1 and Olig2, which promote formation of oligodendrocytes (hence the name "Olig"), were identified via their expression pattern in the developing spinal cord (Lu et al., 2000; Takebayashi et al., 2000; Zhou et al., 2000).

The role of Olig transcription factors in brain development and disease

In this thesis, I begin with a review of the bHLH transcription factors Olig1 and Olig2 by comparing their genetic targets, co-regulator proteins and post-translational modifications (Chapter 1). As will be seen, early gain-of-function and loss-of-function genetic experiments have shown that *Olig1* and *Olig2* have essential "pro-neural" functions in specification of neural cell types, such as motor neurons and oligodendrocytes. The pro-neural functions of Olig1 in the formation of white matter are reflected in murine models of multiple sclerosis wherein Olig1 plays a pivotal role in repair of demyelinated lesions. In addition to its pro-neural functions mentioned above, Olig2 has early anti-neural functions in supporting proliferation of neural progenitor cells. Recent studies have revealed a pathobiological correlate of this anti-neural function in malignant glioma.

Chapter 2 of my thesis addresses this distinctive anti-neural feature of Olig2. As mentioned above, all of the bHLH transcription factors involved in the formation of neurons are either anti-neural or pro-neural in function. How can Olig2 perform execute both pro-neural and anti-neural functions during brain development? I describe and experimentally prove the role of a triple phosphor-

ylation site on the N-terminus of Olig2. This developmentally regulated phosphorylation motif explains how Olig2 multi-tasks during brain development. Specifically, the phosphoserine motif is important for anti-neural progenitor proliferation, but nonessential for pro-neural subtype specification.

The main part of my thesis (Chapter 3) describes the molecular mechanism of Olig2 phosphorylation. In particular, Olig2 phosphorylation suppresses p53 functions, and this is tightly linked to Olig2's role as a transcription factor, i.e. DNA binding. Furthermore, I show that Olig2 triple phosphorylation regulates intranuclear localization, with a subsequent change in preference for Olig2 co-regulatory proteins. The anti-p53 responses of Olig2 are reflected in its role in promoting brain tumor growth in a mouse model for glioblastoma multiforme and in human primary glioma tissue.

In Chapter 4, I address therapeutic opportunities with Olig2 for patients with malignant glioma. Olig2 serves as an attractive therapeutic target because it is specific to the central nervous system and largely expendable for mature CNS function. In collaboration with a chemist, I use a "stapled peptide" approach to design peptidomimetics based on the bHLH domain of Olig2. An electrophoretic gel shift screen is presented as a way to test the peptidomimetics for interfering with Olig2 function.

Finally, I will propose how structural studies could provide insight into the functional divergence of Olig1 and Olig2 in vertebrate CNS development (Chapter 5). Particularly, structural knowledge of the Olig transcription factors could assist rational design of a new generation of small molecule inhibitors for Olig1 and Olig2.

1 The functional and molecular divergence of Olig1 and Olig2

Dimphna H. Meijer, Michael F. Kane, Shwetal Mehta, Hongye Liu, Christopher M. Taylor, David H. Rowitch and Charles D. Stiles

Adapted from: Nature Reviews Neuroscience (2012) 13, 189–831

Abstract

The basic helix-loop-helix transcription factors oligodendrocyte transcription factor 1 (Olig1) and Olig2 are structurally similar and, to a first approximation, coordinately expressed in the developing CNS and postnatal brain. Notwithstanding these similarities, it was apparent from early on after their discovery that Olig1 and Olig2 have non-overlapping developmental functions in patterning, neuron subtype specification and the formation of oligodendrocytes. Here, we summarize more recent insights into the separate functions of these transcription factors in the postnatal brain during repair processes and in neurological disease states, including multiple sclerosis and malignant glioma. We discuss how the unique biological functions of Olig1 and Olig2 may reflect their distinct genetic targets, co-regulator proteins and/or post-translational modifications.

Introduction

The appearance of myelinating oligodendrocytes represented a major step forward in the evolution of the vertebrate CNS, as these cells enabled more efficient axon insulation and conduction of action potentials and, consequently, much greater brain complexity. The essential roles of oligodendrocytes in myelin production, establishing the nodal architecture of the axon, and saltatory conductivity were recognized by the late 1960s. The biological relevance of the structures and functions enabled by oligodendrocytes came from the gradual realization that damage to the myelin sheath, subsequent demyelination and focal depletion of myelinating oligodendrocytes constitute the cellular basis of

multiple sclerosis (MS) (Charcot, 1868; Lucchinetti et al., 1999; Marburg, 1906; Prineas and Connell, 1979). The typical relapsing–remitting course of this disorder highlighted the repair potential of oligodendrocytes and focused attention on two important unresolved issues in myelin development, namely the anatomical origins of oligodendrocytes and the lineage relationships between oligodendrocytes and other neural cell types.

The progress towards answering these questions was initially slow and the findings from early studies were contentious. For example, on the subject of anatomical origins, tissue explant studies suggested that oligodendrocytes arise exclusively from the ventral neural tube (Pringle and Richardson, 1993; Timsit et al., 1995; Warf et al., 1991; Yu et al., 1994). However, quail–chick grafting experiments suggested a more complex picture, with some oligodendrocytes originating from dorsal regions of the neural tube (Cameron-Curry and Le Douarin, 1995). With respect to lineage relationships, tissue explant studies identified glial-restricted progenitor cells from the optic nerve and the spinal cord, suggesting a lineage relationship between oligodendrocytes and astrocytes (Lee et al., 2000; Raff et al., 1983; Rao et al., 1998). However, grafting experiments and analysis of pattern formation in the developing spine highlighted the role of anatomy in glial specification and suggested that oligodendrocytes and astrocytes arise from separate, bipotent progenitor cells (for a review, see Jessell, 2000).

A major advancement in the field came with the cloning and characterization of the basic helix–loop–helix (bHLH) transcription factors oligodendrocyte transcription factor 1 (Olig1) and Olig2. They were so named because early *in situ* hybridization experiments revealed that these transcription factors showed pronounced expression in myelinating oligodendrocytes and oligodendrocyte progenitors (Lu et al., 2000; Takebayashi et al., 2000; Zhou et al., 2000). Gain-of-function and loss-of-function genetic assays involving *Olig1* or *Olig2*, together with Cre-lox fate-mapping experiments, resolved long-running polemics on the cellular and anatomical origins of oligodendrocytes in the developing CNS (Lu et al., 2002; Lu et al., 2000; Takebayashi et al., 2000; Zhou and Anderson, 2002; Zhou et al., 2000). With respect to anatomical origins, it is now clear that oligodendrocyte progenitors arise from both the ventral and dorsal regions of the developing CNS. Most oligodendrocytes in the adult spinal cord are derived

from ventral progenitors. By contrast, oligodendrocytes in the mature forebrain are derived from dorsal progenitors (Cai et al., 2005; Fogarty et al., 2005; Vallstedt et al., 2005). Regarding lineage relationships, the notion that oligodendrocytes and astrocytes arise from a common, bi-potent glial-restricted progenitor proved to be incompatible with genetic analysis and fate mapping studies focusing on *Olig1* and *Olig2* (Lu et al., 2002; Zhou and Anderson, 2002). It is now evident that oligodendrocyte progenitor origins are more closely aligned to neuron subtype progenitors than to astrocytes—at least in the developing CNS.

More recent studies have revealed biological functions for *Olig1* and *Olig2* in the postnatal brain during neurogenesis (Menn et al., 2006) and reactive gliosis (Buffo et al., 2005; Fancy et al., 2004), and in repair functions in experimental models of MS (Arnett et al., 2004). Preliminary, but nevertheless provocative, studies have also suggested that these genes have links to schizophrenia (Georgieva et al., 2006; Huang et al., 2008; Sims et al., 2009) and to the cognitive deficiencies associated with Down's syndrome (Chakrabarti et al., 2010). Overshadowing these links to development and disease is a broad body of literature linking one of these genes—*Olig2*—to a cohort of primary brain cancers known collectively as the diffuse gliomas(Bouvier et al., 2003; Ligon et al., 2004; Lu et al., 2001; Marie et al., 2001; Ohnishi et al., 2003).

Against initial expectations based on expression patterns and striking similarities in their DNA-targeting bHLH motifs, the biological functions of Olig1 and Olig2 are for the most part separate and non-overlapping. In this Review, we examine facets of Olig1 and Olig2 molecular biology that may account for their diverse functional repertoires. In the fullness of time, genetic targets, co-regulator proteins and post-translational modifications unique to Olig1 or Olig2 may lend themselves to development of targeted drugs for CNS injuries and for a variety of neurological disease states, including cerebral palsy, MS and malignant glioma.

Olig structure and expression

The human genome encodes approximately 125 transcription factors that are defined by a canonical bHLH motif (Gray et al., 2004; Ledent et al., 2002). OLIG1 and OLIG2, together with a third transcription factor, Olig3, form a recognizable

subset of proteins in the bHLH family by virtue of their amino acid sequence homology—especially within the bHLH regions, which mediate transcription factor dimerization and DNA targeting (Box 1).

Olig1 and *Olig2* are expressed exclusively within the CNS (Lu et al., 2000; Takebayashi et al., 2000; Zhou et al., 2000) (Table 1).

To a first approximation, these genes are coordinately expressed in both space and time, although there are some important distinctions in their patterns of expression—especially at the level of subcellular localization of the two Olig proteins (see below).

Olig2 expression is detected at very early time points in CNS development within the radial glia of the neural tube that ultimately give rise to motor neurons and oligodendrocytes (Malatesta et al., 2003; Tsai et al., 2012). Expression of *Olig2* in multipotent progenitor cells of developing forebrain is recapitulated *in vitro* in cultures of multipotent neurospheres, in which most mitotic cells are Olig2-positive (Ligon et al., 2007).

Anatomically refined studies of *Olig1* and *Olig2* expression have been carried out in developing spinal cord. Here, both *Olig1* and *Olig2* have been shown to be downstream targets of the ventralizing signal Sonic hedgehog (SHH) (Lu et al., 2000; Zhou et al., 2000). *Olig1* is first expressed in the dorsal portion of the 'p3' progenitor domain of the ventral neural tube and then becomes confined to the pMN (progenitors of motor neurons) domain by embryonic day (E) 10.5. *Olig2* expression is also observed at early development stages prior to neural tube closure in the ventral-most p3 domain and then becomes confined to the pMN domain by approximately E9–E9.5. By the time that *Hb9* (homeobox protein Hb9) is expressed (E9-E9.5), *Olig1* and *Olig2* expression is down-regulated in motor neuron lineage cells. Studies by Chen *et al.* show that a microRNA (*mir-17-3p*) may be the effector of this down-regulation—at least for *Olig2* (Chen et al., 2011). Both *Olig1* and *Olig2* show sustained expression in oligodendrocyte precursor cells as these cells progress to become mature oligodendrocytes (Fig. 1) (Lu et al., 2000; Takebayashi et al., 2000; Zhou et al., 2000).

In contrast to *Olig1* and *Olig2*, *Olig3* is expressed in the dorsal-most domains of the developing spinal cord, patterned by bone morphogenetic proteins (BMP), and is also expressed in multiple tissues outside of the CNS (Table 1) (Liu et al., 2008; Takebayashi et al., 2002; Takebayashi et al., 2000).

	Olig1	*Olig2*	*Olig3*	*References*
Developmental				
Ventral spinal cord (pMN domain)	++	+++	–	(Lu et al., 2000), (Zhou et al., 2000)
Dorsal spinal cord	–	–	+++	(Liu et al., 2008), (Muller et al., 2005)
Early oligodendrocyte progenitors	+++	+++	–	(Lu et al., 2000), (Zhou et al., 2000)
Postnatal				
SVZ transit-amplifying cells	+++	+++	NT	(Menn et al., 2006)
NG2-positive glia	+++	+++	NT	(Miyoshi et al., 2007)
Myelinating oligodendrocytes	+++	+++	NT	(Lu et al., 2000), (Zhou et al., 2000)
External to CNS	–	–	++	(Takebayashi et al., 2000)

TABLE 1. **Developmental and postnatal expression of *Olig* genes.** Expression levels (arbitrary units) ranging from no expression (-) to strong expression (+++). NT, not tested.

Roles in development

Although structurally related and, to a large extent, coordinately expressed in developing embryos, the biological functions of *Olig1* and *Olig2* are only partially redundant (Table 2).

Olig1 and *Olig2* each contribute to patterning of the spinal cord, although *Olig2* plays the dominant role (Fig. 1A). Indeed, in the spinal cord, Olig2 exclusively promotes the specification of motor neurons and early oligodendrocyte progenitors that express platelet-derived growth factor receptor α (Pdgfrα) (Fig. 1B). The switch from maintaining immature pMN progenitors to the production of motor neurons involves regulation of Olig2 levels as well as phosphorylation of this protein at a site within its bHLH domain (see below) (Lee et al., 2005; Li et al., 2011). Loss-of-function studies also indicate roles for *Olig2* in neuron development within the ventral forebrain, particularly in cholinergic neuron populations (Furusho et al., 2006).

Ablation of *Olig1* has no impact on the formation of motor neurons and early oligodendrocyte progenitors (Fig. 1B). However, subsequent maturation of oligodendrocyte progenitors within the spinal cord is delayed in *Olig1* knockout mice (Lu et al., 2002; Xin et al., 2005). The maturational functions of *Olig1* become more prominent in remyelination models of multiple sclerosis (see below).

BOX 1. **The oligodendrocyte transcription factor family: a closer look at structure.** In humans, the genes encoding oligodendrocyte transcription factor 1 (Olig1) and Olig2 are localized within 40 kb of each other on chromosome 21 (syntenic to mouse chromosome 16). Co-localization of these genes is also observed in numerous other species and the chromosomal region in question is well conserved (Frazer et al., 2001). By contrast, Olig3 maps to human chromosome 6 (mouse chromosome 10) (Takebayashi et al., 2000).

Olig1, Olig2 and Olig3 are recognizable as a core subset of genes in the family of basic helix–loop–helix (bHLH) transcription factors by nucleotide sequence homologies in regions encoding to the bHLH domain and amino and carboxy termini of the corresponding proteins (see part a; the phylogenetic tree was generated utilizing ClustalW2).

Standard amino acid sequence alignment algorithms utilizing Clustal Omega and further adjusted to "best-fit" by eye, indicate that at the protein level, Olig2 is more closely related to Olig3 than to Olig1. Minimal conservation of domains outside the bHLH domains of Olig1 and Olig2 is suggested (see Fig. B, percentages reflect conserved substitution weighting following ClustalW2, Gonnet Pam250). However, the close relationship between Olig1 and Olig2 becomes more compelling when the alignment is adjusted to highlight short regions of homology, multiple insertions and deletions, and to utilize the conservation of the spacing of presumed conserved structural elements, such as proline (Fig. S1).

The amino terminal domain of Olig1 is smaller than that of Olig2 (89 amino acids versus 108 amino acids in humans). Also, the overall amino acid identity between Olig1 and Olig2 in this region is low, despite the presence of a distinctive serine–threonine-rich 'ST box' in both proteins (see part b). The Olig3 amino terminus is even smaller (83 amino acids in humans) than that of Olig1 and lacks the ST box; however, the amino termini of Olig2 and Olig3 are rather similar. Importantly, both contain a critical triple serine motif (see main text). It should be noted that the ST box common to Olig1 and Olig2 in humans and rodents is actually not well-conserved in Olig1 and Olig2 in other species (see Fig. S1).

The bHLH region is very highly conserved across all homologues in the Olig family. However, the bHLH domain of Olig1 is distinctive even within the broader family of bHLH transcription factors in several respects. In particular, the loop region of this domain has several unusual features in Olig1. First, it is nearly twice the length of the loops from the other members of the Olig family. Second, it has an extremely rare shift in the position of the helix 1-breaking proline. Third, the proline that precedes helix 2 is displaced. Last, it lacks the serine that directly precedes helix 2 in Olig2 and which is a predicted candidate for phosphorylation.

Sequence identity of the C-terminal domain in Olig1 and Olig2 is very low. By contrast, Olig2 and Olig3 are homologous in this region even though Olig3 lacks a set of distinctive alanine and glycine-rich domains that is seen in Olig2. The Olig2 / Olig3 similarities extend well past the end of helix 2 of the bHLH domain and include a distinctive multi-proline motif directly next to the cysteine domain. The only domain common to all three Oligs and conserved in all orthologues is a cysteine motif (CxCxxC) close to the C terminus. Cysteine residues and domains are implicated in multiple processes, including disulphide-bond formation, post-translational modifications such as S-palmitoylation, and recruitment of histone-modifying activities to chromatin (el-Husseini Ael and Bredt, 2002; Muskal et al., 1990; Smith and Shilatifard, 2010).

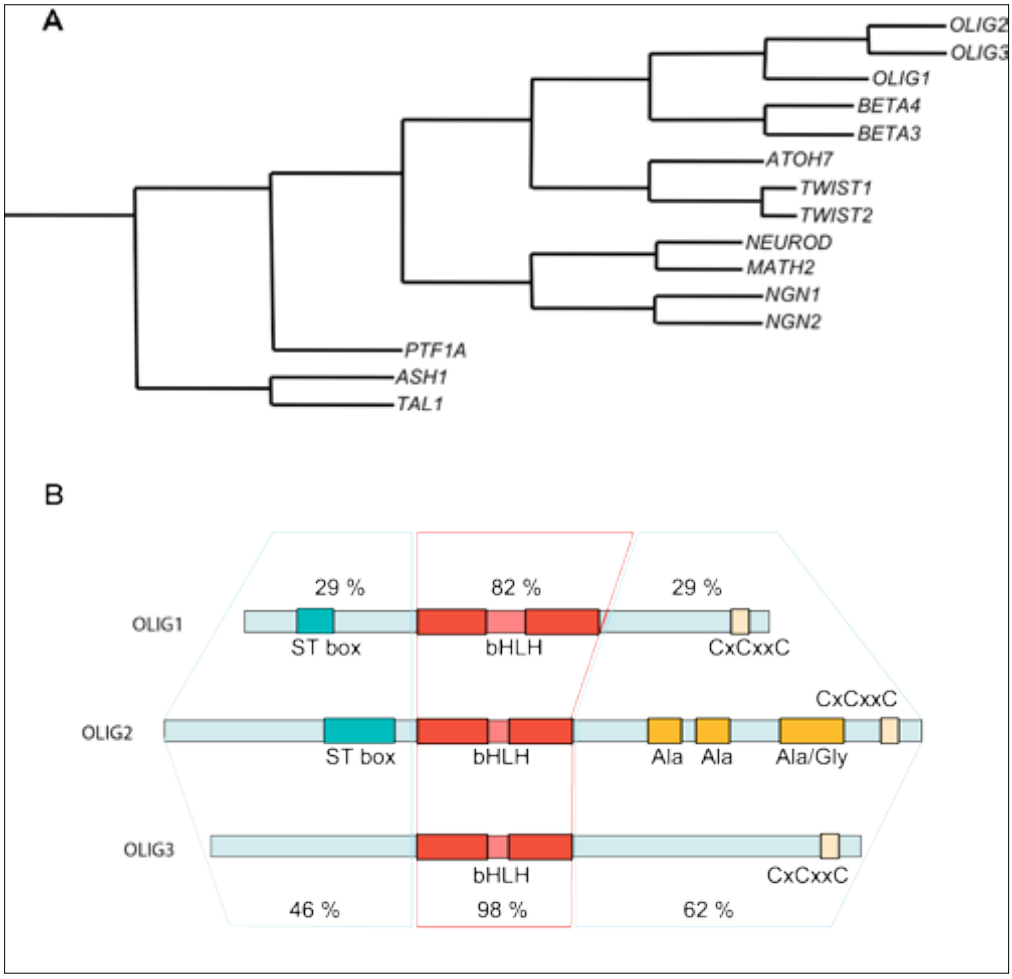
A
OLIG2
OLIG3
OLIG1
BETA4
BETA3
ATOH7
TWIST1
TWIST2
NEUROD
MATH2
NGN1
NGN2
PTF1A
ASH1
TAL1
B
29 %
82 %
29 %
OLIG1
ST box
bHLH
CxCxxC
CxCxxC
OLIG2
ST box
bHLH
Ala
Ala
Ala/Gly
OLIG3
bHLH
CxCxxC
46 %
98 %
62 %

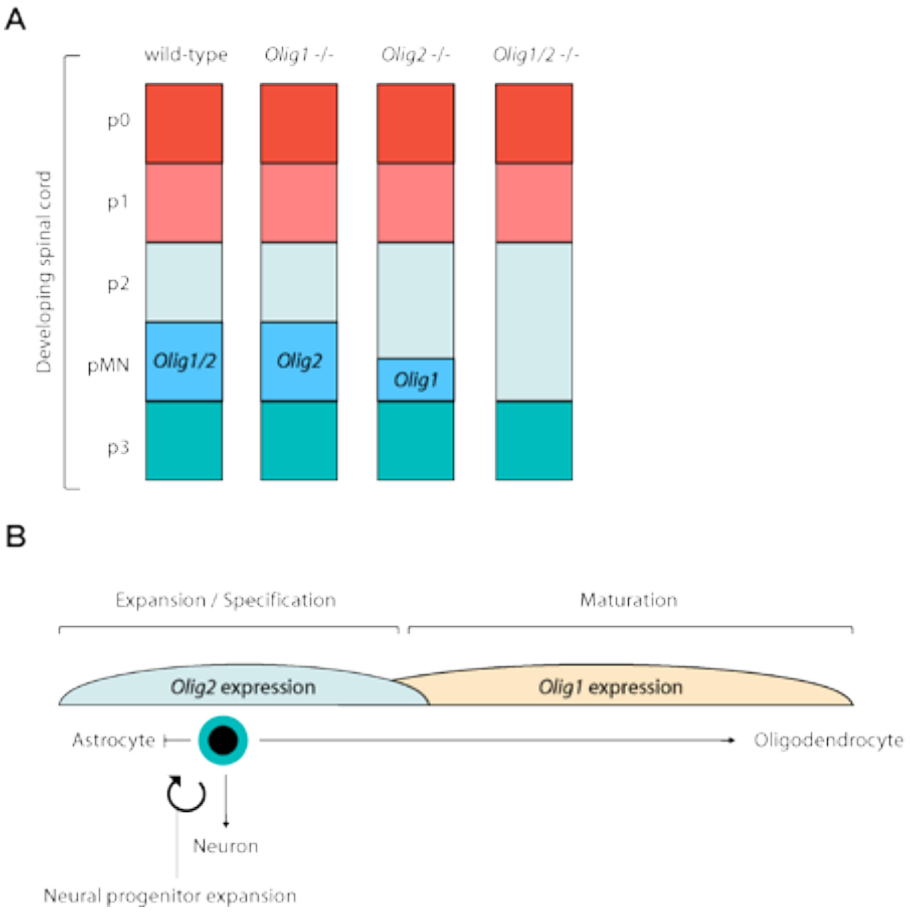

FIGURE 1. The developmental roles of Olig1 and Olig2. **(A)** Impact of *Olig1* and/or *Olig2* ablation on spinal cord patterning in mice. The combinatorial interactions of homeodomain proteins organize the ventral spinal cord of developing mouse embryos into five distinct regions, namely the p0, p1, p2, pMN and p3 domains. Different classes of ventral interneurons arise from the p0–p3 domains, whereas motor neurons and oligodendrocytes are derived from progenitors in the pMN domain (see Jessel, 2000 for a review). Knockout of *Olig1* has little affect on maintenance of the pMN domain, whereas knockout of *Olig2* results in ventral expansion of the p2 domain. Combinatorial knockout leads to the complete disappearance of the pMN domain (see (Rowitch, 2002) for a review). **(B)** Non-overlapping roles for *Olig1* and *Olig2* in proliferation and differentiation of neural progenitors. Olig1 promotes the differentiation of committed oligodendrocyte progenitors, a function that may be even more readily apparent in repair scenarios than in development. By contrast, Olig2 functions at earlier developmental stages. Initially, Olig2 acts to oppose cell differentiation and sustains the replication competent state so as to expand the pool of progenitors. At later stages of development, Olig2 promotes the fate choice decision to form early oligodendrocyte progenitors and certain types of neurons, notably motor neurons in the developing spinal cord. Generally speaking, Olig2 suppresses the formation of astrocytes, although there may be regional exceptions to this rule and it has been suggested that Olig2 has a role in reactive gliosis.

	Olig1	Olig2	Olig1/ 2	Olig3	References
Developmental					
Spinal cord patterning	–	+	+++	–	Lu et al., 2000, Zhou et al., 2000
Expansion of progenitor pool	–	+++	+++	–	Ligon et al., 2007
Specification of motor neurons	–	+++	+++	–	Lu et al., 2000 Zhou et al., 2000
Specification of other neurons	–	+	+	+++	Chakrabarti et al., 2010; Furusho et al., 2006; Hack et al., 2005; Liu et al., 2008; Miyoshi et al., 2007; Muller et al., 2005
Specification of NG2-positive glia	–	+++	NT	NT	Miyoshi et al., 2007
Specification of oligodendrocytes	+/–	++	+++	–	Lu et al., 2000 Zhou et al., 2000
Maturation of oligodendrocytes	+	NT	NT	–	Lu et al., 2000
Postnatal					
Malignant glioma	+/–	+++	+++	NT	Ligon et al., 2007 Mehta et al., 2011
Myelin repair	+++	NT	NT	NT	Arnett et al., 2004
Reactive gliosis	–	+++	NT	NT	Chen et al., 2008
Down syndrome	NT	NT	+++	NT	Chakrabarti et al., 2010
Alzheimer's / Schizophrenia *	NT	+	NT	NT	Georgieva et al., 2006; Huang et al., 2008; Sims et al., 2009
Rheumatoid arthritis *	NT	NT	NT	+	Plenge et al., 2007 Thomson et al., 2007

TABLE 2. **Functions of Olig proteins.** *Genome-wide association studies correlate certain *Olig2* single nucleotide polymorphisms to these disorders. These observations have not progressed beyond the correlative level. Function (arbitrary units) ranging from no involvement (–) to essential for the specific process (+++). NT not tested.

Moreover, occasional foci of Pdgfrα-positive oligodendrocyte progenitors are seen in the forebrain of *Olig2* knockout mouse embryos and these PDGFRα-expressing cells are even more abundant in the hindbrain (Lu et al., 2002). Combinatorial knockout of *Olig1* and *Olig2* is required to ablate these last vestiges of oligodendrocyte formation completely (Zhou and Anderson, 2002), suggesting that the role of Olig1 in the specification phase of oligodendrocyte formation is partially redundant in the presence of Olig2.

In rodents and humans, expression of *Olig2* in the parenchyma is generally considered to identify a cell of the oligodendrocyte lineage, but there are several exceptions to this characterization. First, *Olig2* expression in putative astrocyte precursor cells has been reported in the postnatal day (P) 7 neonatal rodent brain. Second, Cahoy *et al*. reported that a small percentage (~3%) cells (Marshall et al., 2005). Using the in the adult mouse brain that were positive for the astrocytic marker Aldh1l1, also expressed *Olig2* (Cahoy et al., 2008). Third, *Olig2* expression has been reported in proliferating reactive astrocyte precursor cells (Chen et al., 2008). However, *Olig2* expression is down-regulated upon terminal differentiation of astrocytes, an observation confirmed *in vitro* (see below).

One critical neurogenic function seems to be unique to Olig2. Generally, the bHLH transcription factors that control neurogenesis can be classified as being either anti-neurogenic (pro-mitotic) or neurogenic (anti-mitotic). At early stages of development, expression of anti-neurogenic (pro-mitotic) transcription factors prevents cell cycle exit and thereby expands the pool of neural progenitors. At later stages of neural development, expression of neurogenic (anti-mitotic) factors promotes cell cycle exit, subtype specification and differentiation (Kageyama and Nakanishi, 1997; Lee, 1997; Parras et al., 2004). In this context, Olig2 stands apart, showing functional characteristics of both sets of transcription factors in multipotent neural progenitor cells. In the embryonic spinal cord, for example, Olig2 is required for specification and the ultimate differentiation of motor neurons and oligodendrocytes (Lu et al., 2002). However, at early time points in development in the pMN domain, Olig2 functions in pattern formation as an anti-neurogenic factor (pro-mitotic factor), to sustain the replication competent state of some pMN progenitors that are destined for the second wave gliogenesis (Lee et al., 2005). An emerging body of literature suggests that this early anti-neurogenic (pro-mitotic) function of Olig2

may be co-opted by the stem-like 'tumor-initiating cells' of malignant glioma (see below).

The developmental functions (Table 1) and expression (Table 2) of *Olig3* are divergent from those of *Olig1* and *Olig2*. Accordingly, Olig3 will not be discussed beyond this point.

Roles in disease and neural repair

A broadening body of literature documents non-overlapping postnatal roles for Olig1 and Olig2 in neurological diseases and in response to injury (Table 2). For example, both proteins are expressed in fresh surgical isolates of human diffuse gliomas (Bouvier et al., 2003; Ligon et al., 2004; Lu et al., 2001; Marie et al., 2001; Ohnishi et al., 2003). However, human gliomas have been reported to contain a subpopulation of highly tumorigenic cells (Singh et al., 2004) and *Olig2,* but not *Olig1,* is selectively expressed in such cells (Ligon et al., 2007). Beyond merely marking glioma progenitors, Olig2 is required for intracranial tumor formation in genetically relevant murine models of human glioma (Appolloni et al., 2012; Bao et al., 2008; Barrett et al., 2012; Ligon et al., 2007) and for the proliferation of authentic human glioma cells implanted into the brains of severe combined immunodeficiency (SCID) mice (Mehta et al., 2011). These findings do not rule out a role for Olig1 in gliomas, but show that it is dispensable—unlike Olig2—in certain subtypes of these tumors.

As indicated in Table 2, a postnatal role for Olig1 is demonstrated in the repair of white matter injury. Xin *et al*. have described an *Olig1*-null mouse in which myelination is severely retarded, leading to early postnatal lethality. However, the originally reported *Olig1*-null mouse strain exhibits only a mild developmental delay in oligodendrocyte maturation, even when both copies of *Olig1* are ablated, and survives to develop fully myelinated axons in the brain and spinal cord (Lu et al., 2002; Xin et al., 2005). The two mouse strains differ in terms of the targeting of the *Olig1* locus and genetic background, and these differences might underlie the observed differential of the strong versus mild knockout phenotypes. In any case, the relatively benign developmental phenotype of the original *Olig1* knockout strain allows scrutiny of *Olig1* functions in murine models of MS, and Arnett *et al*. have showed that the functions of

Olig1 in response to demyelinating injury are more readily apparent than the developmental functions. Indeed, *Olig1*-null mice were severely limited in their ability to repair demyelinated lesions that were induced by various gliotoxins (cuprizone, lysolecithin and ethidium bromide). The loss of *Olig1* had no effect on the genesis or recruitment of early oligodendrocyte progenitors expressing NG2, Olig2 or homeobox protein Nkx2.2 into the lesion. Rather, the *Olig1*-null progenitors were markedly impaired in their ability to differentiate into myelinating oligodendrocytes and wild-type levels of Olig2 could not compensate for the absence of Olig1 in this regard (Arnett et al., 2004).

One distinctive feature of Olig1 in the developing CNS is recapitulated in the repair of demyelinating insults in murine models and also in postmortem brain tissues from patients with MS. During mouse embryonic development, Olig1 is localized to the nucleus of oligodendrocyte progenitors (Fig. 2).

However, in mature oligodendrocytes in the CNS from 2 weeks after birth, Olig1 is mostly located in the cytoplasm. Translocation of Olig1 from the nucleus to the cytoplasm is a precise marker of the terminal differentiation of oligodendrocytes (Kitada and Rowitch, 2006). By contrast, Olig2 is localized to the nucleus at all stages examined and in all regions of the CNS. The differential localization of Olig1 and Olig2 is also seen in the adult human brain. Arnett *et al.* showed that demyelinating injuries to the adult mouse CNS create an environment that recruits immature oligodendrocyte progenitors with nuclear localization of Olig1 (Arnett et al., 2004). The relocalization of Olig1 observed in murine models of MS is recapitulated in postmortem brain tissue from patients with MS (Arnett et al., 2004). Cells containing cytosolic Olig1 are present in normal-appearing white matter of the human brains but nuclear Olig1 is present at the edges of active MS lesions. Collectively, these findings fit into an emerging theme in human white matter injuries as diverse as adult MS and neonatal brain injury leading to cerebral palsy. In these scenarios various cell-intrinsic and environmental influences may limit the repair response by arresting maturation of oligodendrocyte progenitors, resulting in fixed demyelinated lesions (Billiards et al., 2008; Chang et al., 2002; Fancy et al., 2011; Kuhlmann et al., 2008; Verney et al., 2012).

Two other facets of the body's response to demyelination in both rodents and humans are the proliferation of microglia and astrocytes (known as reactive

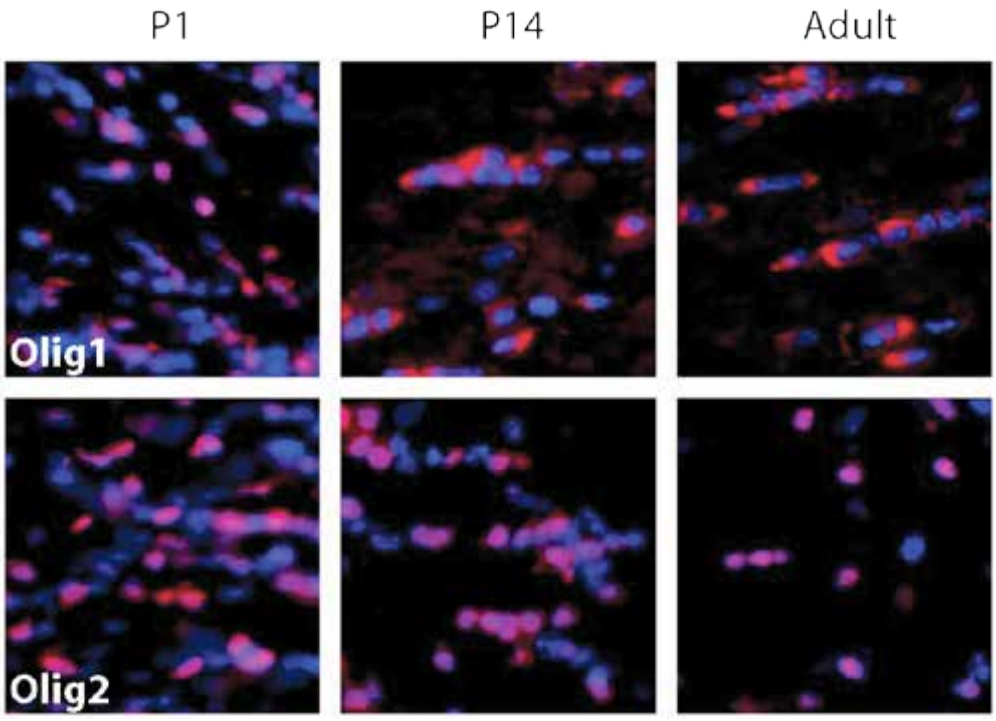

FIGURE 2. **Olig1 and Olig2 localization.** Olig1 and Olig2 (both visualized in red) are both present in the nuclei (blue) of oligodendrocytes and their progenitors at postnatal day (P) 1 in the mouse brain. Olig2 continues to have a nuclear localization at all developmental stages, whereas Olig1 is found almost completely in the cytoplasm in the adult mouse brain.

gliosis; reviewed in Pekny *et al*.) (Pekny and Nilsson, 2005). Neither of these reactive responses to demyelination was impaired in the *Olig1*-null mice (Arnett et al., 2004). However, a series of mouse studies supports a functional role for *Olig2* in reactive gliosis. Within several days following a cortical stab-wound injury, the number of *Olig2*-expressing cells increased in the lesioned area, but there was no rise in the number of *Olig1*-expressing cells (Buffo et al., 2005). Going beyond the correlative level, Chen *et al*. showed that targeted ablation of *Olig2*fl/fl with a Gfap-Cre driver, reduced the number of reactive astrocytes following injury, whereas ablation of *Olig2* in neuronal cells or oligodendroglial cells had no impact on this phenotype (Chen et al., 2008).

The Olig2-positive cell type that gives rise to reactive astrocytes is somewhat of a mystery. Early studies showed that neither *Olig1* nor *Olig2* is expressed in mature astrocytes(Lu et al., 2000; Zhou et al., 2000) and that Olig2 develop-

mentally acts as a repressor of astrogenesis (Gabay et al., 2003; Muroyama et al., 2005; Setoguchi and Kondo, 2004). Moreover, fate-mapping studies in the developing CNS failed to reveal any lineage relationship between Olig-positive cells and astrocytes(Dimou et al., 2008; Lu et al., 2002). In the postnatal brain, *Olig* expression is confined almost exclusively to transit-amplifying cells of the subventricular zone, NG2-positive glia and mature myelinating oligodendrocytes. NG2-positive glia do have progenitor-like qualities. However, fate-mapping studies indicate that these cells are probably not the progenitors of reactive astrocytes (Komitova et al., 2011; Tripathi et al., 2010; Zawadzka et al., 2010). It is conceivable that injury scenarios trigger transient re-expression of *Olig2* in an as yet poorly characterized type of progenitor of reactive astrocytes, which appears to express excitatory amino acid transporter 1 (Eaat1; also known as Glast), as well as other astroglial markers (Buffo et al., 2008). A transient non-lineage-restricted period of *Olig2* expression would be consistent with several reports on reactive gliosis that document the early export of Olig2 from the nucleus of proliferating progenitors followed by apparent degradation of the cytosolic protein (Cassiani-Ingoni et al., 2006; Furusho et al., 2006; Magnus et al., 2007; Zhao et al., 2009).

The most common genetic cause of intellectual disability is triplication of chromosome 21, giving rise to Down syndrome. *Olig1* and *Olig2* are co-localized to chromosome 21 within or near a region on the long (q) arm (the so-called Down syndrome critical region) that is thought to be most tightly associated with the cognitive facets of the Down syndrome phenotype. Does overexpression of the two *Olig* genes contribute to the neurological facets of Down syndrome? Chakrabarti *et al*. have generated support for this view in their studies with a well-characterized murine model of trisomy 21, the Ts65dn mouse (Chakrabarti et al., 2010). The parental Ts65dn mouse shows many of the cognitive and neuro-anatomical defects associated with Down syndrome. In careful anatomical studies, Chakrabarti *et al*. first noted that the Ts65dn mice have a substantial increase in the number of forebrain inhibitory neurons. This observed increase in forebrain inhibitory neurons resonated with earlier studies suggesting that a major functional defect underlying the behavioral abnormalities in Ts65dn mice is an imbalance between excitation and inhibition (Belichenko et al., 2004; Fernandez and Garner, 2007). A total of 128 genes are triplicated

in the Ts65dn mouse. Chakrabarti intercrossed these mice with a heterozygous *Olig1/2* double knockout mouse (*Olig1/2*$^{+/-}$), so as to selectively reduce the dosage of *Olig1* and *Olig2* from three copies to two (Chakrabarti et al., 2010; Haydar and Reeves, 2012; Lu et al., 2012). This genetically precise reduction in gene dosage rescued the overproduction of interneurons. Cognitive tests were not performed on the *Olig1*/*Olig2*-rescued animals; however, the published observations show a plausible molecular and cellular route towards the neurological facets of Down syndrome wherein Olig1 and Olig2 have pivotal roles.

Reports that have yet to undergo functional validation link *Olig2*, but not *Olig1*, to schizophrenia and Alzheimer's disease. Genome-wide association work identified several single nucleotide polymorphisms (SNPs) in *Olig2* that are associated with schizophrenia in a UK population (Georgieva et al., 2006). One of the SNPs identified by the UK team (SNP rs762178) has been confirmed in a study of schizophrenia in a Chinese Han population (Huang et al., 2008). Two of the above-mentioned *Olig2* SNPs (SNP rs762237 and rs2834072) have also been linked to a cohort of Alzheimer's disease patients with psychotic symptoms (Sims et al., 2009).

Genetic targets

As discussed above and summarized in Table 2, data from multiple studies indicate that Olig1 and Olig2 have largely non-overlapping roles in development, tissue repair and disease. Paradoxically, these two genes are co-localized within 40 kb of each other on human chromosome 21 and their expression patterns are largely overlapping. Moreover, Olig1 and Olig2 have highly homologous DNA-targeting bHLH motifs. In this, and subsequent sections, we explore ways in which their non-overlapping biological functions may reflect separate genetic targets, co-regulator proteins and post-translational modifications. We begin with discussion of their genetic targets.

Expression profiling studies of *Olig1* and *Olig2* knockout mice versus their wild-type counterparts show that various non-overlapping sets of genes are up-regulated or down-regulated in the absence of *Olig1* or *Olig2* (Ligon et al., 2007; Wang et al., 2006) (S. Mehta, H. Liu, J. Alberta, E. Huillard, D. Rowitch, C. Stiles, unpublished observations) (Fig. 3).

However, expression profiling cannot discriminate between direct genetic targets of Olig1 and Olig2 and downstream sequelae of their deletion. The basic domain of bHLH transcription factors mediates the interaction between these proteins and DNA sequences that contain the core hexanucleotide motif CANNTG, known as an E-box (reviewed in Massari and Murre, 2000). For Olig2, specification of motor neurons following E-box binding seems to be channeled largely through its functions as a transcription repressor. In chick embryo electroporation assays, involving ectopic motor neuron formation as a biological readout, the neurogenic effect of Olig2 is mimicked when the Olig2 DNA-binding domain is fused to the transcription repressor domain of engrailed. Equivalent fusions to the transcription activator VP-16 lack neurogenic activity (Mizuguchi et al., 2001; Novitch et al., 2001; Zhou et al., 2001). One important downstream effector gene of the Olig2 repressor function seems to be *Hb9* (Lee et al., 2005). Lee *et al*. have shown that Olig2 binds to an E-box element in the *Hb9* promoter. The Olig2–*Hb9* promoter interaction results in repression of *Hb9* transcription, preventing differentiation into post-mitotic motor neurons and sustaining the replication competent state of pMN neural progenitors during neural tube development (Lee et al., 2005). Olig2 also binds to promoter elements of the cell cycle repressor gene *p21* and suppresses its expression (Ligon et al., 2007). Suppression of *p21* transcription by Olig2 may contribute in part to the growth of normal and malignant neural progenitors and to the notorious resistance of p53-positive human gliomas to radiation and genotoxic drugs (Mehta et al., 2011).

All that being said, it is unclear if Olig2 solely acts as a transcriptional repressor. Expression profiling reveals multiple genes that are down-regulated in *Olig2*-null neural progenitors compared with wild-type counterparts, consistent with the view that Olig2 might stimulate expression of such genes (Ligon et al., 2007). Recent data show that in mice, Olig2 binds to an enhancer site upstream of *Sox10*, thereby inducing its expression and increasing oligodendroglial activity (Kuspert et al., 2011). More recently, two groups have used ChIP-seq protocols to identify new Olig2 target genes (Mazzoni et al., 2011; Weng et al., 2012). Weng *et al*. identified *Sip1* as a direct, inducible target gene of Olig2. Specifically, they showed that Olig2 stimulates expression of *Sip1*, which goes on to promote the maturation of oligodendrocyte progenitors via inhibition of Smad signaling (Weng et al., 2012).

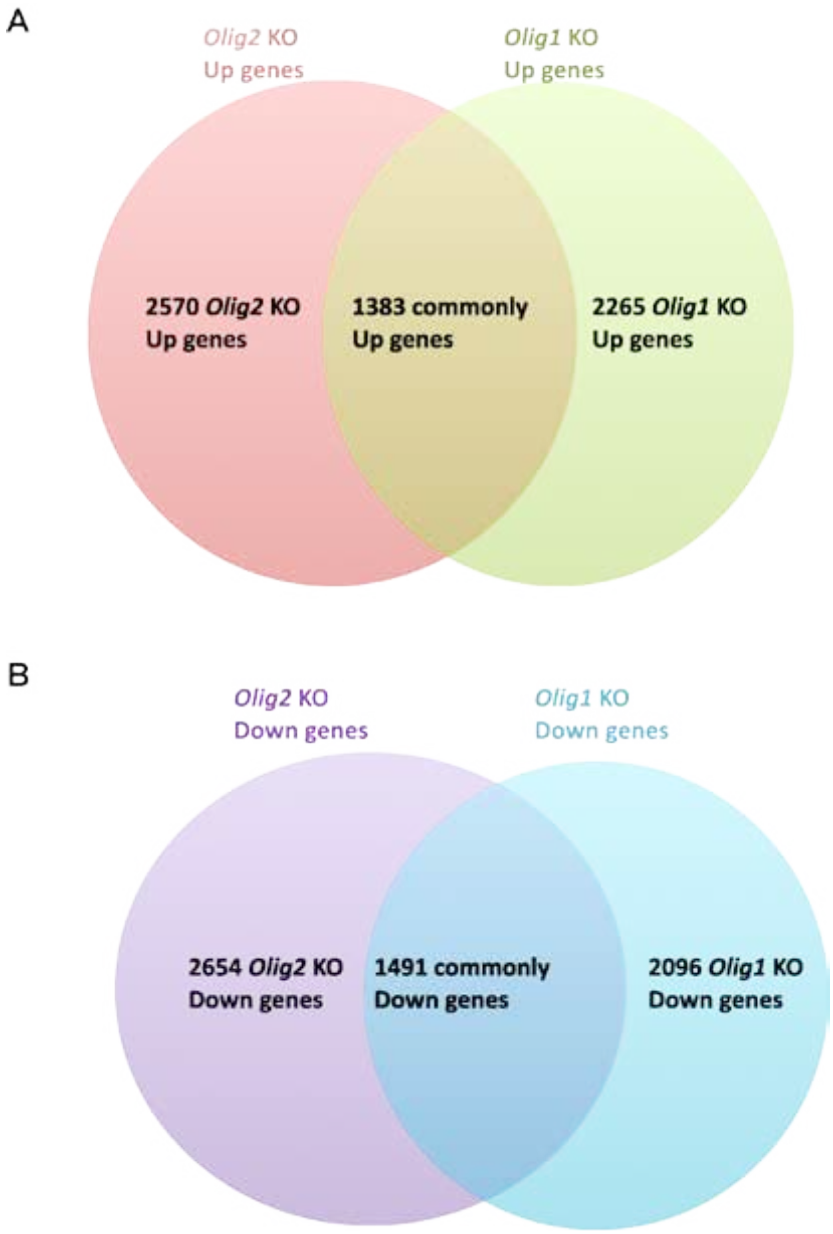

FIGURE 3. **Olig1 and Olig2 downstream gene targets.** The gene sets regulated by Olig1 and Olig2 only partially overlap. **(A)** The number of genes that show upregulated expression in *Olig1* and/or *Olig2*-null neural progenitor cells compared with wild-type neural progenitor cells. **(B)** The number of genes that show down-regulated expression in *Olig1* and/or *Olig2*-null neural progenitor cells compared with wild-type counterparts. The *Olig2* data set is taken from Ligon et al., 2007, whereas the *Olig1* expression profiling data sets (S. Mehta, H. Liu, J. Alberta, E. Huillard, D. Rowitch, C. Stiles, unpublished observations) are available from the NCBI GEO database (GSE39706).

What about genetic targets of Olig1? As noted in the section on disease and neural repair, the truly distinctive feature of Olig1 is that it is localized to the cytosol in the postnatal brain where it cannot possibly have any direct genetic targets (Arnett et al., 2004). Indeed, as nuclear localization is essential for transcription factor function, it can be surmised that the critical phase of Olig1 transcriptional activity in oligodendrocyte differentiation has been completed by the time it becomes localized to the cytoplasm. Genetic targets of Olig1 have been inferred from gene expression profiles of wild-type versus *Olig1*-null tissues. Compared with their wild-type counterparts, optic nerve, spinal cord and brain tissue from *Olig1*-null mice show reduced mRNA and protein levels for several genes involved in oligodendrocyte maturation, including myelin basic protein (*Mbp*), myelin oligodendrocyte glycoprotein (*Mog*) and *Plp* (Arnett et al., 2004; Chen et al., 2009; Guo et al., 2010; Wang et al., 2006; Xin et al., 2005). Olig1 directly binds to the promoter region of *Mbp*, thereby inducing its expression (Li et al., 2007; Xin et al., 2005). The *Mbp* promoter contains one E-box that is entirely conserved between human, mouse, rat, chick and zebrafish (Li et al., 2007). Mutation of this E-box reduces the binding affinity of Olig1 for the *Mbp* promoter in luciferase promoter assays and gel mobility shift assays (Li et al., 2007). Olig1 also induces expression of zinc finger protein 488 (*Zfp488*), as shown in a luciferase reporter assay. There are 20 conserved E-box sequences in the *Zfp488* promoter region, but it has not been tested whether Olig1 directly or indirectly activates *Zfp488* expression (Wang et al., 2006).

Co-regulator proteins

All bHLH transcription factors function in a dimeric state as homodimers or as heterodimers with another bHLH protein. Once in contact with promoter or enhancer elements of a target, bHLH homodimers and heterodimers serve as scaffolding upon which a multimeric complex of transcriptional co-regulator proteins can be assembled (Beckett, 2001; Featherstone, 2002; Ravasi et al., 2010; Torchia et al., 1998). Transcriptional co-regulators serve many functions, but broadly speaking they can be assigned into two groups—those that are components of the basal transcriptional machinery and those that modify the structure of chromatin92. Against this backdrop, the non-overlapping biological

functions of Olig1 and Olig2 could reflect differential dimeric partners for the two transcription factors and/or differential interactions with co-regulator proteins.

As a general rule, tissue-specific bHLH transcription factors (termed class B factors) form heterodimers with ubiquitously expressed class A bHLH transcription factors such as E12, E47 (also known as Tcf3) or Tcf12 (Massari and Murre, 2000). Olig2, which is highly tissue-specific, might favour homodimerization over heterodimerization with class A bHLH transcription factors. Indeed, although Olig2 : E12 and Olig2 : E47 heterodimers have been detected (Lee, 2005)(Samanta and Kessler, 2004), Lee *et al.* found that Olig2 homodimers are the preferred product when Olig2 and E47 are co-expressed in yeast two-hybrid experiments (Lee et al., 2005). In addition, Olig2 will form heterodimers with Olig1 and, under certain conditions, HLH transcription factors such as DNA-binding protein inhibitor Id2, and Id4. These Olig : Id interactions are detected when differentiation of progenitors towards the oligodendrocyte lineage is suppressed by BMPs (Samanta and Kessler, 2004). Lacking a basic domain, HLH factors cannot interact with DNA. Accordingly, HLH transcription factors are thought to function as natural dominant-negative agents for bHLH transcription factors by forming heterodimers that cannot bind to E-box elements of their target genes (Benezra et al., 1990).

Physical interactions between bHLH proteins and members of the homeodomain protein family regulate the development of several other tissues, including the pancreas, the pituitary gland and muscle (Babu et al., 2008; Makarenkova et al., 2009; Poulin et al., 2000). Olig2 has been shown to interact with Nkx2.2, a homeodomain protein that defines the p3 progenitor domain of developing spinal cord and is specifically required for production of v3 interneurons and maturation of oligodendrocytes (Sun et al., 2001).

Another co-regulator protein that has been linked to Olig2 is histone acetyltransferase p300 (Fukuda et al., 2004; Ravasi et al., 2010), which, via its associated histone acetyl transferase activity, functions to decondense the structure of chromatin and thus promotes transcription (Fukuda et al., 2004; Ogryzko et al., 1996; Ravasi et al., 2010). The presence of p300 as a co-regulator resonates with data suggesting that Olig2 can stimulate the expression of some genes (Kuspert et al., 2011). Considering the known function of Olig2 as a transcription repressor in the genesis of motor neurons, it is somewhat surprising that

studies to date have not identified any known members of the general transcription co-repressor complex in association with Olig2. Conceivably, directed antibody pull down experiments and unbiased yeast-two-hybrid screens lack sensitivity or cell-type specificity to display these interactions.

Most HLH-containing proteins that have been identified as Olig2-binding partners show some binding affinity for Olig1 as well (the exception is cyclin-D1-binding protein 1 (Ccndbp1). This is not surprising since the bHLH domains of Olig1 and Olig2 show more than 80% amino acid identity (BOX 1). Ccndbp1 is a helix–loop–helix protein that lacks a DNA-binding region. Ikushima *et al*. showed that this protein inhibits transcription of transforming growth factor β (Tgf-β)-induced genes that require the Smad complex for their activation(Ikushima et al., 2008). They demonstrated in NmuMG and U373MG cells (normal murine mammary gland and glioma cell lines, respectively) that Ccndbp1 recruits Olig1, thereby interfering with the Olig1–Smad interaction. A comprehensive list of all co-regulator proteins that have been associated with Olig1 and Olig2 can be found in the Supplemental Table.

Post-translational modifications

How are the proliferative and developmental functions of Olig1 and Olig2 regulated at different developmental stages and in different cell types? Most neurogenic bHLH transcription factors (for example, mammalian achaete-scute homologue 1 (Mahs 1), mammalian atonal homologue Math, neurogenin 1 (Ngn1) and Ngn2) are only expressed transiently in progenitor cells at times when their functions are required. Notably, neither neurogenic nor anti-neurogenic bHLH transcription factors are generally expressed in fully formed, terminally differentiated neurons (Kageyama and Nakanishi, 1997; Lee, 1997; Parras et al., 2004). However, expression of *Olig1* and *Olig2*, initiated in oligodendrocyte progenitors, is sustained throughout development and occurs in the postnatal brain, where initial *in situ* hybridization images indicate that the two genes are expressed in white matter tracts of the corpus callosum, the optic nerve and cerebellum (Lu et al., 2000; Takebayashi et al., 2000; Zhou et al., 2000). Thus, for Olig1 and Olig2, post-translational modifications, rather than the timing of gene expression per se, might be the key to the developmental

control of their functions. Obviously, factor-specific post-translational modifications could contribute to differential interactions with co-regulator proteins and genetic targets as discussed above.

Phosphorylation regulates Olig2 function

Computer algorithms reveal a number of conserved potential phosphorylation sites in Olig2 and recent studies indicate that several of these sites are functional (Fig. 4A and Fig. S1).

Developmentally regulated phosphorylation events may account for the functional versatility of Olig2 in cell cycle regulation and differentiation. A striking structural feature of Olig2 is a string of 12 contiguous serine and threonine residues at position Ser77-Ser88 in its N-terminal region (known as the ST box). Huillard *et al*. showed that a murine Olig2 protein fragment containing the ST box, fused to glutathione S-transferase, was a substrate for the serine–threonine protein kinase Ck2 (Huillard et al., 2010). Tryptic peptide digests revealed phosphorylation of the Olig2 fragment at residues Ser85 and Ser87 within the ST box. Interestingly, targeted disruption of the gene encoding Ck2β (an essential regulatory subunit of Ck2) results in impaired oligodendrocyte differentiation *in vivo* and *in vitro*. These observations largely resemble the differentiation phenotype of the *Olig2* knockout mice. Moreover, an *Olig2* deletion mutant that lacks the entire ST box is unable to rescue the formation of oligodendrocyte progenitor cells when it is transduced in *Olig2*-null neural progenitor cells. Collectively, these observations provide circumstantial evidence that the phosphorylation state of the ST box could regulate separate functions of Olig2 in proliferation and differentiation.

One concern, however, is that phosphorylation of the ST box has never been detected in living cells. Sun *et al*. isolated endogenous Olig2 from mouse neural stem cells, human malignant gliomas and ectopic Olig2 transfected into COS7 cells and screened these isolates for post-translational phosphorylation events by mass spectrometry. Phosphorylation of the ST box in the Olig2 extracts was not detected (Sun et al., 2011). Conceivably, phosphorylation of the ST box *in vivo* is a spatially and temporally restricted event that was not duplicated in the cell types assessed by Sun and colleagues. However, it is also possible that misfold-

ing of the Olig2 fragment in the *in vitro* experiment described above exposed CK2 substrates that are normally occluded in native Olig2. It may be noteworthy that the ST box itself is not especially well conserved through phylogeny, especially when compared with several other phosphorylation motifs interesting Olig2 (see Fig. 4A and Fig. S1). Thus, the biological functions of the ST region have yet to be fully resolved *in vivo*.

Cortical progenitor cultures that have been expanded by incubation with basic fibroblast growth factor (Fgf) and epidermal growth factor (Egf) for two weeks contain 90% Olig2-positive cells (Ligon et al., 2007). Following withdrawal of Fgf and Egf and exposure to ciliary neurotrophic factor (Cntf), Olig2 is exported from the nucleus to the cytosol where it is rapidly degraded. In an elegant series of studies, Setoguchi and Kondo showed that this Cntf-induced relocalization of Olig2 coincides with activation of the serine–threonine protein kinase Akt (Setoguchi and Kondo, 2004). Moreover, they showed that Ser30 in the N-terminus of Olig2 is phosphorylated by Akt *in vitro*. A phosphomutant version of Olig2 containing a Ser30Ala mutation, is retained in the nucleus of neural progenitor cells. This coincides with impaired Cntf-induced astrocytic differentiation after Fgf and Egf withdrawal, compared to cells overexpressing vector control. Together, their observations are consistent with a model wherein the phosphorylation state of Olig2 at Ser30 dictates a fate choice decision for cortical progenitor cells to differentiate into astrocytes or remain as uncommitted neuronal progenitors.

Setoguchi *et al*. did not demonstrate Ser30 phosphorylation of endogenous Olig2 in Cntf-treated cortical progenitor cells. In addition, Sun *et al*. did not detect Ser30 phosphorylation in Olig2 that was isolated from proliferating mouse neurospheres or glioma progenitor cells (Sun et al., 2011). However, Olig2 in cycling neurosphere cultures is localized strictly to the nucleus, and Sun *et al*. did detect some Ser30 phosphorylation in Olig2 that was isolated from COS7 cells, in which an appreciable amount of the protein is found in the cytosol (Sun et al., 2003; Sun et al., 2011). These observations would be consistent with the nuclear export and degradation function of Ser30 phosphorylation, as was suggested by Setoguchi and Kondo (Setoguchi and Kondo, 2004). One caveat regarding the functional relevance of the Ser30 site is that this site is not well conserved in Olig2 from different animal species (Fig. 4A).

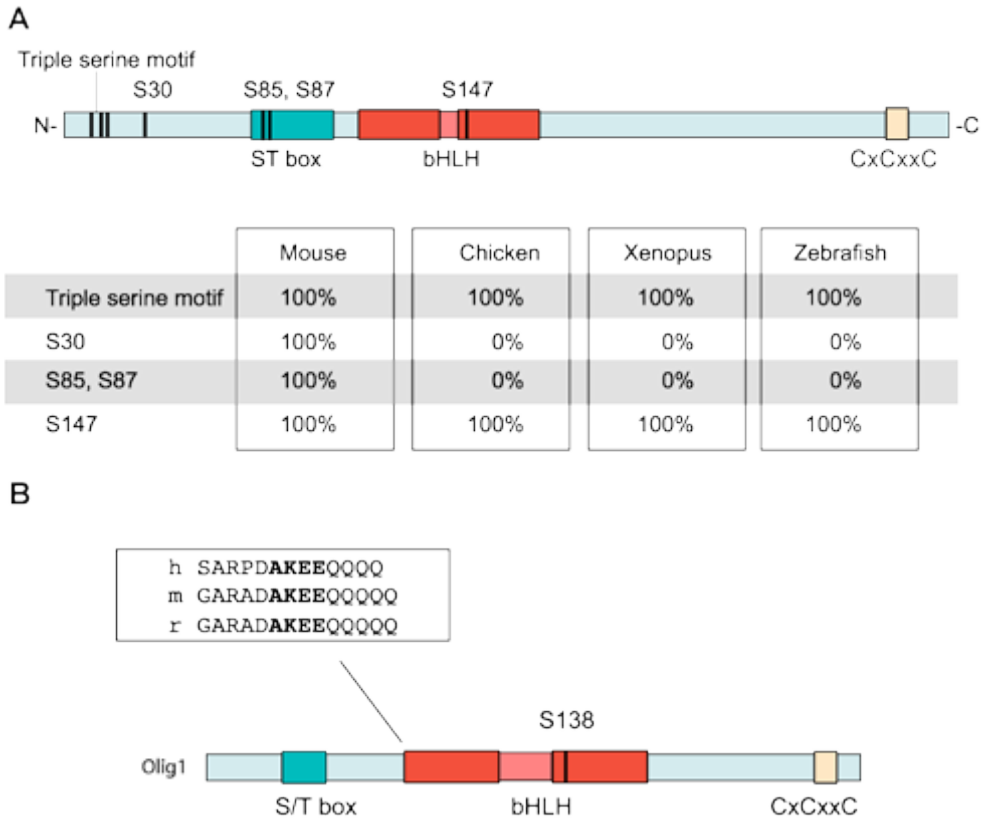

	Mouse	Chicken	Xenopus	Zebrafish
Triple serine motif	100%	100%	100%	100%
S30	100%	0%	0%	0%
S85, S87	100%	0%	0%	0%
S147	100%	100%	100%	100%

FIGURE 4. Post-translational modification motifs in Olig1 and Olig2. **(A)** Human Olig2 contains a number of serine phosphorylation sites, which are conserved in mouse Olig2. The triple serine motif in N terminus of human Olig2 and Ser147 are entirely conserved in chicken, *Xenopus laevis* and zebrafish. **(B)** Human Olig1 contains a serine residue at position 138 that seems to correspond to Ser147 in Olig2. Protein alignment of Olig1 orthologues from human, mouse and rat reveals a conserved putative SUMOylation motif close to the basic helix–loop–helix (bHLH) domain (inset).

As noted above in our comments on development, one important function of Olig2 in the early stages of development is to sustain the replication-competent state of neural progenitors (Lee et al., 2005). At later stages of development however, Olig2 is pivotal for specification of motor neurons and oligodendrocytes (Fig. 1B and Table 2). Studies by Sun *et al.* show that the proliferative functions of Olig2 are largely controlled by developmentally regulated phosphorylation of a triple serine motif comprising Ser10, Ser13 and Ser14 (Sun et al., 2011). When phosphorylated at these positions, Olig2 maintains pro-mitotic functions in normal neural progenitors. Using a phosphorylation state-specific antibody to

the triple serine motif, Sun *et al.* showed that endogenous Olig2 is phosphorylated at these residues during early stages of embryonic development when oligodendrocyte progenitors are proliferating. In postnatal white matter, the same serine residues are in a non-phosphorylated state. Strikingly, cells expressing a phosphomimetic mutant version of Olig2 (wherein the negatively charged amino acids aspartate or glutamate were substituted for Ser10, Ser13 and Ser14) were more tumorigenic in a murine model of high-grade glioma. Conversely, cells expressing a phosphonull mutant of Olig2 (with the neutral amino acids glycine or alanine were substituted for the three serine residues) were less tumorigenic. On a final note, Olig2 expressed in p53-positive human gliomas is phosphorylated at the triple serine motif. The data presented by Sun *et al.* and in a related paper by Mehta *et al.* suggest that phosphorylated Olig2 inhibits the genetic and biological responses to p53 (Mehta et al., 2011). Collectively, these data suggest that phosphorylated Olig2 may contribute to the notorious resistance of human gliomas to radiation and genotoxic drugs. This Olig2 triple serine motif is stringently conserved throughout evolution (Fig. 4A). In fact, these serines and their flanking amino acids are nearly as well conserved as the bHLH motif itself. To date, the protein kinases and phosphatases that regulate the phosphorylation state of this triple serine motif have not been identified.

As described above (Table 2), Olig2 is essential for specification of motor neurons as well as oligodendrocytes in the pMN domain of the developing spinal cord. Li *et al.* identified a phosphorylation site in the bHLH domain of Olig2 that regulates the motor neuron to oligodendrocyte transition (Li et al., 2011). A bio-informatic search for predicted phosphorylation sites and conserved amino acids in Olig2 drew the authors' attention to a predicted protein kinase A (PKA)-phosphorylated serine at position 147 in the second helix of Olig2. A phospho-specific antibody showed that Ser147 is phosphorylated in the developing mouse spinal cord during the window of time wherein Olig2 specifies the formation of motor neurons. The phosphorylation state of Ser147 reaches a maximum at day E9.5 during the peak of neurogenesis in the pMN and then decreases over time, disappearing entirely after E12, when the switch towards oligodendrocyte production takes place. Li *et al.* also generated mice that expressed *Olig2* encoding a serine-to-alanine substitution at position 147 (Ser147Ala Olig2) to study the biological function of Ser147 phosphorylation *in vivo*.

Ser147Ala Olig2 mice have a diminished pMN domain (revealed by *Pax6* and *Nkx*2.2 expression), as do *Olig2*-null mice. Also, as noted with *Olig2*-null mice, Ser147Ala Olig2 mice die at birth, because they do not generate motor neurons.

At a biochemical level, Li *et al*. showed that Ser147Ala Olig2 less readily forms Olig2 homodimers and Olig2–Olig1 heterodimers relative to wild-type Olig2 (Li et al., 2011). Conversely, Ser147Ala Olig2 binds NGN2 with higher affinity than does wild-type Olig2. The authors speculate that dephosphorylation of Olig2 in the developing pMN domain sequesters Ngn2, thereby preventing motor neuron development. In a perfect world, this sequestration of Ngn2 would be antagonized by substitution of a negatively charged amino acid (aspartic acid or glutamic acid) at Ser147, as per rescue experiments with the phosphomimetic mutant for the triple serine motif, described by Sun and colleagues (Sun et al., 2011). However, rescue experiments of this sort are not always successful and Ser147Asp and Ser147Glu Olig2 seem to be phenotypically equivalent at a biochemical level to the Ser147Ala Olig2—at least with respect to their diminished capacity to form Olig2 homodimers (Li et al., 2011). Interestingly, the Ser147 phosphorylation motif is conserved in the bHLH domain of Olig1 (Ser138), which is not involved in motor neuron development (Fig. 4B and Table 2). It would be interesting to see if the bHLH domain of Olig1 could be substituted for the Olig2 bHLH domain in 'domain swap' experiments focusing on motor neuron formation.

Is Olig1 protein post-translationally regulated?

Regardless of the structural similarities in Olig1 and Olig2, neither the Olig2 triple serine motif nor the Akt phosphorylation site at Ser30 have equivalents in Olig1. However, as mentioned above, the predicted Pka-phosphorylated serine at Ser147 in the bHLH domain of Olig2 is represented at an equivalent position in Olig1 (Ser138). As described earlier, one of the features of Olig1 is its nuclear to cytoplasm relocalization during oligodendrocyte development (Arnett et al., 2004). Niu *et al*. transduced *Olig1*-null rat oligodendrocyte progenitor cells with a Olig2 phosphomutant construct (Ser138Ala) or with its rescue construct (Ser-138Asp) (Niu et al., 2012). They showed that Ser138Ala Olig1 is expressed primarily in the nucleus of oligodendrocyte progenitor cells, whereas Ser138Asp

Olig2 has a cytoplasmic localization. Future work should clarify whether this serine has a functional role *in vivo*, as this study did not include any direct analysis of the phosphorylation state of this serine with either a phosphorylation state-specific antibody or mass spectrometry, or any *in vivo* mouse work.

One other intriguing protein modifier that is relevant to transcription factor biology is SUMO (small ubiquitin-like modifier). SUMOylation has been implicated in numerous biological functions within the nucleus, including transcription factor activity, protein–protein interactions, promyelocytic leukemia (PML) nuclear body integrity, DNA repair and sub-nuclear localization (Gill, 2004; Hay, 2005; Johnson, 2004; Verger et al., 2003). SUMOylation of NF-κB essential modulator (Nieddu et al.), which regulates NF-κB, is sufficient for nuclear import (Hay, 2004; Huang et al., 2003). By contrast, several studies show an increase in substrate SUMOylation concurrent with substrate nuclear export (Imoto et al., 2008; Martin et al., 2007). It is unclear whether SUMOylation initiates export or occurs in the cytoplasm, perhaps as a mechanism to retain proteins in the cytoplasm through masking of a nuclear localization signal or context-dependent protein–protein interactions. As shown in Fig. 4B, Olig1 does contain a conserved SUMOylation motif, and it was predicted to be a target of SUMOylation in a genome-wide screen for this modification (Zhou et al., 2005). Accordingly, it is at least conceivable that a SUMOylation event dictates the developmentally regulated localization of Olig1 observed in remyelinating white matter (Fig. 2) (Arnett et al., 2004).

Conclusions and future directions

This chapter has highlighted disparate aspects of the biology of Olig1 and Olig2 during development and in human disease. Despite much progress in elucidating this biology, many important questions remain regarding Olig protein functions and activity. Indeed, given their multiple stage-specific roles, we have argued that insight into the post-translational regulation of Olig1 and Olig2 activity is crucial for understanding the functional roles of these proteins.

The phenotype of *Olig2* knockout mice is severe and the biological functions of the Olig2 are readily apparent (Table 2). By contrast, the phenotype of *Olig1*-null mice is relatively nuanced (Lu et al., 2002). Investigators naturally grav-

itate to systems that are 'black and white' rather than 'shades of gray' and an Olig2 bias is readily apparent in the literature. Indeed, the PubMed database at the National Library of Medicine currently shows a four to one ratio of papers with Olig2 in their title to those with Olig1. *Olig1* and *Olig2* lie in close proximity to each other in humans, rodents and numerous other species in a region that is genetically well conserved (Frazer et al., 2001). In our view, the biological functions of Olig1 in development and disease are understudied and deserving of more attention. Indeed, many questions regarding its function remain. For example, are there early roles for Olig1 in forebrain neurogenesis? Can Olig1 compensate in part for Olig2 during gliomagenesis? What are the important factors regulating Olig1 at the post-translational level?

Overshadowing these technical challenges and underserved areas of inquiry are a series of therapeutic opportunities. Small molecule activators of Olig1 and Olig2 could have practical applications in MS and spinal cord injury respectively. Conversely, recent data suggest that small molecule antagonists of Olig2 might serve as highly targeted therapeutics for malignant glioma. Against these therapeutic opportunities lies one formidable challenge. Transcription factors are generally considered to be unattractive targets for drug development because their interactions with DNA and heterodimeric partner proteins involve large and complex surface area contacts. Surrogate targets for Olig drug development may be embedded within enzymatically active gene targets, partner proteins or post-translational modifying enzymes.

	Olig1	Olig2	References
Olig1	Affinity Purification	Affinity Purification	Li et al., 2007
Olig2	Affinity Purification	Two-hybrid, Affinity Purification	Lee et al., 2005; Li et al., 2007
E12	Affinity Purification	Affinity Purification	Li et al., 2007; Samanta and Kessler, 2004)
E47	Affinity Purification	Two-hybrid, Affinity Purification	Lee et al., 2005; Samanta and Kessler, 2004)
ID2	Two-hybrid, Affinity Purification *	Two-hybrid, Affinity Purification *	Chen et al., 2009; Guo et al., 2011; Samanta and Kessler, 2004)
ID4	Two-hybrid, Affinity Purification *	Two-hybrid, Affinity Purification *	Samanta and Kessler, 2004
NfiA		Affinity Purification	Deneen et al., 2006
Ngn2		Two-hybrid, Affinity Purification	Lee et al., 2005
Ngn3		Affinity Purification	Li et al., 2007
Zfp488		Affinity Purification	Wang et al., 2006
Nkx2.2		Two-hybrid, Affinity Purification	Li et al., 2007; Ravasi et al., 2010; Sun et al., 2003)
p300		Two-hybrid, Affinity Purification *	Fukuda et al., 2004; Ravasi et al., 2010)
Sox8		Two-hybrid, Affinity Purification	Ravasi et al., 2010; Wissmuller et al., 2006)
Sox10	Affinity Purification	Two-hybrid, Affinity Purification	Li et al., 2007; Ravasi et al., 2010; Wissmuller et al., 2006)
Sry		Affinity Purification	Wissmuller et al., 2006
Zfp292	Two-hybrid		Ravasi et al., 2010
Brca1	Two-hybrid		Ravasi et al., 2010
Lass4	Two-hybrid		Ravasi et al., 2010
Gtf2E1	Two-hybrid		Ravasi et al., 2010
Gtf2A1	Two-hybrid		Ravasi et al., 2010
Ccndbp1	Affinity Purification *		Ikushima et al., 2008
Smad2/3	Affinity Purification *		Ikushima et al., 2008
Srm160		Affinity Purification	McCracken et al., 2005

**endogenous interaction*

SUPPLEMENTAL TABLE. Dimerization partners and co-regulators of Olig1 and Olig2

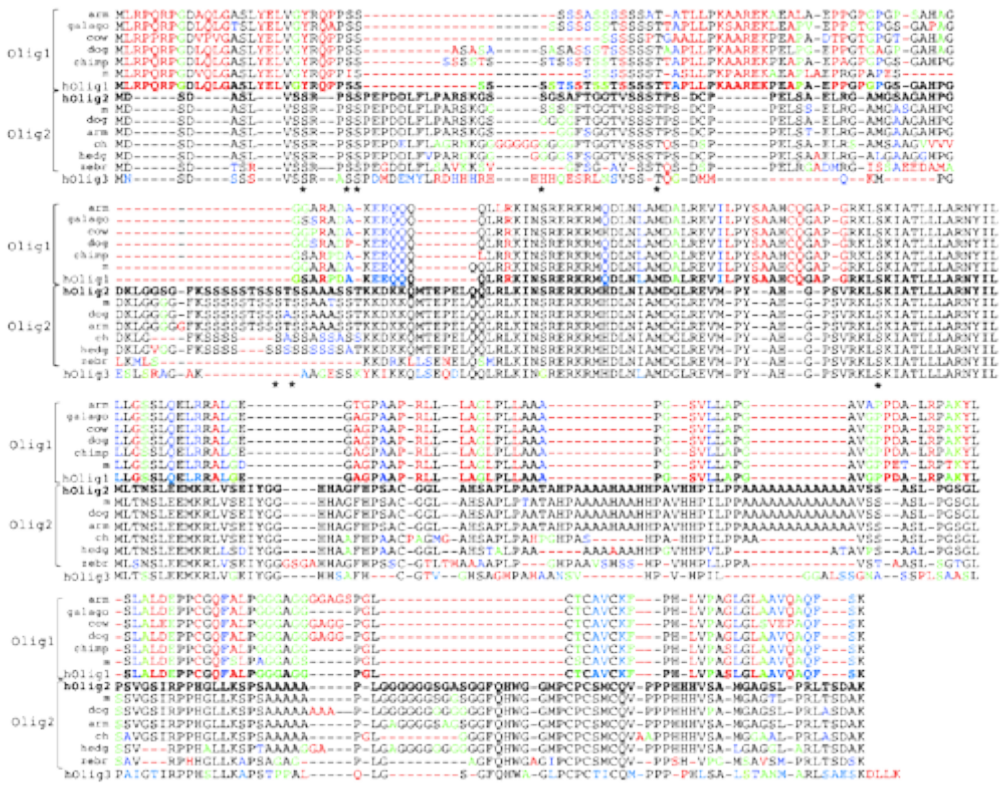

SUPPLEMENTAL FIGURE S1. Protein alignment of Olig1 and Olig2. Orthologues of Olig1 and Olig2 were obtained from Genbank. Sequences were first aligned utilizing Clustal Omega and then further adjusted to "best-fit" by eye. The alignments and weighting are based on human Olig2. Substitution weighting follows ClustalW2 (Gonnet Pam250), black indicates identity, blue indicates conserved substitution, green indicates semi-conserved substitution, red indicates non-conserved residues. Sites found to be phosphorylated in Olig2 are indicated by * (see text). Conspicious by its absence is sequence data for an avian *Olig1*. An avian *Olig2* gene is localized to chromosome 1 of the chick. However, at the present time there are still large gaps in the sequencing data for chick chromosome 1. It seems most likely that chick *Olig1* is contained in the gap region, although the possibility that *Olig1* is missing in birds cannot be excluded.

2 Phosphorylation state of Olig2 regulates proliferation of neural progenitors

Yu Sun, Dimphna H. Meijer, John A. Alberta,
Shwetal Mehta, Michael F. Kane, Sophie Runquist,
An-Chi Tien, I. David H. Rowitch and Charles D. Stiles

Adapted from: Neuron (2011) 69, 906–917

Abstract

The bHLH transcription factors that regulate early development of the central nervous system can generally be classified as either anti-neural or pro-neural. Initial expression of anti-neural factors prevents cell cycle exit and thereby expands the pool of neural progenitors. Subsequent (and typically transient) expression of pro-neural factors promotes cell cycle exit, subtype specification and differentiation. Against this backdrop, the bHLH transcription factor Olig2 in the oligodendrocyte lineage is unorthodox, showing anti-neural functions in multipotent CNS progenitor cells but also sustained expression and pro-neural functions in formation of oligodendrocytes. We show here that the proliferative function of Olig2 is controlled by developmentally regulated phosphorylation of a conserved triple serine motif within the amino terminal domain. In the phosphorylated state, Olig2 maintains anti-neural (i.e. pro-mitotic) functions that are reflected in human glioma cells and in a genetically defined murine model of primary glioma.

Introduction

During central nervous system (CNS) development, regulation of pool size for diversified neuronal and glial progenitor populations involves complex interactions of spatially restricted organizing signals, mitogens and other developmental cues that promote differentiation through intracellular signaling and activation of a variety of transcription factors (Edlund and Jessell, 1999). Pro-neural bHLH transcription factors (e.g. Ascl1) and anti-neurogenic bHLH

and HLH transcription factors from the Hes, Hey and Id families play pivotal roles in specification and differentiation of neurons and glia. At early times in development, anti-neurogenic factors prevail over their pro-neurogenic counterparts so as to sustain replication competence and expand the pool of neural progenitors. At later times, pro-neurogenic factors become dominant as to promote cell cycle exit, neuronal differentiation and subtype specification (Jessell, 2000; Ross et al., 2003; Rowitch, 2004).

Oppositional functions of anti-neurogenic and pro-neurogenic transcription factors can be regulated at the level of gene expression or protein activity. In the developing telencephalon for example Delta/Notch signaling stimulates expression of anti-neural Hes transcription factors (reviewed in Justice and Jan, 2002) which in turn directly suppress expression of neural factor Ascl1. Conversely, suppression of Notch/Delta signaling (through relief of lateral inhibition) is needed for expression and function of pro-neural factors (reviewed in Beatus and Lindhal) (Beatus and Lendahl, 1998). According to the prevailing view of neurogenesis, the transient expression of pro-neural bHLH transcription factors such as Mash1, Ngn1 or Ngn2 induces a second sustained wave (or waves) of bHLH neuronal differentiation transcription factors (e.g. NeuroD, NeuroD2), which then promote terminal differentiation. Notably, neither pro-neural nor anti-neural bHLH transcription factors are generally expressed in fully formed, terminally differentiated neurons (Kageyama and Nakanishi, 1997; Lee, 1997). The pro-neural factor Ascl1 also plays a role in specification of oligodendrocytes (Parras et al., 2004). Even in this gliogenic context, however, Ascl1 expression is confined to immature precursors and is not seen in differentiated oligodendrocytes.

One neurogenic factor that defies this simple binary functional characterization is Olig2—a bHLH transcription factor that shows both anti-neural functions and pro-neural functions at different stages in the formation of the oligodendrocyte lineage. In the embryonic spinal cord for example, *Olig2* is expressed initially in the pMN domain where it functions at early times in pattern formation (Lu et al., 2002) and as an anti-neural factor to sustain the replication competent state of those pMN progenitors that are destined for second wave gliogenesis (Lee et al., 2005) (see Discussion). *Olig2* is likewise expressed in multipotent neurospheres derived from the embryonic forebrain, where it

is required for optimum proliferation *in vitro* (Ligon et al., 2007). As development proceeds, Olig2 acquires a pro-neural function to specify formation of oligodendrocyte progenitors. However unlike other pro-neural factors with roles in gliogenesis such as Ascl1 that are not expressed in their terminally differentiated end products (Parras et al., 2004), *Olig2* expression is sustained in oligodendrocyte progenitors and in mature oligodendrocytes (Lu et al., 2000) where it appears to have ongoing biological functions (Cai et al., 2007). A similar anti-neural/pro-neural dichotomy is observed in the postnatal brain where *Olig2* is expressed in rapidly cycling transit amplifying cells ("Type C" cells) of the subventricular zone as well as in terminally differentiated myelinating oligodendrocytes that arise from these cells (Jackson et al., 2006; Menn et al., 2006).

Intuitively, it would seem that Olig2 can not be doing the same thing in replication competent progenitor cells and in terminally differentiated oligodendrocytes. The regulatory functions of Olig2 in proliferation of neural progenitors are of special interest due to provocative links to the literature on human gliomas. Tissue microarray and *in situ* hybridization studies show that *Olig2* is expressed in 100% of the human diffuse gliomas irrespective of grade. Beyond merely marking the glioma cells, *Olig2* expression is actually required for intracranial tumor formation in a murine model of glioma that recapitulates the genetics and histology of high-grade glioma in humans. The tumorigenic "gatekeeper" function of Olig2 reflects, at least in part, the fact that the gene encoding *p21WAF1/CIP1*, a tumor suppressor and inhibitor of stem cell proliferation (hereafter referred to as "p21"), is directly repressed by Olig2 in murine neural progenitors and human gliomas (Ligon et al., 2007).

How might the distinct functions of Olig2 be dynamically modulated to suit biological context? Using mass spectroscopy, phosphorylation state-specific antibodies and site-directed mutagenesis, we show here that the separate functions of Olig2 in progenitor self renewal and oligodendrocyte development are controlled in part by developmentally regulated phosphorylation of a conserved triple serine motif within the amino terminal domain. The pro-mitotic functions of this triple serine motif are reflected in human glioma neurosphere cultures and in a murine model of primary glioma (the most common manifestation of the disease in humans) (Kleihues and Cavenee, 2007).

Results

Identification of a triple phospho serine motif in Olig2

Using immunoaffinity chromatography, we purified microgram quantities of endogenous Olig2 protein from both normal murine neurosphere cultures and from gliomas generated by orthotopic transplant of primary human tumor neurospheres (Fig. s1). High confidence phosphorylation sites within Olig2 were mapped by mass spectroscopy (Figs. 1, s1D and s2).

As indicated in Fig. s1, a number of potential phosphorylation sites within Olig2 can be detected by computer algorithm. However, mass spectroscopy reveals that very few of these potential sites are actually utilized in endogenous Olig2 isolated from these murine and human progenitor cell types (see "Discussion"). Notably, no phosphorylated residues were detected within a serine/threonine rich "box" that is a distinctive feature of all mammalian Olig2 homologs (Lu et al., 2000; Takebayashi et al., 2000; Zhou et al., 2000). Instead, high confidence phosphorylation sites within endogenous Olig2 were confined to Ser10, Ser13, Ser14 and Thr43 within the amino terminal domain (Figs. 1A, s1 and s2).

The triple phospho serine motif in Olig2 regulates proliferation of neural progenitors in secondary neurosphere assays

Olig2-null progenitor cells can be cultured as neurospheres *in vitro*. However the population doubling time of *Olig2*-null progenitors is significantly extended relative to their wild-type counterparts (~43 hrs versus ~35 hrs respectively) (Ligon et al., 2007). The four S/T residues comprising the high confidence phosphorylation sites were mutated singly or in combinatorial fashion to glycine or valine so as to create phospho-null Olig2 mutant proteins (Fig. 1B). These phospho-null variants were transduced into *Olig2*-null neural progenitor cells and secondary neurosphere assays were conducted to examine their roles in proliferation.

As indicated (Figs. 1C,D) the phosphorylation state of Olig2 is irrelevant to the total number of neurospheres that are produced in secondary neurosphere assays. However, the viable cell count within these neurospheres (and hence

the size of the secondary neurospheres) is greatly reduced by phospho-null substitutions at Ser10, Ser13 and Ser14 (triple phospho-null, TPN). Conversely, the substitution of negatively charged "phospho-mimetic" amino acids (S->D or S->E) at this triple serine motif (triple phospho-mimetic, TPM) rescues the proliferative functions of wild-type Olig2 (Figs. 1C, 1E and 1F). The effects of these TPN and TPM amino acid substitutions on proliferative functions of Olig2 were further confirmed by pulse labeling experiments with BrdU (Fig. S3).

Western blotting and immunostaining experiments show that the triple phospho-null and triple phospho-mimetic substitutions affect neither the expression nor the subcellular location of Olig2; moreover, the total amount of ectopic wild-type or mutant Olig2 proteins (produced as transcription/translation products of our retroviral expression vectors) is roughly equivalent to the abundance of endogenous Olig2 protein in normal neural progenitor cells (Fig. S4). Single or double substitutions at Ser10, Ser13, Ser14 proved to have minimal effect on neurosphere growth (Fig. 1B). Accordingly, all of our further studies focused on the TPN and TPM variants shown in Fig. 1B.

Phosphorylation state of the Olig2 Ser10/13/14 motif is developmentally regulated

Using synthetic phosphopeptides and affinity chromatography, we prepared a phosphorylation state-specific antibody to the Olig2 triple serine motif. Specificity of this antibody preparation was validated by western blot analysis of cells transduced with wild-type or phospho-null variants of Olig2 (Fig. 2A) and also by peptide competition western blots (Fig. S5).

Using this antibody, we examined the phosphorylation state of endogenous Olig2 in developing mouse embryos. Spinal cord is an anatomically simple region of the CNS where the bifunctionality of Olig2 has been clearly documented. As indicated (Fig. 2B) the phosphorylation state of Olig2 undergoes a dramatic decrease as proliferating *Olig2*-positive progenitors in the embryo mature into terminally differentiated, myelinating oligodendrocytes of the postnatal spinal cord. Developmental regulation of Olig2 phosphorylation can also be observed *in vitro* when cycling progenitor cells are plated in factor-free medium and allowed to differentiate (Fig. 2C). In cell culture, it

FIGURE 1. **Triple serine phosphorylation motif in the N-terminus of Olig2 is required for proliferation of neural progenitor cells. (A)** Four phosphorylation sites were identified in the N-terminus of Olig2 by mass spectroscopy. Three serine sites are in a tight cluster in the N-terminus. **(B)** We created a panel of single and multiple mutants of the phosphorylation sites. *Olig2*-null neural progenitor cells were transduced with each construct of *Olig2* via retroviral infection. Secondary neurosphere assays were performed. Each construct was compared to *Olig2* WT and total viable cell population was used as an index for measuring neurosphere proliferative ability. **(C)** Representative neurospheres generated from cells transduced with control vector (EGFP), *Olig2* WT, *Olig2* TPN (triple phospho-null), and *Olig2* TPM (triple phospho-mimetic) reveal size differences. **(D)** Secondary neurosphere numbers were compared. Transduced cells were plated in 6-well plate at 10 cells/μl (2 ml total volume) in EGF (20ng/ml) and bFGF (20ng/ml) containing medium. 7 days later neurospheres from each well were counted using a dissection microscope. ***, One-way ANOVA, $p>0.05$. NS, neurosphere; error bars, SEM. **(E)** Total viable cell population was compared. One-way ANOVA and posthoc Newman-Keuls test, $p<0.001$; error bars, SD. **(F)** Neurosphere sizes were measured with ImageJ software and areas were compared. One-way ANOVA and posthoc Newman-Keuls test, $p<0.01$; NS, neurosphere; error bars, SEM. See also Figs. S1, S2 and S4.

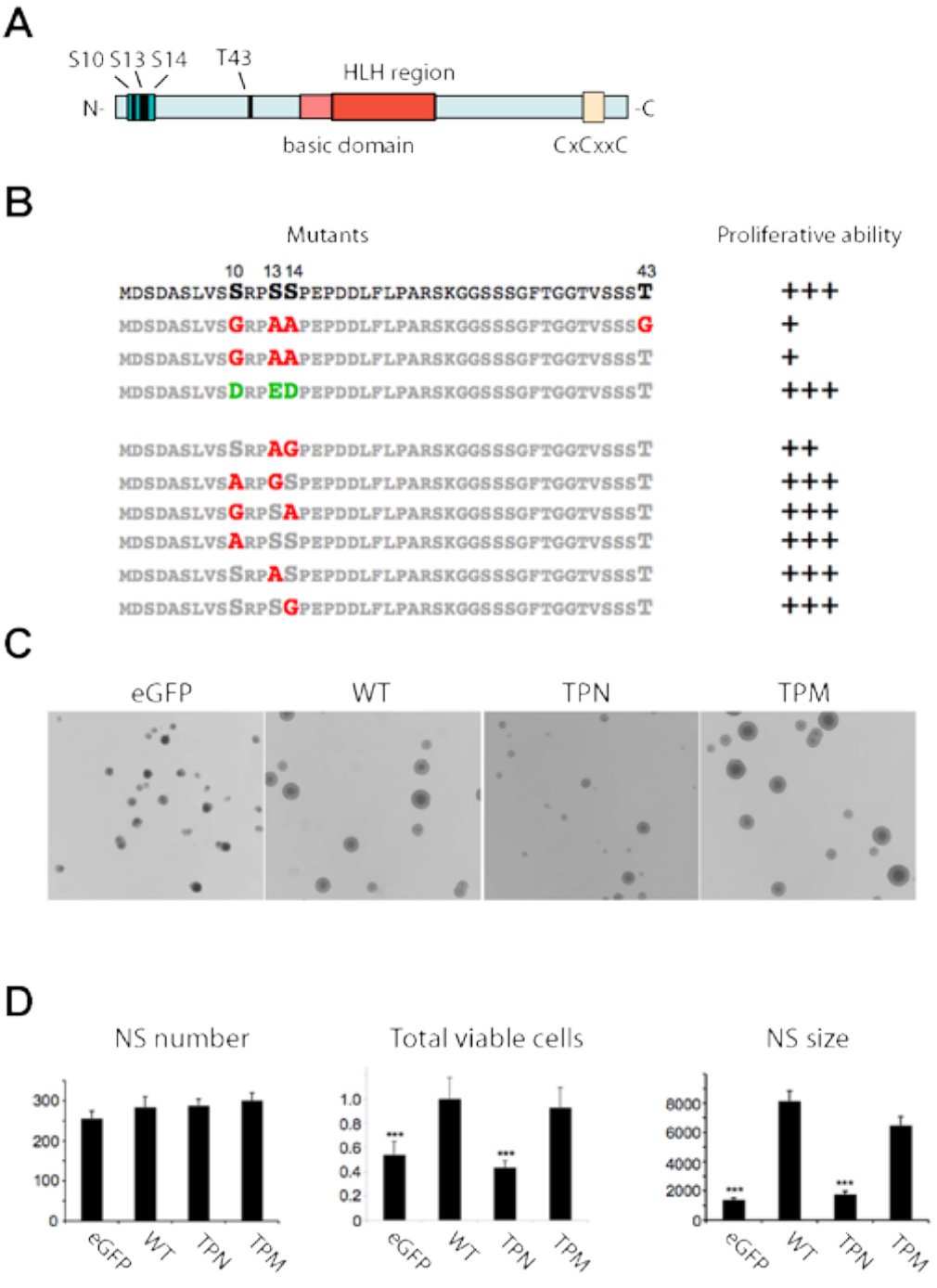
A
S10 S13 S14
T43
HLH region
N-
-C
basic domain
CxCxxC
B
Mutants
Proliferative ability
10 13 14 43
MDSDASLVSSRPSSPEPDDLFLPARSKGGSSSGFTGGTVSSST +++
MDSDASLVSGRPAAPEPDDLFLPARSKGGSSSGFTGGTVSSSG +
MDSDASLVSGRPAAPEPDDLFLPARSKGGSSSGFTGGTVSSST +
MDSDASLVSDRPEDPEPDDLFLPARSKGGSSSGFTGGTVSSST +++
MDSDASLVSSRPAGPEPDDLFLPARSKGGSSSGFTGGTVSSST ++
MDSDASLVSARPGSPEPDDLFLPARSKGGSSSGFTGGTVSSST +++
MDSDASLVSGRPSAPEPDDLFLPARSKGGSSSGFTGGTVSSST +++
MDSDASLVSARPSSPEPDDLFLPARSKGGSSSGFTGGTVSSST +++
MDSDASLVSSRPASPEPDDLFLPARSKGGSSSGFTGGTVSSST +++
MDSDASLVSSRPSGPEPDDLFLPARSKGGSSSGFTGGTVSSST +++
C
eGFP
WT
TPN
TPM
D
NS number
Total viable cells
NS size
300
200
100
0
1.0
0.8
0.6
0.4
0.2
0
8000
6000
4000
2000
0
***
eGFP
WT
TPN
TPM

is possible to conduct pulse labeling experiments with ^{32}P and these experiments indicate that the developmentally regulated decline of phosphorylated Olig2 reflects diminished activity of an Olig2 protein kinase(s) (Fig. 2D). Together these data indicate that the triple phosphorylation of Olig2 is correlated with proliferation of neural progenitor cells and is much diminished after differentiation.

Phosphorylation of Olig2 is dispensable for specification of oligodendrocytes

Targeted disruption of *Olig2* results in nearly complete ablation of the oligodendrocyte lineage *in vivo* and *in vitro* (Lu et al., 2002; Zhou and Anderson, 2002). As shown in Figs. 3A and 3B, the ability of *Olig2-null* progenitors to develop into O4-positive cells can be rescued by lentiviral transduction of wild-type *Olig2*; however, unlike the case with secondary neurosphere assays (Fig. 1) the TPN and TPM variants of Olig2 are equipotent to WT Olig2 for this developmental function (Figs. 3C and 3D).

We conclude that phosphorylation of Olig2 is dispensable for specification of oligodendrocyte lineage cells. These results do not rule out the possibility that phospho-mimetic Olig2 might antagonize oligodendrocyte differentiation *in vivo*.

Phosphorylation state of the Olig2 triple serine motif correlates with oncogenic potential

Olig2 is expressed in 100% of the human diffuse gliomas irrespective of grade (Ligon et al., 2004). Beyond merely marking malignant gliomas, *Olig2* expression is required for intracranial tumor formation in a genetically relevant model of malignant glioma (Ligon et al., 2007). In this model, neural progenitor cells from *p16*^{Ink4a}/*p19*^{Arf}-null mice are transduced with the mutated, constitutively active *EgfrvIII* variant of the epidermal growth factor receptor (Bachoo et al., 2002). These genetically engineered "tumor neurospheres" recapitulate two stereotypical genetic lesions that drive a high percentage of human gliomas (Kleihues and Cavenee, 2007; Network, 2008).

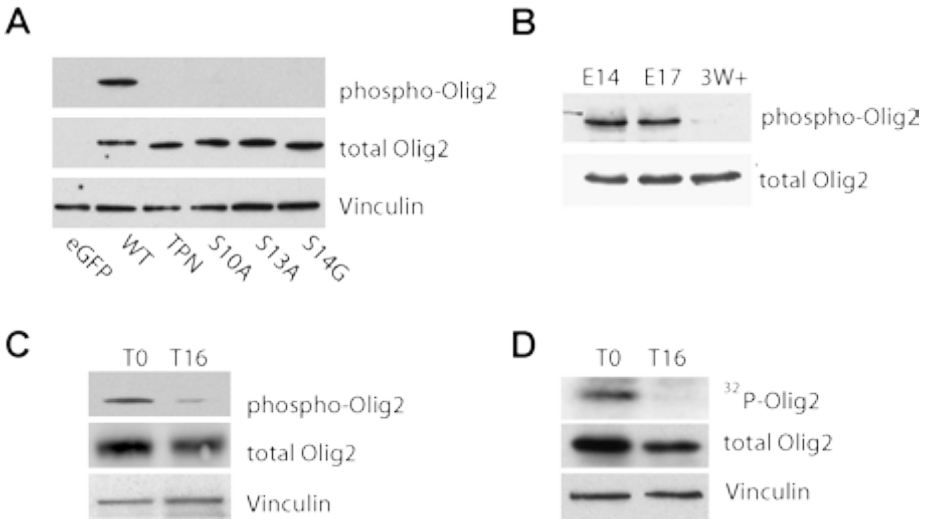

FIGURE 2. **Triple serine phosphorylation state in Olig2 is regulated developmentally. (A)** Olig2 phospho-specific antibody detects phosphorylation in wild-type *Olig2* but not in triple phosphomutant or any single serine mutant. *Olig2*-null neural progenitor cells bearing different *Olig2* phosphorylation mutants were lysed and the state of phosphorylation at Ser10, Ser13 and Ser14 was analyzed by western blot using phospho-specific Olig2 antibody. The blot was then stripped and reprobed with polyclonal antibody to total Olig2. **(B)** Olig2 triple serine phosphorylation state decreases with increasing developmental stage of spinal cord. Whole spinal cords were dissected from E15, E17 embryos and P23-25 CD1 mice. Protein lysates (40 μg) in RIPA buffer were loaded for immunoblotting, probed for phospho-Olig2 antibody, and then reprobed with a monoclonal Olig2 antibody. **(C)** Triple serine phosphorylation decreased as neurospheres are allowed to become adherent and differentiate in growth-factor free medium. *Olig2* WT neurospheres were rinsed once with ice-cold PBS medium and then plated in B27 containing medium in poly-l-ornithine coated plates. 16 hours later, cell lysates were collected and compared to undifferentiated neurosphere lysate (T0) by western blot. **(D)** ^{32}P-pulse labeling of neurospheres in the presence (T0) or absence of Egf and Fgf. No ^{32}P incorporation in Olig2 is observed after overnight differentiation (16 hours). Autoradiogram (phosphorylated Olig2), and western blot, total Olig2 and vinculin loading control. See also Fig. S5.

As indicated in Fig. 4, the malignant potential of *Olig2*-null tumor neurospheres is much impaired. Even when a high number (~10^5) of *Olig2*-null tumor neurospheres are inoculated into the brain, tumor penetrance is low and latency is long. Tumor formation is rescued by transduction of wild-type Olig2 and the two Olig2 variants; however endpoint dilution experiments reveal a phosphorylation-dependent differential in the malignant phenotype. Relative to wild-type Olig2, both the lag time to tumor development and the minimum

FIGURE 3. **Triple serine phosphorylation in Olig2 is negligible in specification of oligodendrocytes.** **(A)** Olig2 is required for the generation of O4 positive oligodendrocytes. Neural progenitor cells were isolated from the E12 LGE region, plated at clonal density and cultured in Fgf containing medium. Cells were stained with antibody to total Olig2 or O4 at day 7. Scale bar, 100 μm. **(B)** The frequency of O4 positive cells was compared among *Olig2*+/+, *Olig2*+/–, and *Olig2*-null embryos (***, ANOVA and posthoc Newman-Keuls test, $p<0.0001$; three embryos for each genotype; error bars, SEM; ND, none detected). **(C)** Triple serine phospho-null, phospho-mimetic and *Olig2* WT reveal similar abilities in rescuing O4 positive cells. Lentivirus bearing WT, TPN or TPM was used to infect *Olig2*-null E12 LGE progenitor cells at MOI 1:1. Cells were analyzed at day 9–10. Scale bar, 100μm. **(D)** The ratios of O4 positive cells among the infected cells (identified with either GFP or Olig2 staining) were compared (**, ANOVA and posthoc Newman-Keuls test, $p<0.001$; N=3 independent experiments; ND, none detected; error bars, SEM).

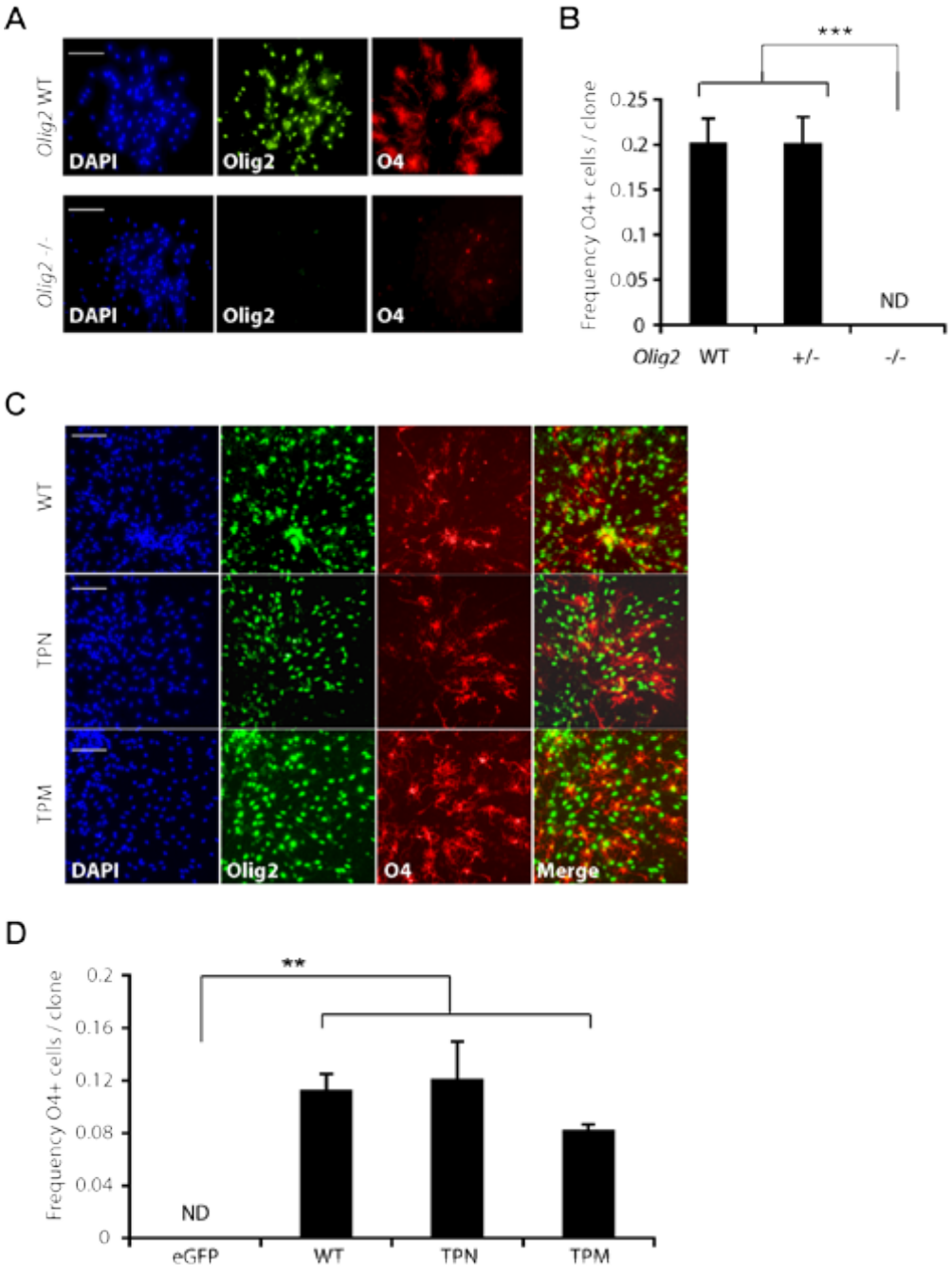
A
Olig2 WT
DAPI
Olig2
O4
Olig2 -/-
DAPI
Olig2
O4
B
***
Frequency O4+ cells / clone
0.25
0.2
0.15
0.1
0.05
0
ND
Olig2 WT
+/-
-/-
C
WT
TPN
TPM
DAPI
Olig2
O4
Merge
D
**
Frequency O4+ cells / clone
0.2
0.16
0.12
0.08
0.04
0
ND
eGFP
WT
TPN
TPM

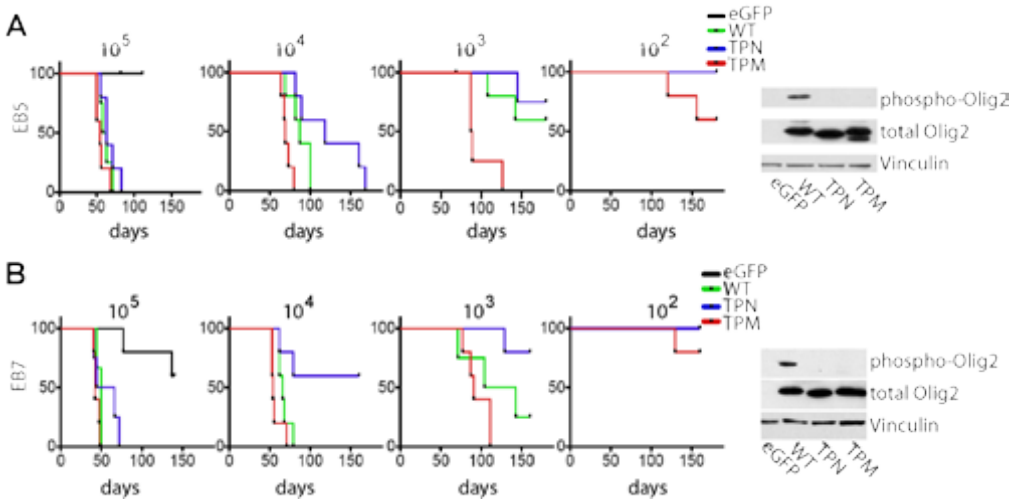

FIGURE 4. **Phosphorylation state of the Olig2 triple serine motif correlates with oncogenic potential.** **(A)** *p16*^{Ink4a}*/p19*^{Arf}*/Olig2*-null *Egfrviii* murine neural progenitor cell line EB5 was stably transduced with EGFP, *Olig2* WT, *Olig2* TPN ,or *Olig2* TPM via retroviral infection. Tumorigenic potential of each line was compared using a limiting dilution assay. For each construct, 10^5, 10^4, 10^3, or 10^2 dissociated neural progenitor cells were injected intracranially and the survival of each mouse was recorded (for the EGFP control group, 10^5 were injected). Right Panel: Expression levels of each *Olig2* construct in the EB5 line were examined by western blot for phosphorylated Olig2 and total Olig2. Vinculin expression was used as a loading control. **(B)** Same as A but with another independently derived *p16*^{Ink4a}*/p19*^{Arf}*/Olig2*-null *EGFRVIII* murine neural progenitor cell line, EB7.

inoculum of tumor cells required for tumor formation are increased with the phospho-null form of Olig2. Conversely, the phospho-mimetic form of Olig2 is more tumorigenic than either wild-type or phospho-null Olig2.

What about human gliomas? While technically impractical to assess the function of Olig2 phosphorylation in the human tumors, we did use our phosphospecific antibody to interrogate Olig2 phosphorylation state within six human glioma neurosphere cultures. As reference points, we used Olig2 from cycling mouse neurosphere cultures and from terminally differentiated oligodendrocytes in the mouse corpus callosum. As indicated (Fig. 5) the phosphorylation state of Olig2 was analogous to that of cycling murine progenitor cells rather than corpus callosum for five out of the six lines tested.

Interestingly, the exception (1/6 lines tested) was a *p53*-null tumor cell line. In other studies, we have found an intrinsic oppositional relationship between Olig2 and p53 (Mehta et al., 2011), such that Olig2 function (and presumably phos-

phorylation) is irrelevant in a *p53*-null context. Together, these findings indicate that Olig2 phosphorylation at the serine triple motif is present in human glioma and regulates tumor growth in a genetically relevant mouse orthotopic model.

Olig2 phosphorylation state regulates p53 function

What is the molecular mechanism that links Olig2 phosphorylation to neurosphere growth and formation of malignant gliomas? A companion paper by Mehta *et al*. describes an intrinsic oppositional relationship between Olig2 and p53 (Mehta, 2011). Put briefly, Mehta *et al*. show that expression of Olig2 suppresses the post- translational acetylation of p53, which is known to be required for optimum transcriptional functions (Barlev et al., 2001; Dornan et al., 2003). Concurrent with hypoacetylation, the interactions of p53 with promoter/enhancer elements of its stereotypical target genes (e.g. *p21,.Bax*, *Mdm2*) are much attenuated in wild-type neural progenitors relative to their *Olig2*-null counterparts. Accordingly, p53-mediated biological responses to genotoxic damage are suppressed by Olig2.

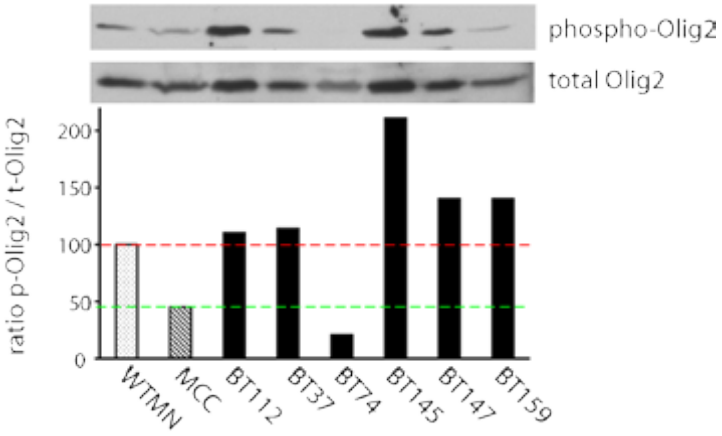

FIGURE 5. **Phosphorylation of Olig2 in human glioma cell lines.** Several human glioma cell lines were examined for their levels of Olig2 phosphorylation using the phosphorylation state specific antibody by western blot. WTMN, wild-type mouse neurospheres; MCC, mouse corpus callosum; BT, brain tumor cell line. Western blots were quantitated using a Typhoon Imaging System, and values in the graph are representative of three independent repeats. BT74 denotes the only human tumor cell line in this study that harbors a mutant form of p53.

Experiments summarized in Fig. 6 show that this oppositional relationship between Olig2 and p53 is regulated by the phosphorylation state of the triple serine motif. Wild-type and also phospho-mimetic Olig2, suppress the radiation-induced increase in both total p53 (Fig. 6A) and acetylated p53 (Fig. 6B). Likewise, wild-type and phospho-mimetic Olig2, suppress radiation-induced expression of the canonical p53 target gene p21 (Fig. 6C insert). Concurrent with suppression of p21 expression, Olig2 WT and TPM promote the survival of irradiated neural progenitors as noted by Mehta et al (Fig. 6C). In marked contrast, Olig2 TPN is deficient in all of these functions.

In previous studies, we have shown that basal levels of *p21* expression seen in cycling neural progenitor cells are also suppressed by Olig2 (Ligon et al., 2007). As shown in Fig. 7A (inset), Olig2 WT and TPM suppress basal levels of p21 protein while Olig2 TPN shows little or no effect. The phospho-Olig2 mediated suppression of p21 protein is exerted largely at transcriptional level, as indicated by diminished expression of *p21* MRNA (Fig. 7A).

Expression of a p21 luciferase reporter gene is likewise controlled by Olig2 in a phosphorylation state-dependent manner (Supplementary Fig. 6). This suppression of basal state p21 MRNA reflects, at least in part, phospho-Olig2 regulated changes in the amount of p53 that is associated with promoter/enhancer elements of the *p21* gene (Fig. 7B). The differential loading of p53 onto p21 promoter enhancer element is nuanced but statistically significant and also in good accord with the basal state levels of acetylated p53 seen in Fig. 6B.

On a final note, the phosphorylation state dependent effects of Olig2 on neurosphere proliferation noted in Fig. 1 are completely dependent on p53 status. As seen in Figs. 7C and 7D the phosphorylation state of Olig2 is irrelevant in p53-null neurospheres—at least with respect to cell proliferation. Collectively these data show that p53 is a significant target of phosphorylated Olig2 in neural progenitors.

Discussion

The BHLH transcription factor Olig2 is expressed in multipotent progenitors of the embryonic brain (Petryniak et al., 2007) and in the postnatal brain within cell types that span a biological continuum from rapidly cycling neural progen-

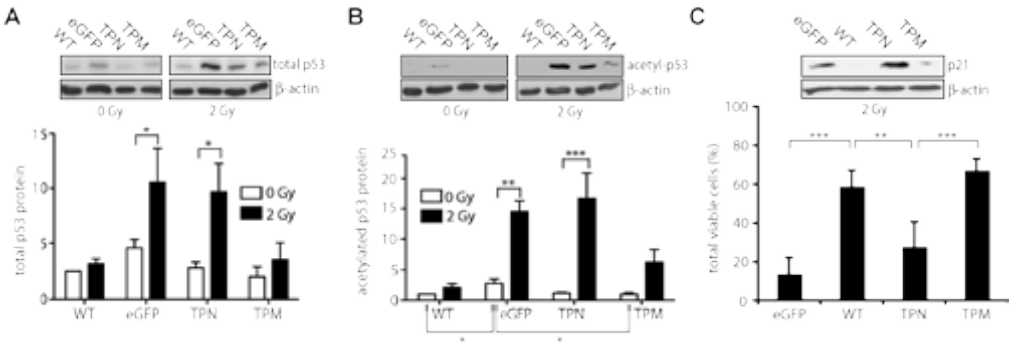

FIGURE 6. **Wild-type and phospho-mimetic Olig2 suppress radiation-induced p53 responses. (A)** Phosphorylation state of Olig2 affects DNA-damage induced accumulation of p53 protein. *Olig2*-null mouse neural progenitor cells were stably transduced with a vector control (EGFP) or with *Olig2* WT, *Olig2* TPN or TPM as indicated. Cells were either untreated or treated with 2Gy of IR and lysates were obtained in presence of Hdac inhibitor, size fractionated and immunoblotted with antibodies recognizing p53 or beta-actin. The experiments were repeated a total of five times. The resulting immunoblots (inset) were normalized for beta-actin and quantified (bar graphs). As indicated, wild-type and also phospho-mimetic Olig2 suppress radiation-induced changes in total p53 but phospho-null Olig2 is without effect (p value: *<0.01, two-way ANOVA and Bonferroni post hoc test). In non-irradiated cells (white bars) the differences in total p53 between the four experimental groups did not approach the level of statistical significance. **(B)** Phosphorylation state of Olig2 affects DNA-damage induced acetylation of p53 protein. Same as panel A above except that cell lysates immunoblotted with antibodies recognizing acetylated p53 (Lys379) or beta-actin. Again, wild-type and phospho-mimetic Olig2 suppress radiation-induced changes in acetylated p53, while phospho-null Olig2 is without effect (p value: *<0.01). Relative to vector controls, wild-type and phospho-mimetic Olig2 create a small, but significant, suppression of acetylated p53 in non-irradiated cells (white bars). (p values: *<0.05, ** <0.01, *** <0.001, two-way ANOVA and Bonferroni post hoc test). **(C)** Inset: Phosphorylation state of Olig2 dictates p21 expression level and cell survival following gamma irradiation. Cells were irradiated with 2 Gy IR. Endogenous p21 expression levels were compared by western blot with beta-actin as a loading control. Bar graph shows relative cell growth after 2Gy irradiation. Total viable cells are defined as the percentage of viable cells 4–5 days after treatment compared to no treatment groups. Data presented are from three independent experiments; error bar, SD. One-way ANOVA, p<0.001, and posthoc Newman-Keuls test, ** = p<0.01; *** = p<0.001.

itors (e.g. type C cells, NG2 cells) to terminally differentiated, myelinating oligodendrocytes (Jackson et al., 2006; Ligon et al., 2006; Lu et al., 2000; Menn et al., 2006; Takebayashi et al., 2000; Zhou et al., 2000). How are the transcriptional functions of Olig2 modulated to suit these divergent biological contexts? We show here that a developmentally regulated phospho-serine motif in the amino terminus is essential for Olig2 proliferative function in both normal and

FIGURE 7. **An oppositional relationship between Olig2 and p53 in cycling neural progenitors. (A)** Endogenous p21 protein (inset) and mRNA (bar graphs) are suppressed by wild-type and phospho-mimetic Olig2 in cycling neural progenitors. *Olig2*-null mouse neural progenitor cells were stably transduced with vector control (eGFP), WT, TPN or TPM. Endogenous protein levels were compared by western blotting with p21 antibody and beta-actin as control. RNA was extracted from cells as described above, and p21 mRNA levels were quantified using premade p21 Taqman gene expression assay. **(B)** Expression of *p21* in cycling neural progenitors correlates with p53 loading on promoter/enhancer elements of the *p21* promoter. Lysates of *Olig2*-null mouse neural progenitor cells stably transduced with vector control (eGFP), WT, TPN or TPM were processed for chromatin immunoprecipitation with p53 antibody. Primers spanning the distal E-box in the *p21* promoter/enhancer region were used for qRT-PCR analysis. Bar graph shows *p21* promoter binding normalized for non-target site enrichment. Note that the differences in p53 loading, between the four groups, though nuanced, are statistically significant (p values: ** <0.001, *** <0.0001) and in good accord with differences noted in acetylated p53 seen in cycling cells (Fig. 7B). **(C)** Phosphorylation state of Olig2 is irrelevant in *p53*-null neurospheres. *Olig2* cre/cre mice were intercrossed to *p53*fl/fl mice to obtain neural progenitors that were *Olig2*/*p53*-null. These progenitors were transduced with eGFP, wild-type *Olig2* or the triple phospho-null mutant of *Olig2* as indicated. Secondary neurosphere assays were performed on these cells and on matched *p53* +/+ controls as per Fig. 1.

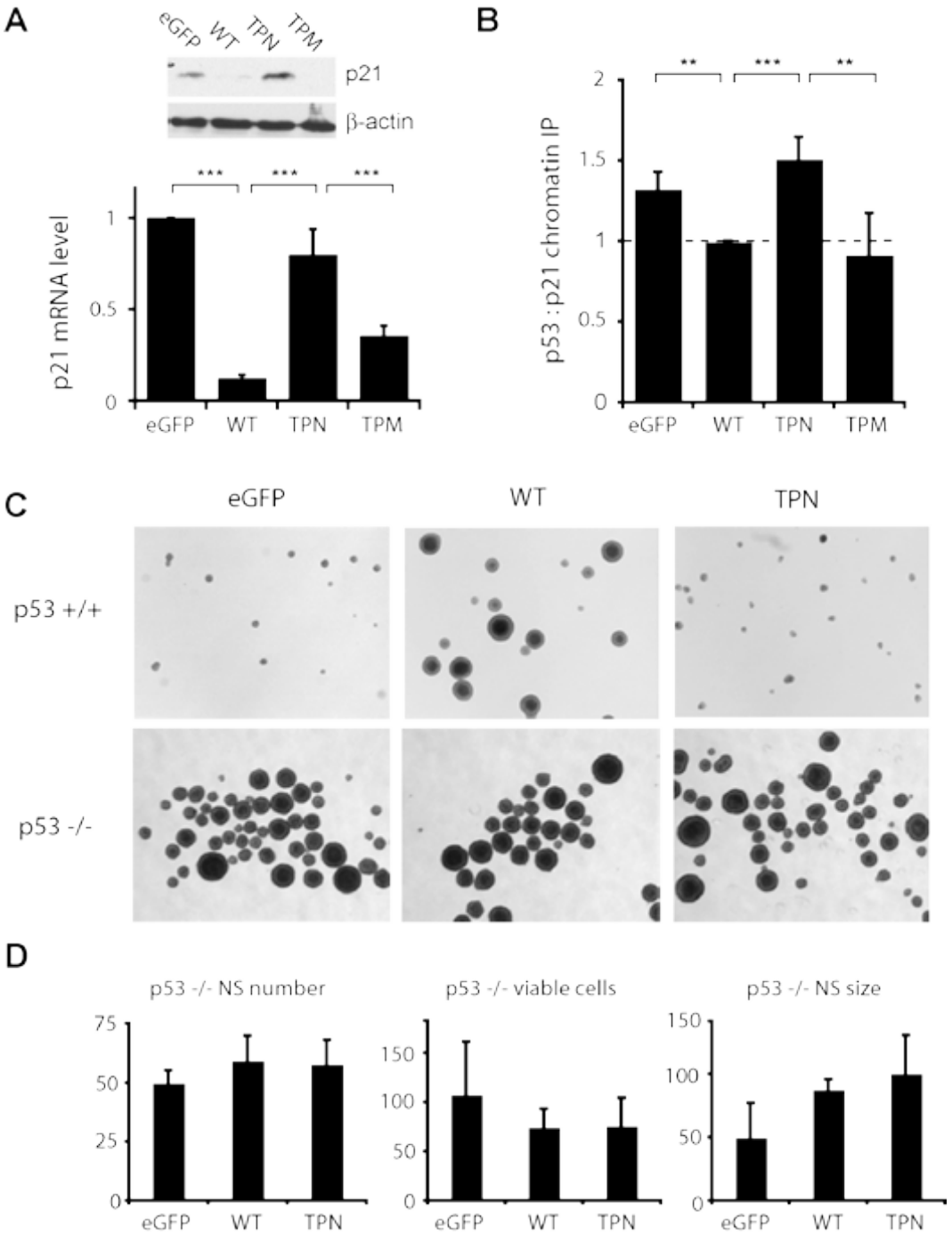
A
eGFP
WT
TPN
TPM
p21
β-actin
p21 mRNA level
***
***
***
1
0.5
0
eGFP
WT
TPN
TPM
B
p53 : p21 chromatin IP
**
***
**
2
1.5
1
0.5
0
eGFP
WT
TPN
TPM
C
eGFP
WT
TPN
p53 +/+
p53 -/-
D
p53 -/- NS number
75
50
25
0
eGFP
WT
TPN
p53 -/- viable cells
150
100
50
0
eGFP
WT
TPN
p53 -/- NS size
150
100
50
0
eGFP
WT
TPN

malignant neural progenitors. On a mechanistic level, the pro mitotic activity of this triple serine motif appears to reflect a suppression of p53 functions. In contrast to proliferative functions, specification and terminal differentiation of oligodendrocytes are completely independent of Olig2 triple serine phosphorylation state. In the fullness of time, the ability to uncouple proliferative and developmental functions of Olig2 may thus practical applications in glioma medicine. In the interim, the observations summarized here raise several interesting and unresolved scientific questions.

Are there other physiologically-relevant phosphorylation sites on Olig2?

Computer algorithms reveal a number of potential phosphorylation sites on Olig2 (Fig. S1A). To determine which, if any, of these potential sites are actually utilized in neural stem cells, we developed a simple two-step protocol to purify microgram quantities of endogenous Olig2 from human glioma and murine neurosphere cultures. For comparative purposes, we also purified ectopic Olig2 from COS7 cells transfected with a human *Olig2* expression vector. Only a subset of the potential Olig2 phosphorylation sites catalogued are actually detected in these cells. Four amino acid residues, Ser10, Ser14, Ser14 and Thr43 scored as "high confidence" phosphorylation sites in all three of the cell types we examined.

It is possible that a small percentage of the Olig2 protein, below the detection limits of our mass spectroscopic analysis, is phosphorylated at other positions in biologically relevant cell contexts. This caveat must be considered in particular for potential phosphorylation motifs in the carboxyl terminal domain of Olig2 where proteolytic digestion sites are rather sparse. That said, we actually did detect a high confidence phosphorylation site in the carboxyl terminus (Ser263) in ectopic Olig2 purified from transfected COS7 cells (data not shown). Another phosphoserine residue was found at Ser81 in the "ST box" of COS7 cell-purified Olig2 (see below). However, we find no evidence that Ser81 or Ser263 are phosphorylated on the endogenous Olig2 protein expressed in neural cell types. As previously reported, a considerable fraction of ectopic Olig2 in transfected COS7 cells is mislocalized to the cytosol (Sun et al., 2003). The level of ectopic Olig2 generated by COS7 cell expression vectors is so high that we did

not need to use isolated nuclei as a source of starting material for our protein preparations and instead extracted both nuclear and cytosolic Olig2. For these reasons, we are inclined to regard the Ser81 and Ser263 phosphorylation events as cytosol-specific artifacts of the cos7 cell system.

Setoguchi and Kondo have suggested (on the basis of *in vitro* phosphorylation studies) that Akt-mediated phosphorylation of Ser30 causes Olig2 to relocalize from the nucleus to the cytosol where it is subsequently degraded to allow formation of astrocytes from neural progenitor cells (Setoguchi and Kondo, 2004). We did not detect any evidence of Ser30 phosphorylation in nuclear extracts of the neural cell types we studied. However, Ser30 was detected as a low confidence phosphorylation site in cos7 cell extracts. The detection of low levels of phospho Ser30 in our mass spectroscopy analysis of cos7 cell Olig2 may have been enabled by the large amounts of cytosolic Olig2 in the cos7 cell preparations and would thus be consistent with a degradative role of Ser30 as suggested by Setoguchi and Kondo (Setoguchi and Kondo, 2004) (but see below).

Developmental regulation of replication competence by Olig2 in the CNS

In this study we have focused on evolving functions of Olig2 in multipotent progenitors of the developing forebrain and in myelinating oligodendrocytes of the post-natal brain. However, in the developing spinal cord, *Olig2* is expressed initially in the pMN domain where it functions at early times to sustain the replication competent state of those pMN progenitors that give rise to oligodendrocytes (Lee et al., 2005). Olig2 function is also required for neural patterning and specification of motor neurons and oligodendrocyte progenitors (Lu et al., 2002; Novitch et al., 2001; Park et al., 2002; Takebayashi et al., 2002; Zhou and Anderson, 2002). So, might phosphorylation of the Olig2 triple serine motif also be responsible for the developmental switch from pMN progenitor proliferation to cell fate specification in the embryo? The answer to this question may be complex. Indeed, *Olig2*-null animals show no obvious proliferation phenotype in spinal cord or brain (Lu et al., 2002; Novitch et al., 2001; Park et al., 2002; Takebayashi et al., 2002; Zhou and Anderson, 2002). This lack of a proliferation phenotype is most probably accounted for by the dramatic changes in

neural patterning in *Olig2*-null embryos, whereby the pMN domain is re-specified to p2 fate, coupled with the fact that the p2 domain contains independent mechanisms for cell cycle regulation capable of supporting similar levels of progenitor proliferation. Further work using knock-in mutants of phospho-null *Olig2* is therefore required to investigate possible roles for Olig2 in embryonic progenitor proliferation and such studies are in progress.

Regulation of p53 functions by the triple serine motif

In a companion paper, Mehta et al show that Olig2 suppresses radiation-induced functions of p53 in both normal and malignant neural progenitors (Mehta, 2011). We show here that this intrinsic oppositional relationship between Olig2 and p53 is regulated by the Olig2 triple serine motif. Wild-type and also phospho-mimetic Olig2 suppress the classic radiation-induced accumulation of p53 protein whereas Olig2 TPN is permissive for this response (Fig. 6A). We have generated cRNA expression profiles on Olig2 wild-type, Olig2-null, Olig2 phospho-null and Olig2 phospho-mimetic neurospheres. These profiles reveal no impact of Olig2 proteins on the level of p53 mRNA levels (data not shown). Rather, it appears that Olig2 WT and TPM suppress radiation-induced post-translational acetylation events that enhance both the stability (Li et al., 2002) and the transcriptional functions (Barlev et al., 2001) of p53 (Fig. 6B).

In addition to their guardian functions in response to genotoxic damage, p53 and p21 are known to regulate the proliferation of normal neural progenitors (Kippin et al., 2005; Meletis et al., 2006). As shown in Fig. 7, wild-type and phospho-mimetic Olig2 suppress basal expression of p21 protein and mRNA in cycling cells. These effects are reflected, at least in part, by diminished levels of p53 protein associated with promoter/enhancer elements of the *p21* gene. However, the pronounced impact of Olig2 phosphorylation on expression of p21 protein and mRNA (Fig. 8A) stands somewhat in contrast to the more nuanced differences in total p53 bound to *p21* promoter/enhancer elements (Fig. 7B). Expression of p21 protein and mRNA is likely to reflect the cumulative impact of reduced p53 recruitment to the p21 promoter, reduced transcriptional function of hypoacetylated p53 at the promoter (Barlev et al., 2001) and possible post transcriptional effects on stability of the p21 protein (Coleman et al., 2003;

Gong et al., 2003). In addition, we have shown in previous studies have shown that Olig2 can interact directly with the promoter/enhancer elements of *p21* (Ligon et al., 2007). Since Olig2 has been characterized as a transcription repressor (Novitch et al., 2001; Zhou et al., 2001) it is possible that the attenuation of p53 transcriptional functions are further augmented by direct Olig2-mediated suppression of *p21* expression (however, see below). Notwithstanding the complexity of p21 regulatory mechanisms, the experiment summarized in Figs. 7C and D show clearly that p53 is a prime target of the Olig2 proliferative phenotype.

Regulation of Olig2 functions by the triple serine motif

How does phosphorylation of the triple serine motif affect transcriptional functions of Olig2? Members of the bHLH transcription factor family function as homodimers or as heterodimers with E12/E47 proteins to bind to canonical E-box elements in the promoter/enhancer regions of their target genes (Ross et al., 2003). The bHLH motif is almost exclusively responsible for both heterodimerization and DNA targeting to the E-box. It seems unlikely that phosphorylation events in the amino terminus would have any direct affect on these functions of Olig2 and preliminary chromatin immuneprecipitation studies failed to show changes in Olig2 : p21 targeting that could account for the effects on basal p21 expression of p21 seen in Fig. 8A.

The fact that all three serine residues at positions 10, 13 and 14 must be mutated to achieve a strong loss-of-function or gain-of-function phenotype suggests that the proliferative function associated with the Olig2 phosphorylation state involves a significant conformational change in the amino terminus of Olig2. This conformational change could affect the interaction of Olig2 with DNA or important co-regulator proteins and thus affect the transcriptional activity of Olig2 upon target genes that affect p53 function. One final possibility that cannot be ruled out by the data is that the p53 antagonist function of Olig2 is independent of its function as a bHLH transcription factor. It is possible, for example, that phosphorylated Olig2 competes directly with p53 for binding to proteins that promote p53 acetylation or prevent its deacetylation. In fact, preliminary observations of Mehta et al suggest such a mechanism (Mehta et al., 2011).

Phosphorylation state of Olig2 and malignant potential

In a murine model of primary glioma, the tumor penetrance is quite low and latency is prolonged in the absence of *Olig2* expression (Fig. 4 and also Ligon et al 2007). A forced phospho-mimetic Olig2 state actually enhances intracranial tumor formation relative to wild-type Olig2. We speculate that the enhanced performance of the phospho-mimetic Olig2 relative to the wild-type protein *in vivo* reflects the fact that some of the implanted cells expressing wild-type *Olig2* undergo differentiation with attendant dephosphorylation, whereas the mutant form of *Olig2* is locked into a phosphomimetic configuration.

An unexplained feature of the limiting dilution assays for tumor growth (Fig. 4) is that Olig2 TPN, though clearly inferior to WT and TPM, is able to support tumor growth when large numbers of cells are transplanted. Based on the p21 suppression results, particularly the inability of the TPN mutant form of Olig2 to suppress p21, one might predict that phospho-null Olig2 would be completely non-tumorigenic. How does one account for the residual tumorigenic potential of Olig2 TPN? In a companion paper to this one, Mehta et al. show that the major role of Olig2 in promoting intracranial tumor formation is to suppress the functions of p53 (Mehta, 2011). However, these authors also noted a somewhat nuanced p53-independent function(s) of Olig2 in tumor formation. It is possible that the p53-independent functions of Olig2 in tumor formation noted by Mehta et al are likewise independent of phosphorylation state.

The triple serine motif as a drug target for malignant glioma

Chemical tool compounds and hairpin RNA expression vectors, used in combination with our phospho-specific antibody (Fig. 2) should ultimately lead to identification of protein kinases that regulate the phosphorylation state of Ser10, Ser13 and Ser14. Phosphorylation modeling programs such as Scansite, GPS and PredPhospho as well as direct evaluation yields some overlapping predictions for kinase candidates, but also different predictions for each of the three serine residues. Among the best represented predictions are Cdk5, Erk kinases (Erk1/2, Mapk), Gsk3 and casein kinases (Ck1/2). In neurosphere proliferation assays, we were unable to narrow the phenotype of TPN Olig2

down to a single serine site, which argues against the existence of a priming site. However an intramolecular cascade may be operative if Gsk3 acts at Ser10 as predicted by the computer algorithms. Gsk3 would require prephosphorylation of Ser14 to create the motif S/TxxxpS/pT. Likewise, phosphorylation of Ser13 is prerequisite for Ck2 to phosphorylate Ser10 (Phosphomotif, www.hprd.org).

Olig2 is a lineage-restricted regulatory transcription factor whose expression is confined to the CNS. The expression pattern of *Olig2* in human tissue microarrays (Ligon et al., 2004), combined with mouse modeling studies of human glioma (Ligon et al., 2007), have suggested to us that a small molecule inhibitor of Olig2 might serve as a targeted therapeutic for a wide range of pediatric and adult gliomas. However, an anti-tumor therapy that generally targets all Olig2 activity in the brain (e.g., by shRNA) would likely have detrimental, off-target effects in non-tumor cells such as oligodendrocytes potentially limiting tolerance/utility. Moreover, transcription factors are generally considered unattractive targets for drug development because their interactions with DNA and with co-regulator proteins involve large and complex surface area contacts.

In contrast to transcription factors, protein kinases lend themselves readily to the development of potent and specific small molecule inhibitors. Our studies indicate that Olig2 functions critical for glioma growth (Fig. 4) and radiation resistance (Fig. 6) but not development (Fig. 3) are distinguished by the triple serine phosphorylation. The ability to uncouple these functions one from the other suggests an avenue to specifically target Olig2-dependent tumors within the brain while sparing normal white matter. In the fullness of time, small molecule inhibitors of Olig2 protein kinases could have practical overtones for patients with glioma, and provide a more specific means of therapy with minimized off-target effects in oligodendrocytes.

Methods

Animal procedures

Animal husbandry was performed according to DFCI and UCSF guidelines under IACUC-approved protocols for all experiments reported. The strains used have

been described previously (Lu et al., 2002; Schuller et al., 2008). *Shiverer* mice were obtained from Jackson Laboratory. Neural progenitor cells were isolated from lateral ganglionic eminence (LGE) of E12-E14 embryos from time-pregnant mice using techniques previously described (Qian et al., 1998).

Neurosphere culture

For neurosphere culture, dissociated single cells were cultured at 10 or 20 cells μl^{-1} into poly (2-hydrocyethylmethacrylate, Sigma) coated plates in serum-free medium containing B27 (Stemcell Technology), N2 (Invitrogen), Fgf (Millipore) 20ng ml^{-1}, Egf (Millipore) 20ng ml^{-1}. (Ligon et al., 2007) Neurospheres were fed every three days and passaged every 7–8 days. For neurosphere differentiation experiments, neurospheres were collected and rinsed with ice-cold PBS, then plated onto poly-l-ornithine coated plates in serum-free medium without Fgf and Egf. O4 cell generation assay was performed using dissociated neural progenitor cells (single cell suspension) and plating into poly-l-ornithine coated plates in serum free medium containing bFGF (10ng ml^{-1}) at 4000 cells per well of a 24-well culture plate. Lentivirus bearing various mutants of *Olig2* was applied to the cultures the next day at an MOI of 1:1. Media was refreshed every three days. 7–10 days later, cells were incubated with anti-O4 IgM antibody (gift from Dr. Tim Vartanian) at 1:5 dilution for 30 minutes then fixed and stained with polyclonal anti-Olig2 antibody (1:20,000) (Arnett et al., 2004) or anti-GFP antibody (1:1000, Sigma). Total O4 positive cells and total number of cells in each transduced clone (identified with Olig2 or GFP staining) were counted. For the generation of cell lines, media containing blasticidine (2 ug ml^{-1}) was used following transduction.

Retroviral Vectors and Virus Production

Full-length mouse Olig2 or GFP was cloned into the PWZL-BLAST retroviral vector as previously described (Ligon et al., 2007). Phosphorylation sites identified by mass-spectrometry were reproduced as single and multiple mutants utilizing QuikChange Site-Directed Mutagenesis (Stratagene) and subsequently cloned into the PWZL-BLAST backbone and into the PHAGE-CMV-MCS-IZSGreenW

lentiviral vector (kindly provided by Jeng-Shin Lee, Harvard Gene Therapy Initiative-HGTI). Lentivirus was generated as described by Mostoslavasky et al. (Mostoslavsky et al., 2005).

Olig2 protein purification and phosphorylation analysis

Endogenous Olig2 protein was purified from *in vitro* cultured murine LGE neurospheres (5 g total pellet weight; derived from E14 embryos of CD1 time-pregnant mice, Charles River) and human glioma line BT37 mouse xenografts (15g total tissue weight) by generating nuclear extracts that were then subjected to Olig2 antibody affinity column chromatography. The affinity column was generated using Olig2 antibody according to the instructions of AminoLink Plus Immobilization Kit (Pierce). Purified Olig2 protein was subjected to SDS-PAGE gel electrophoresis followed by Coomassie blue staining. Bands corresponding to Olig2 protein were excised and sent to the Taplin Biological Mass Spectrometry Facility (Harvard Medical School) for protein identification and Olig2 phosphorylation analysis using LC/MS/MS.

Secondary neurosphere assay

Olig2-null neural progenitor cell lines were derived from the LGE of individual E14 *Olig2*-null embryos and maintained as neurosphere cultures. After three passages, neurospheres were dissociated into single cells and then transduced with retroviruses containing various mutants of *Olig2* at an MOI of 0.5:1 under neurosphere culture conditions. Transduced cells were selected with blasticidin for 7 days. Primary transduced neurospheres were dissociated into single cells and replated at 10 cells μl^{-1} in 6-well plates for secondary neurosphere formation assays. For each construct, tertiary neurosphere assays were performed to confirm the results seen in secondary neurosphere assay. The expression of each construct was confirmed with western blot and immunocytochemistry. For total cell population analyses, total neurospheres from each 6-well were collected and mechanically dissociated into single cells. Total viable cells were counted with hemocytometer using 0.2% trypan blue exclusion. Total neurosphere numbers were counted under a dissection microscope. The images of

individual neurospheres were taken using a 4x objective and ImageJ software was used for measuring neurosphere size (area).

^{32}P labeling of cells

Cells were labeled for 2 hours in phosphate free media supplemented with 300 μCi ml-1 ^{32}P orthophosphate. Cells were washed in cold PBS and protein extracts generated using RIPA buffer. Olig2 was immune-precipitated using a pan-Olig2 antibody (Arnett et al., 2004) and resolved using SDS-PAGE. Quantitation of the signal was performed using a Typhoon Trio (GE Healthcare).

Generation and characterization of phospho-specific antibodies

Phosphorylation state-specific antibodies were generated and purified as described previously (Alberta and Segal, 2001) using a peptide containing the triple phosphorylation motif (LVSPSRPPSPSPEPDDLC) conjugated to KLH using the Imject Conjugation kit (Pierce) as antigen in rabbits by Covance (Denver, PA).

Limiting dilution tumorigenesis assay

Two *p16^{Ink4a}/p19^{Arf}/Olig2*-null *Egfrv*III neurosphere lines (EB5 and EB7) were generated as described (Ligon et al., 2007), and then stably transduced with EGFP, Olig2 WT and Olig2 mutants of interest via retroviral infection and five passages of neurosphere expansion. For each Olig2 construct, serial dilutions of cells at 1x10^5, 1x10^4, 1x10^3, 1x10^2, were injected into the right striatum of Icr-SCID mice (Taconic Farms, Inc.) at the coordinates, A, -0.5mm, L, 1.50mm and D, 2.65mm relative to the bregma. Animals were sacrificed at the onset of neurological/clinical symptoms.

Chromatin immunoprecipitation

Olig2-null mouse neural progenitor cells were stably transduced with retrovirus expressing EGFP, *Olig2* wt, *Olig2* TPN or *Olig2* TPM as described above. Cells were plated at a density of 10 cells ul-1 and cultured on laminin-coated 6-well plates

(Pollard et al., 2009). Cells were cross-linked with 1% formaldehyde for 10 min at RT. Reaction was quenched with 125 mM glycine for 5 min at RT. The cells were washed twice, and harvested in ice cold PBS, resuspended in 300 µl SDS lysis buffer and sonicated with three pulses of 10 seconds each. Chromatin was diluted in ChIP dilution buffer and pre-cleared for 1 hour at 4°C in the presence of 25 µl Dynal magnetic beads (Invitrogen). For immuneprecipitation, 50 µl beads were incubated with p53 antibody (Santa Cruz) for 5 hours at 4°C. Pre-cleared chromatin and antibody-bound beads were incubated overnight on a rotor at 4°C. Beads were then washed six times in RIPA wash buffer and twice in TE. Beads were resuspended in 100 µl buffer (200mM NaCl, 1% SDS and 0.1M $NaHCO_3$) and reverse cross-linked overnight at 65°C. Immunoprecipitated DNA was cleaned with PCR clean up kit (Qiagen) and eluted in ddH2O.

Quantitative PCR

Chromatin immunoprecipitated DNA was analysed with quantitative PCR in real time PCR system (Applied Biosystems), using SYBR green mix. Primers used for qPCR are as described in detail elsewhere (Mehta et al., 2011). Presented data are delta CT values normalized for WT promoter occupancy.

Radiation sensitivity assay

Olig2-null mouse neural progenitor cells stably transduced with EGFP, *Olig2* WT, *Olig2* TPN or *Olig2* TPM were cultured under adherent culture condition as described above. Cells were allowed to recover for three hours and then treated with 2 Gy irradiation. Control groups remained untreated. At 4–5 days after treatment, viable cells were counted by trypan blue exclusion. Data are presented as percentage of total viable cell number after treatment relative to untreated controls.

Immunoblotting

Total Olig2 immunoblotting was performed according to standard protocols using either a rabbit polyclonal anti-Olig2 antibody (1:100,000) or a monoclonal mouse anti-Olig2 antibody (1:2000) (Arnett et al., 2004).

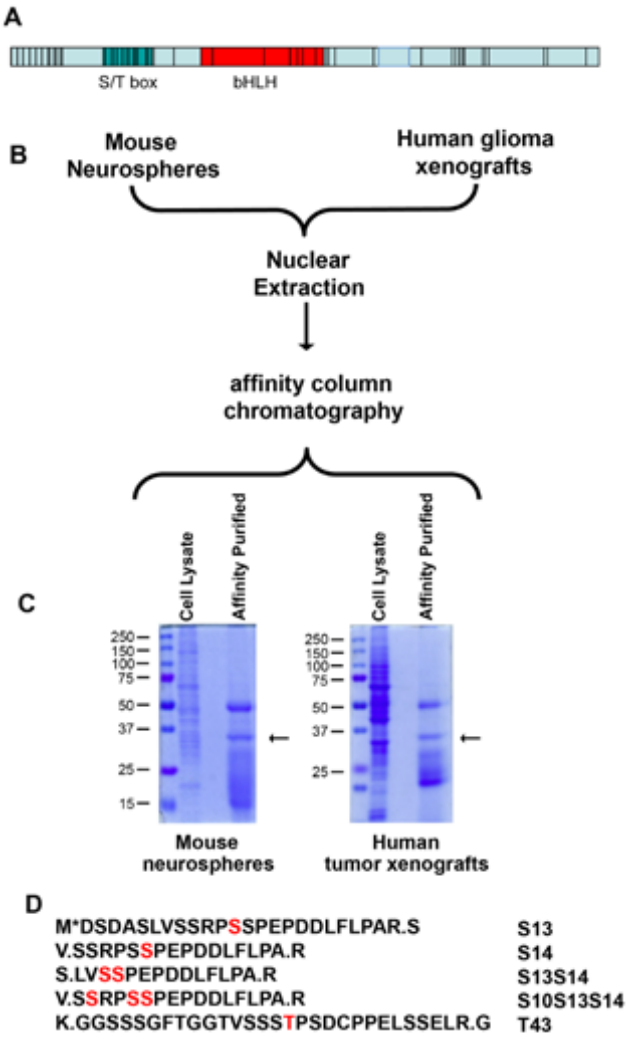

SUPPLEMENTAL FIGURE S1. **Purification and mass spectrometry analysis of murine and human Olig2.** **(A)** Potential phosphorylation sites for Olig2 by the Scansite algorithm (scansite.mit.edu). Potential phosphorylation sites (small vertical lines) are scored utilizing a sliding residue window around the invariant residue comparing the target sequence to a matrix based on experimental data and then compares the score for that motif to all potential similar motifs within all vertebrate sequences in Swiss-Prot. The indicated phosphorylation sites are in general within the top 1.2% of similar sites as reported by Scansite. Several structural motifs of interest in Olig2 are indicated: (red) the bHLH domain; (turquoise) a "box" of 12–20 contiguous serine/threonine residues found in all of the mammalian Oligs and in avian olig2. **(B)** Flow-chart describing the purification of Olig2 from mouse neurospheres or human tumor xenografts. **(C)** Coomassie Blue stained gel showing microgram amounts of Olig2 purified from murine neurosphere cultures and human tumor xenografts. Arrows denote the position of Olig2 in the Affinity Purified lanes. **(D)** Peptides identified in Olig2 by mass spectrometry containing phosphorylated amino acids (red).

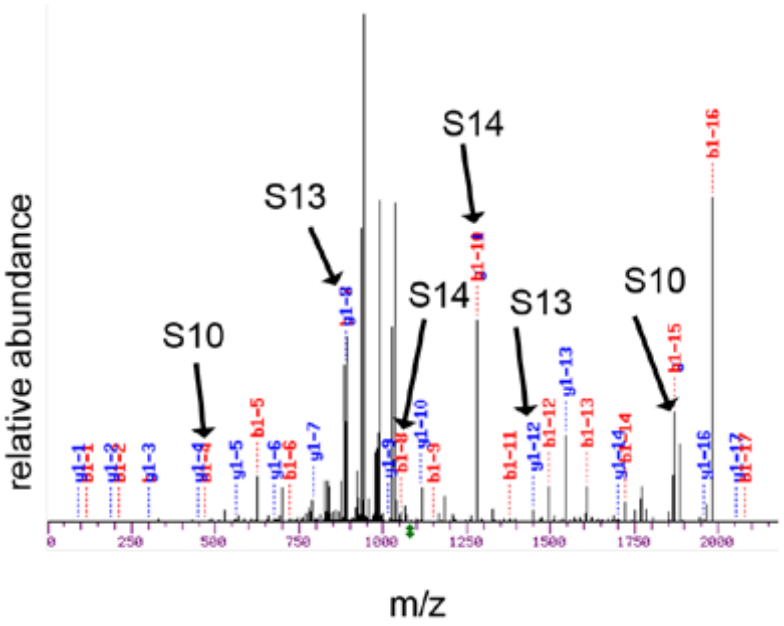

SUPPLEMENTAL FIGURE S2. **Representative mass spectrum of Olig2.** Tandom mass spectrum of an eluted peptide fragment of Olig2 corresponding to the serine 10, 13, and 14 region. Arrows denote peaks representing the specific phosphoserines.

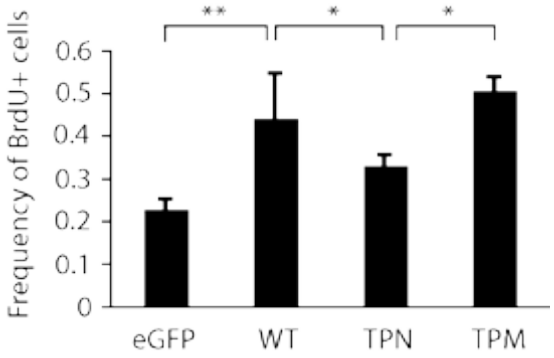

SUPPLEMENTAL FIGURE S3**. Phosphorylation state of Olig2 at triple serine motif shows difference in BrdU incorporation.** *Olig2*-null neurospheres bearing EGFP, *Olig2* WT, *Olig2* TPN and *Olig2* TPM, were dissociated into single cells and then plated with the presence of Egf and Fgf under adherent culture conditions, on the 2nd day, BrdU at 10μM was added to the culture medium for 3hrs, then cells were fixed, and stained for BrdU and counterstained with DAPI. The bar graph indicates the frequency of BrdU positive cells relative to total DAPI positive cells. One-way ANOVA and Posthoc Newman Keuls test, **, $p<0.01$; *, $p<0.05$.

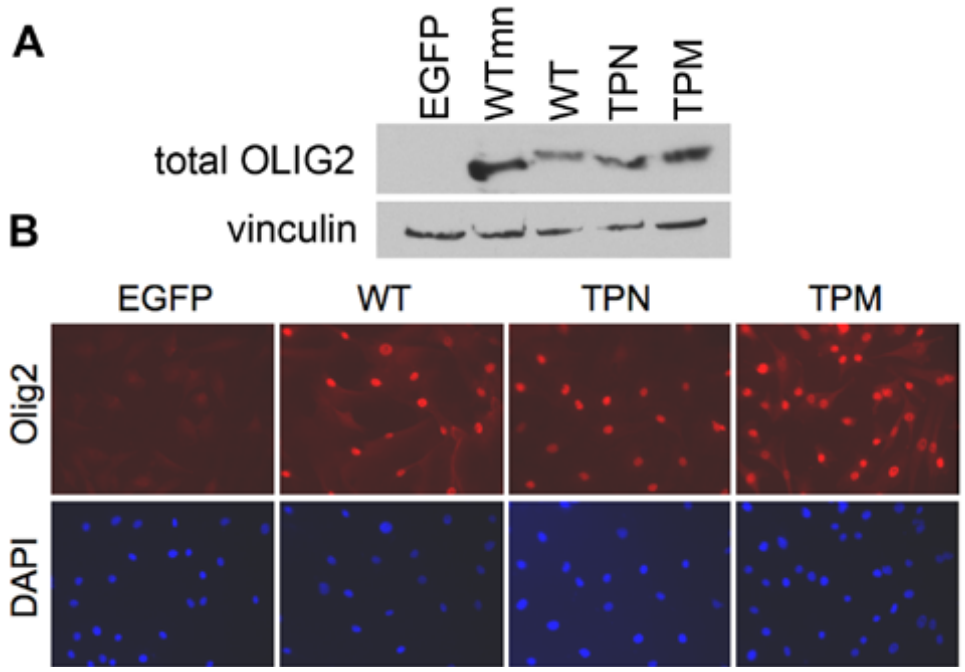

SUPPLEMENTAL FIGURE S4. **Expression of Olig2 in engineered neurosphere lines**. **(A)** Expression levels of transduced WT, TPN and TPM in *Olig2*-null neurospheres are equivalent to those in wild-type mouse neurospheres (WTmn). Western blot analysis using total Olig2 antibody. **(B)** Subcellular localization of Olig2 is independent of phosphorylation at serines 10, 13, and 14. Cells as in A were immunostained with a total Olig2 antibody.

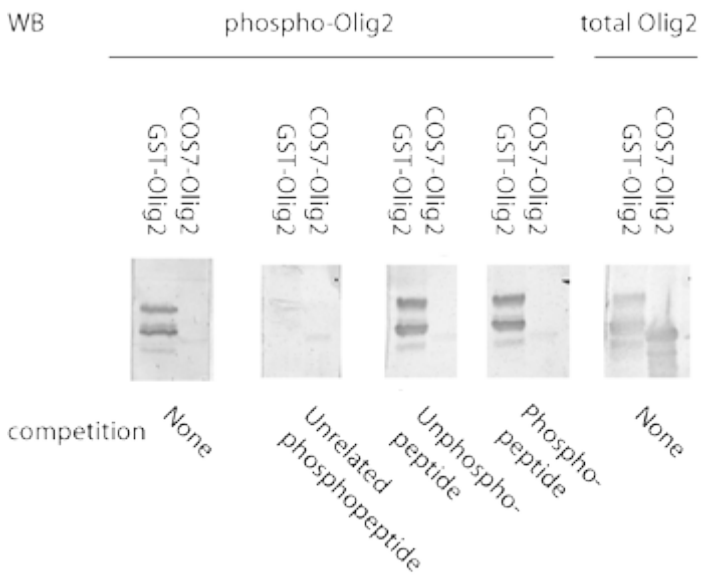

SUPPLEMENTAL FIGURE S5. **Phosphorylation state specific antibodies to the triple phosphorylation motif of Olig2.** Western blot of *Olig2* expressed in COS7 cells (where Olig2 was shown to be phosphorylated) or as a GST fusion protein (where Olig2 is not phosphorylated). The blots were probed with DF449, an antibody generated against a peptide corresponding to the triple phosphorylated form of Olig2 and affinity purified. Various peptides were used as competitors as indicated in the figure.

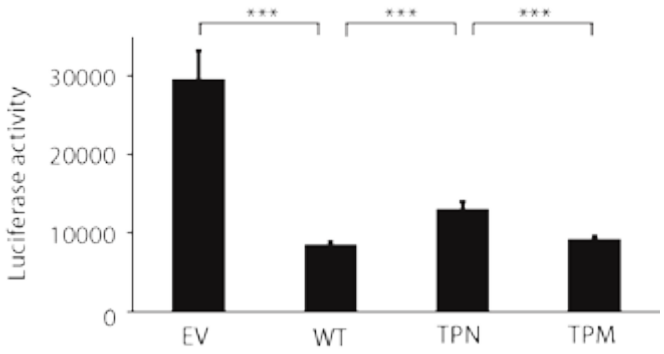

SUPPLEMENTAL FIGURE S6. **Olig2 acts directly on the** p21 **promoter in a phosphorylation dependent manner.** U87 cells were transfected with empty vector (EV) or Olig2 (wild-type, TPN or TPM), a p21 promoter-luciferase construct and lacZ as a transfection control. Two days later, lysates were generated and luciferase activity measured using b-gal activity to normalize for transfection efficiency. For statistical analysis all samples were normalized to wild-type Olig2 in each experiment. ANOVA and Post hoc Neuman-Keuls test, ***, $p < 0.001$, $n=6$.

3 Molecular mechanism of Olig2 phosphorylation: Phosphorylation state controls intranuclear localization of Olig2 in neural progenitor cells

Dimphna H. Meijer, Yu Sun, Shwetal Mehta, Tao Liu,
Michael F. Kane, John Alberta, Guillaume Adelmant,
David Rowitch, Yoshihiro Nakatani, Charles D. Stiles

Abstract

The bHLH transcription factor Olig2 contains a developmentally regulated phosphorylation motif in its amino terminal domain. In its phosphorylated state, Olig2 supports proliferation of both normal and malignant neural progenitors. The pro-mitogenic function of phospho-Olig2 reflects, at least in part, an oppositional relationship with p53 functions. Here, we define the molecular mechanism whereby amino terminal phosphorylation regulates Olig2 function. We show that the gene expression profile of Olig2 is controlled by phosphorylation state of the amino terminal motif. In contrast, target gene binding is not affected by the phosphorylation state. Rather, phosphorylation regulates intranuclear compartmentalization of Olig2 and consequent access to key co-regulator proteins.

Introduction

During development, the fate choice decision of neural progenitors to proliferate symmetrically or divide asymmetrically and differentiate, is largely controlled by transcription factors belonging to the basic helix-loop-helix (bHLH) class (Ross et al., 2003). As a general rule, these neurogenic bHLH transcription factors can be parsed into "pro-neural" and "anti-neural" subsets. At early stages of development, progenitor cells express mostly anti-neural bHLH proteins. These factors sustain proliferation to expand the pool of available neuronal and glial precursors. At later times, expression of these anti-neural factors is sup-

pressed, allowing for the emergence of pro-neural factors, which promote cell cycle exit and neural differentiation. Notably, neither anti-neural, nor pro-neural transcription factors are generally expressed in terminally differentiated neurons of the postnatal central nervous system.

Against this backdrop, the bHLH transcription factor Olig2 defies simple classification as an anti-neural or pro-neural factor. At early stages of central nervous system development, Olig2 functions to prevent premature cell cycle exit and sustain the replication of progenitor cells that give rise to certain types of neurons—notably motor neurons (Lu et al., 2002; Zhou and Anderson, 2002). At later developmental stages however, Olig2 is required for specification of the oligodendrocyte lineage throughout the central nervous system. Moreover, in marked contrast to other neurogenic bHLH factors, expression of *Olig2* is maintained in mature, myelinating oligodendrocytes of the postnatal brain (Lu et al., 2000; Takebayashi et al., 2000; Zhou et al., 2000).

Recent studies have shown that Olig2 is a phospho-protein and that developmentally regulated changes in the phosphorylation state enable its multiple functions in the developing central nervous system (Huillard et al., 2010; Li et al., 2011; Setoguchi and Kondo, 2004; Sun et al., 2011). One developmentally regulated phosphorylation site in the bHLH domain of Olig2 regulates the motor neuron to oligodendrocyte transition (Li et al., 2011). A second developmentally regulated phosphorylation motif at positions Ser10, Ser13, Ser14 in the amino terminus of Olig2 supports proliferation, but is not essential for Olig2-regulated developmental functions (Sun et al., 2011). The mitogenic function of this triple phosphoserine motif reflects, at least in part, an oppositional relationship to p53 (Mehta et al., 2011). Wild-type Olig2 and a triple phospho-mimetic Olig2, where negatively charged aspartate or glutamate residues are substituted for serine 10, 13 and 14 suppress p53-mediated responses to gamma irradiation. By contrast, a triple phospho-null mutant of Olig2, where neutral glycine or alanine residues replace the three serine residues, is equivalent to the *Olig2*-null state with respect to p53 function (Sun et al., 2011). The oppositional relationship between Olig2 and p53 is of some practical interest. Phosphorylation of the Olig2 triple serine motif stimulates tumor formation in a "genetically relevant" murine model of human glioma. Moreover, phosphorylated Olig2 is detected in human gliomas (Sun et al., 2011)

How does a phosphoserine motif in the amino terminus of Olig2 suppress p53 function? Transcription factors with bHLH domains function as homodimers or heterodimers to bind canonical E-box promoter elements on their target genes. Olig2 and also other bHLH factors (e.g. Neurogenin and Twist), have phosphorylation events within the bHLH domain that regulate dimerization and interactions with key co-regulator proteins (Firulli et al., 2007; Li et al., 2011; Ma et al., 2008). In contrast, it is not self-evident how the phosphorylation state of Olig2, at a position more that 100 residues away from the DNA-targeting bHLH motif, might regulate biological functions. Indeed, to date there has been no evidence that the anti-p53 functions of phosphorylated Olig2 are linked to its functions as an E-box binding transcription factor. For example, key genetic functions of the p53 protein are regulated by acetylation. A differential acetylation state of p53 noted in WT relative to *Olig2*-null neural progenitors, supports the testable hypothesis that Olig2 simply competes with p53 for an important co-regulator protein that facilitates acetylation (Mehta et al., 2011).

In a series of studies summarized here, we first show that the pro-mitogenic, anti-p53 functions of phosphorylated Olig2 do indeed reflect its functions as an E-box binding transcription factor. We then show that the phosphorylation state of the amino terminal triple-serine motif regulates the gene expression profile of Olig2. However, the mode of this regulation depends on intranuclear localization. In particular, phosphorylated Olig2 protein is loosely associated with the chromatin, where it has access to a specific set of Olig2 co-regulator proteins.

Results

Pro-mitogenic, anti-p53 functions of the N-terminal triple phosphoserine motif in Olig2 require DNA binding

To determine whether the pro-mitogenic, anti-p53 functions of the triple phosphoserine motif are linked to Olig2 transcriptional functions, we mutated a single amino acid in the basic domain of Olig2 to abrogate DNA binding (N114H or ΔOlig2, see Fig. 1A).

Retroviral expression vectors were used to reintroduce either WT *Olig2* or Δ*Olig2* into *Olig2*-null neural progenitor cells. As shown in Fig. 1B, Δ*Olig2* is

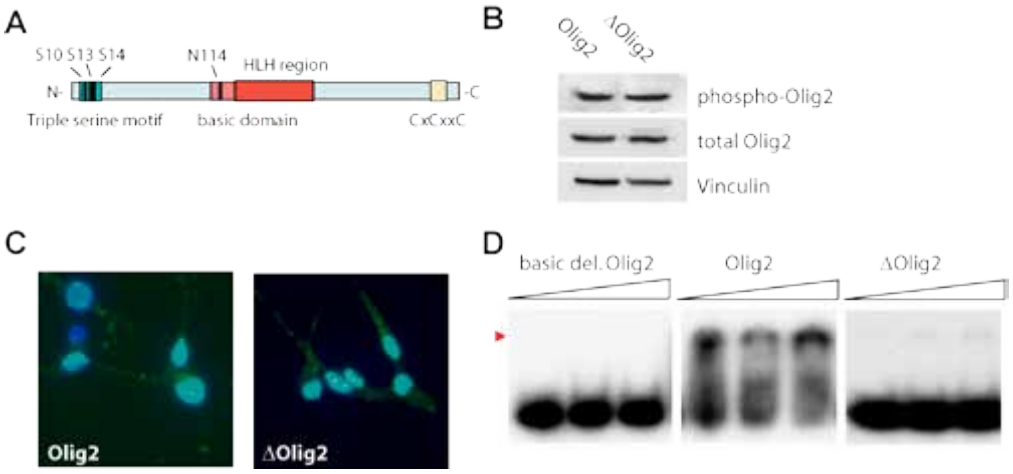

FIGURE 1. **Single amino acid mutation abrogates DNA binding. (A)** Schematic representation of mouse Olig2 protein. Asparagine residue N114 is located in the basic region. **(B)** *Olig2*-null mouse neural progenitor cells expressing *Olig2* WT or N114H mutation (ΔOlig2) show comparable levels of triple phosphorylation, as shown by immunoblot with phosphorylation state-specific antibody. **(C)** *Olig2*-null mouse neural progenitor cells were transduced with *Olig2* WT or Δ*Olig2*. Immunofluorescence staining shows that Olig2 N114H (green) maintains nuclear localization. **(D)** Olig2 WT, an Olig2 deletion construct lacking the basic region (basic del.) or ΔOlig2 was purified from COS7 cells and incubated with radioactive DNA probe containing E-box element CAGATG from the *Hb9* promoter. Deletion of the basic region (amino acids 109–121) abrogates DNA binding, whereas Olig2 WT shifts *Hb9* probe in a dose-dependent matter. In contrast, ΔOlig2 is not able to shift *Hb9* probe.

expressed at levels comparable to WT *Olig2*. Moreover, immunoblotting with a highly specific antibody targeted to the triply phosphorylated serine motif shows that the triple serine motif on the mutant is phosphorylated at levels comparable to WT Olig2 (Fig. 1B) (Sun et al., 2011). In addition, ΔOlig2 is correctly targeted to the cell nucleus (Fig. 1C). However, ΔOlig2 cannot bind to canonical E-box promoter/enhancer elements (Fig. 1D).

The transduced neural progenitor cells together with vector controls were then challenged with gamma irradiation. Unlike WT Olig2, ΔOlig2 cannot protect from gamma irradiation (Figs. 2A, 2B).

Likewise, ΔOlig2 cannot suppress a pair of p53 responses to radiation that were noted in previous studies—namely stabilization and acetylation of p53 (Fig. 2C). Acetylation enhances the interaction of p53 with promoter elements of target genes such as *p21* (Barlev et al., 2001; Li et al., 2002). As shown in Fig.

2D, WT Olig2, but not ΔOlig2 suppresses the interaction of p53 with the *p21* promoter.

To further probe the link between amino terminal phosphorylation, and Olig2 transcriptional functions, we cloned the DNA binding mutation into *Olig2* constructs containing a WT, triple phospho-null (TPN) or triple phospho-mimetic (TPM) element at the N-terminal. As shown in Figs. 3A and 3B, the phosphory-

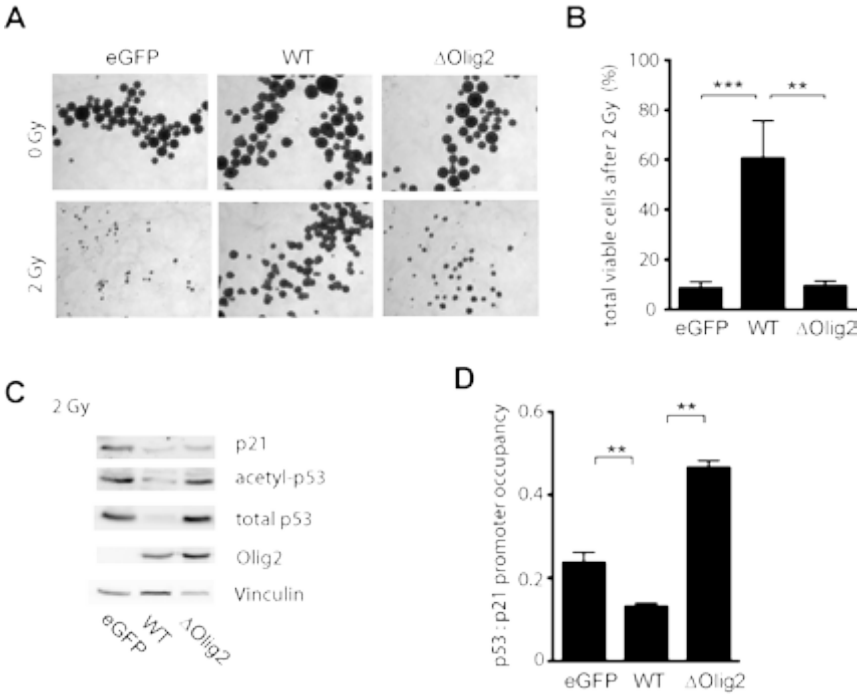

FIGURE 2. **Anti-p53 functions are dependent on Olig2 : DNA interaction. (A)** *Olig2*-null mouse neural progenitor cells were transduced with *Olig2* WT, Δ*Olig2* or EGFP (control). Cells were plated at 10 cells / μL in 6 well plates and treated with or without 2Gy irradiation. Images were taken six days after plating. **(B)** Bar graph shows quantitation of viable cell counts after 2Gy irradiation normalized to cells without irradiation treatment, as an index for neurosphere proliferation. Data presented are from three independent experiments. Error bars, SD. One-way ANOVA, $p<0.001$, ** = $p<0.01$, *** = $p<0.001$ **(C)** *Olig2*-null mouse neural progenitor cells expressing *Olig2* WT, Δ*Olig2* or EGFP were treated with 2 gray irradiation and cells were harvested 6 hours after treatment. Olig2, total p53, acetylated p53 (Lys 379) and p21 protein levels were analysed by immunoblotting, using vinculin as loading control. **(D)** Cell lysates from mouse neural progenitor cells expressing *Olig2* WT, Δ*Olig2* or control protein EGFP were processed for ChIP with p53 antibody. Bar graph shows QRT-PCR analysis of p53 binding to p21 promoter region, calculated over ChIP input. Data shown are three independent repeats. Error bars, SEM. One way ANOVA, $p<0.001$, ** = $p<0.01$

lation state of the N terminal triple serine motif is irrelevant to cell proliferation when Olig2 cannot bind to E-box elements. Collectively, these studies show that the pro-mitogenic and anti-p53 functions of the triple phosphorylation motif noted in previous studies are intimately linked to the ability of Olig2 to recognize canonical E-box promoter/enhancer elements (Sun et al., 2011).

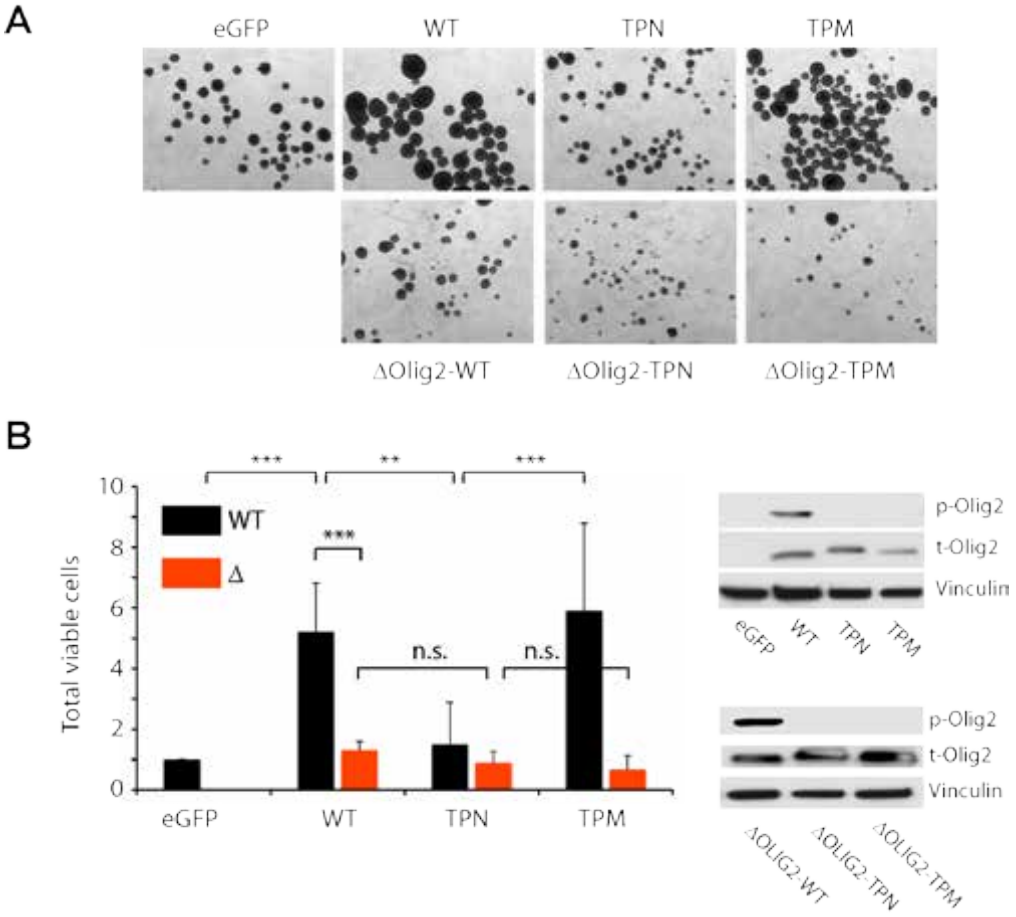

FIGURE 3. **Function of the Olig2 triple phosphorylation relies on DNA binding. (A)** *Olig2*-null neural progenitor cells were transduced with retroviral vectors encoding EGFP, WT, TPN, TPM or ΔWT, ΔTPN, ΔTPM constructs of *Olig2*. Cells were plated at 10 cells / μL in 6 well plates and representative images were taken six days after plating. **(B)** Cell counts, as an index for neurosphere proliferative ability, were normalized to Olig2 EGFP. Inset shows total and phospho-Olig2 protein levels in all cell lines analysed. Data represent average from three independent repeats. t-Olig2, total Olig2; p-Olig2, phospho-Olig2. Error bar, SD. One-way ANOVA, $p<0.001$. Tukey's multiple comparisons test, ** = $p<0.01$, *** = $p<0.001$

Differential expression profiles dictated by TPN and TPM mutants of Olig2

Does the phosphorylation state of the triple serine motif impact gene expression? To address this question, *Olig2*-null neural progenitors were transduced with WT, TPN or TPM variants of *Olig2* (Fig. 4A).

Cells were cultured and expression profiles were then captured by RNA-seq. Relative to *Olig2* TPN-expressing progenitors, we identified 526 genes that are repressed by the *Olig2* TPM mutant and another 400 genes that are upregulated (Fig. 4B, datasets will be made available online in the Gene Expression Omnibus (GEO) repository). Using quantitative PCR, we validated a subset of target genes that are activated by Olig2 TPM and are associated with enhanced growth / proliferation (Fig. 4E, red) (Doetsch et al., 2002; Young et al., 2010). Likewise, we validated a subset of repressed target genes that are potentially anti-proliferative (Fig. 4E, blue) (Aoki et al., 2004; Roussa et al., 2006). The latter list includes the p53-response gene, *p21*, shown previously to be repressed by Olig2 TPM relative to TPN (Sun et al., 2011). We conclude that the expression profile of Olig2 is regulated by phosphorylation state of the amino terminal motif.

Target gene binding is unaffected by Olig2 triple phosphorylation

To determine whether Olig2 phosphorylation regulates gene expression through differential binding of target genes, we performed genome-wide ChIP-seq analysis on the WT, TPM or TPN cell lines. Of note, our high affinity total Olig2 antibody used for the chromatin immunoprecipitation step of this work reacts equally well with all three variants of Olig2 (Fig. S1). The absolute number of target genes detected in ChIP protocols is somewhat arbitrary and contingent upon thresholds set for peak calling (Zhang et al., 2008). Using a new peak-calling algorithm, we arrive at a list of target genes where more than half of the TPN/TPM differentially expressed genes from Fig. 4B correspond to Olig2 binding sites (Fig. 4C). As with our RNA-seq data set, the full cohort of Olig2 binding genes detected by ChIP-seq will be made available online in the GEO repository.

Does the phosphorylation state of Olig2 affect gene target binding? As shown in Fig. 4D, the differentially regulated gene sets from Fig. 4B correspond to

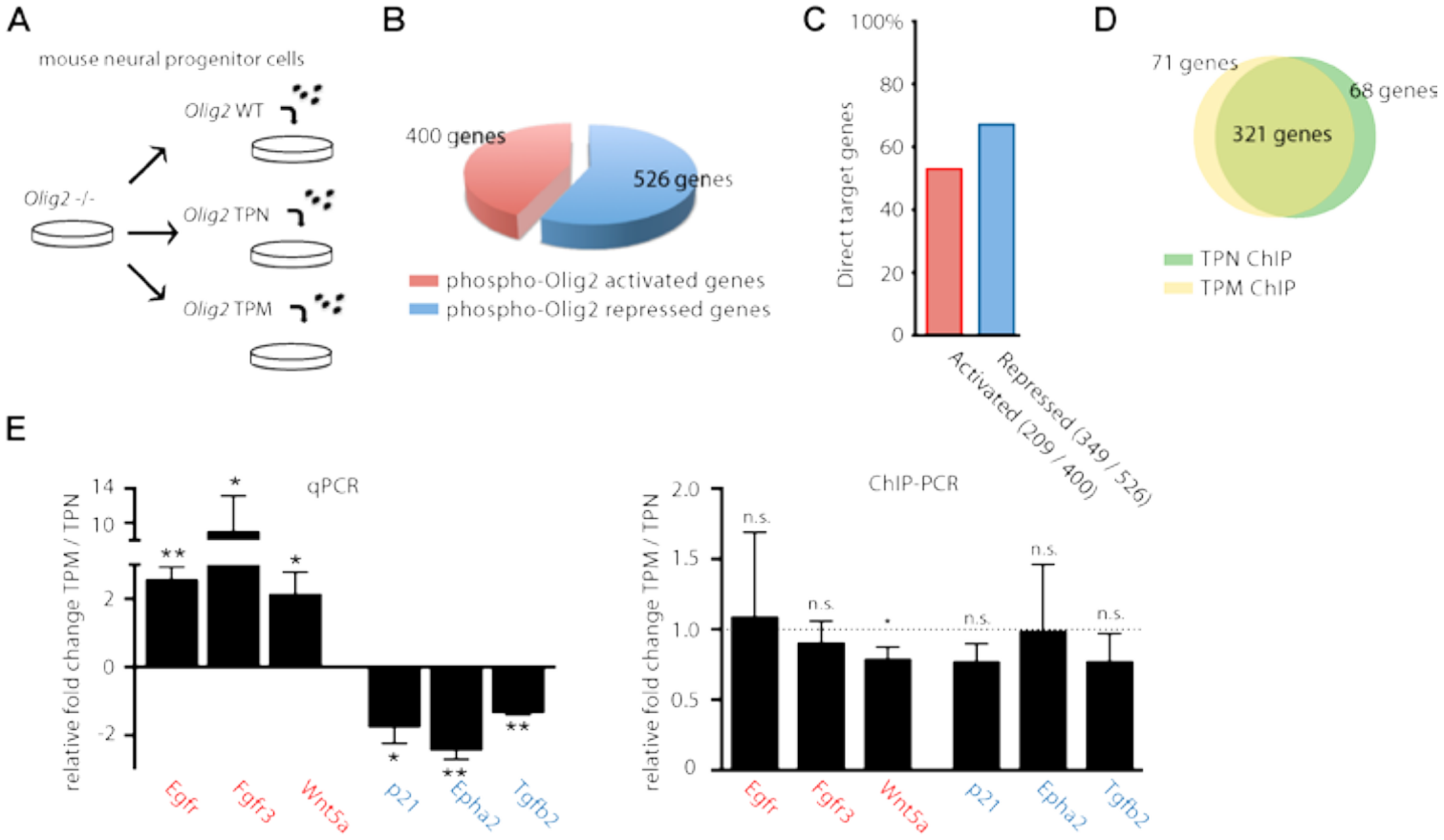
A
mouse neural progenitor cells
Olig2 -/-
Olig2 WT
Olig2 TPN
Olig2 TPM
B
400 genes
526 genes
phospho-Olig2 activated genes
phospho-Olig2 repressed genes
C
100%
80
60
40
20
0
Direct target genes
Activated (209 / 400)
Repressed (349 / 526)
D
71 genes
321 genes
68 genes
TPN ChIP
TPM ChIP
E
qPCR
relative fold change TPM / TPN
14
10
2
0
-2
Egfr
Fgfr3
Wnt5a
p21
Epha2
Tgfb2
ChIP-PCR
relative fold change TPM / TPN
2.0
1.5
1.0
0.5
0
n.s.

FIGURE 4. **Olig2 phosphorylation regulates gene expression but not DNA targeting in mouse neural progenitor cells. (A)** Schematic overview of experimental design. *Olig2*-null mouse neural progenitor cells were transduced with *Olig2* WT, TPN or TPM. Cells were plated at 10 cells / µL and harvested under proliferating conditions. **(B)** RNA was isolated from TPN or TPM mouse neural progenitor cells using Trizol, and sequenced on Illumina Hiseq 2000. Sequencing results were directly compared using Cuffcompare, part of Cufflinks (Trapnell et al., 2010). Genes shown are statistically significant up- or down-regulated between TPN and TPM. **(C)** Olig2 WT cell lysates were processed for ChIP with total-Olig2 antibody. Sequencing was performed on Illumina Hiseq 2000. Comparison of direct Olig2 target gene set and differentially expressed gene sets (see 4B) shows more than 50% overlap for activated and repressed genes. **(D)** Olig2 TPN and Olig2 TPM cells were harvested and processed for Olig2 ChIP. Venn diagram shows overlapping direct target genes for TPN and TPM using the differentially expressed genes (see Fig. 4C). **(E)** Directed qRT-PCR (left graph) and ChIP-PCR (right graph) results confirm set of direct targets that are activated, i.e. Egfr, Fgfr3, Wnt5a, or repressed, i.e. p21, Epha2, Tgfb2, by Olig2 triple phosphorylation. Bar graphs show fold change of TPM over TPN of three independent repeats. Error bar, SD. Unpaired t test, two-tailed, n.s. = not significant, * = $p<0.05$, ** = $p<0.01$

Olig2 binding sites that are almost completely equivalent between TPN and TPM ChIP-seq datasets (> 80% overlap). To further explore the role of Olig2 phosphorylation in target gene binding, we performed directed ChIP-PCR on a subset of genes that are differentially expressed in the TPN cells relative to TPM. As shown in Fig. 4E, six genes that are clearly differentially regulated in TPM cells relative to TPN, show no difference in target gene binding between TPN and TPM (See also Fig. S2).

In a final test of whether Olig2 phosphorylation changes target gene binding, we analysed direct protein:DNA interaction utilizing electromobility shift assays. The bHLH group of transcription factors recognize the E-box motif CANNTG in promoter/enhancer regions of their target genes. Our ChIP-seq data suggest that the preferred E-box for Olig2 in mouse neural progenitor cells is CAGCTG (Fig. S3). We constructed a gel mobility shift probe containing this preferred E-box (*Mycn*). We also constructed a second probe containing a variant E-box (CATCTG) from the *Hb9* promoter, a biologically relevant target of Olig2 in the developing spinal cord (Lee et al., 2005). As indicated in Fig. 5, purified Olig2 TPN and TPM show comparable affinity for the *Hb9* and *Mycn* probes (See also Fig. S3).

As noted in Fig. 4D, whole genome ChIP-seq did show a small percentage of Olig2 binding sites (~20%) that did interact differentially with TPM and TPN. Follow-up studies on 24 of these sites by directed ChIP-PCR failed to show any evidence of differential DNA binding by TPM or TPN (data not shown). Collectively, these data demonstrate that Olig2 phosphorylation does not regulate gene expression through differential binding of target genes.

Triple phosphorylation motif regulates intranuclear compartmentalization

Eukaryotic chromatin exists in two states, loose and condensed. These two compartments, and their associated proteins, can be resolved one from the other by salt extraction and digestion with micrococcal nuclease (Giusti et al., 2009; Kamakaka and Kadonaga, 1994). In general, transcription factors are mainly associated with loose chromatin (Kamakaka and Kadonaga, 1994). To determine whether phosphorylation state of the triple serine motif modulates intranuclear compartmentation of Olig2, we lysed wild-type neural progenitor

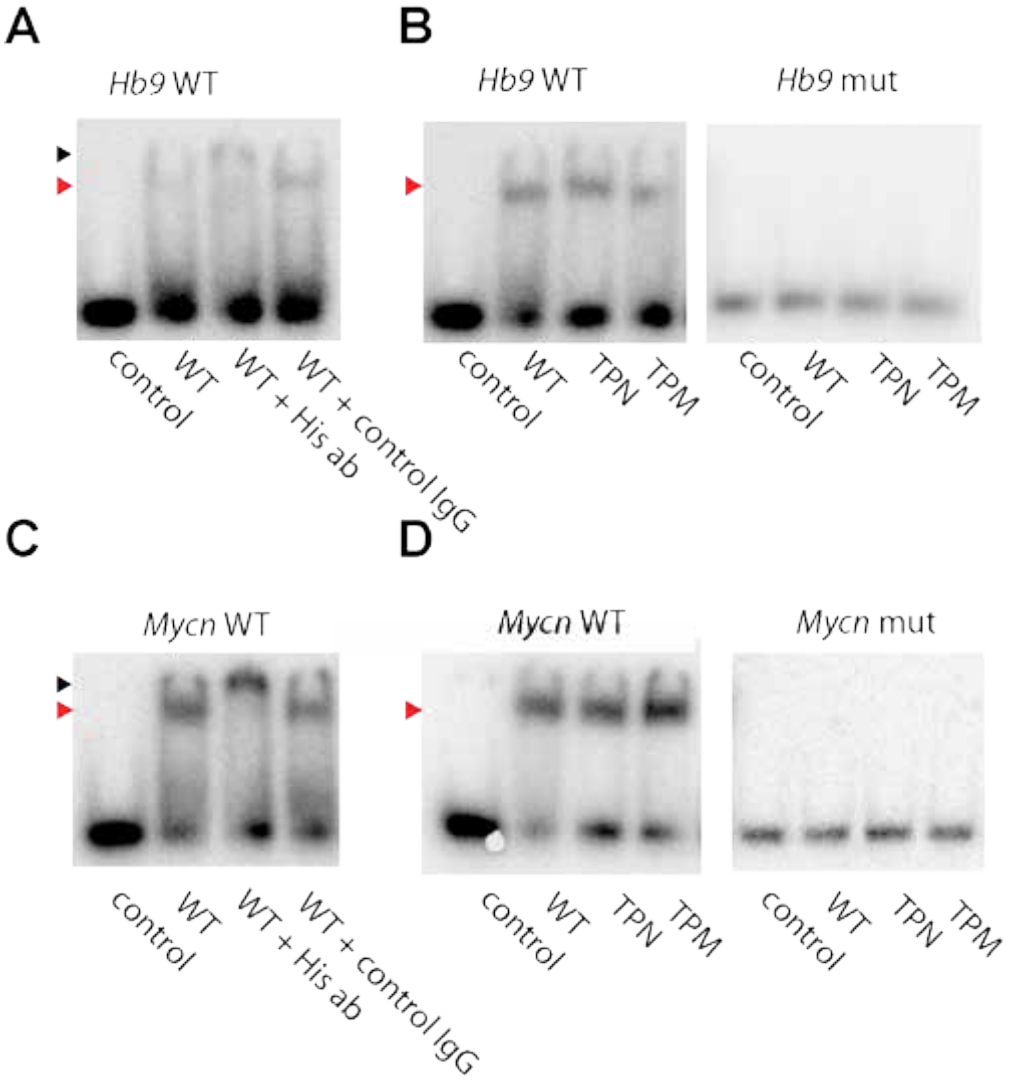

FIGURE 5. **Olig2 phosphorylation does not control E-box recognition**. **(A)** *Olig2* WT was transfected into COS7 cells and purified by V5 and His tag tandem immunoprecipitation (see Fig. S3). Purified Olig2 WT protein was incubated with radioactive DNA probe containing E-box element CAGATG from the *Hb9* promoter, in the presence of His tag or control antibody, and binding was assessed in electrophoretic mobility shift assay. **(B)** Purified Olig2 WT, TPN or TPM was incubated with *Hb9* probe, or *Hb9* mutant containing mutated E-box TAGACT, and analyzed in electrophoretic mobility shift assay. **(C)** Purified Olig2 WT was incubated with *Mycn* probe containing E-box element CAGCTG, in the presence of His tag or control antibody, and binding was assessed in electrophoretic mobility shift assay. **(D)** Purified Olig2 WT, TPN or TPM was incubated with *Mycn* probe, or *Mycn* mutant containing mutated E-box TAGCCT, and analyzed in electrophoretic mobility shift assay. Red arrowhead indicates shift, black arrowheads indicate position of supershift.

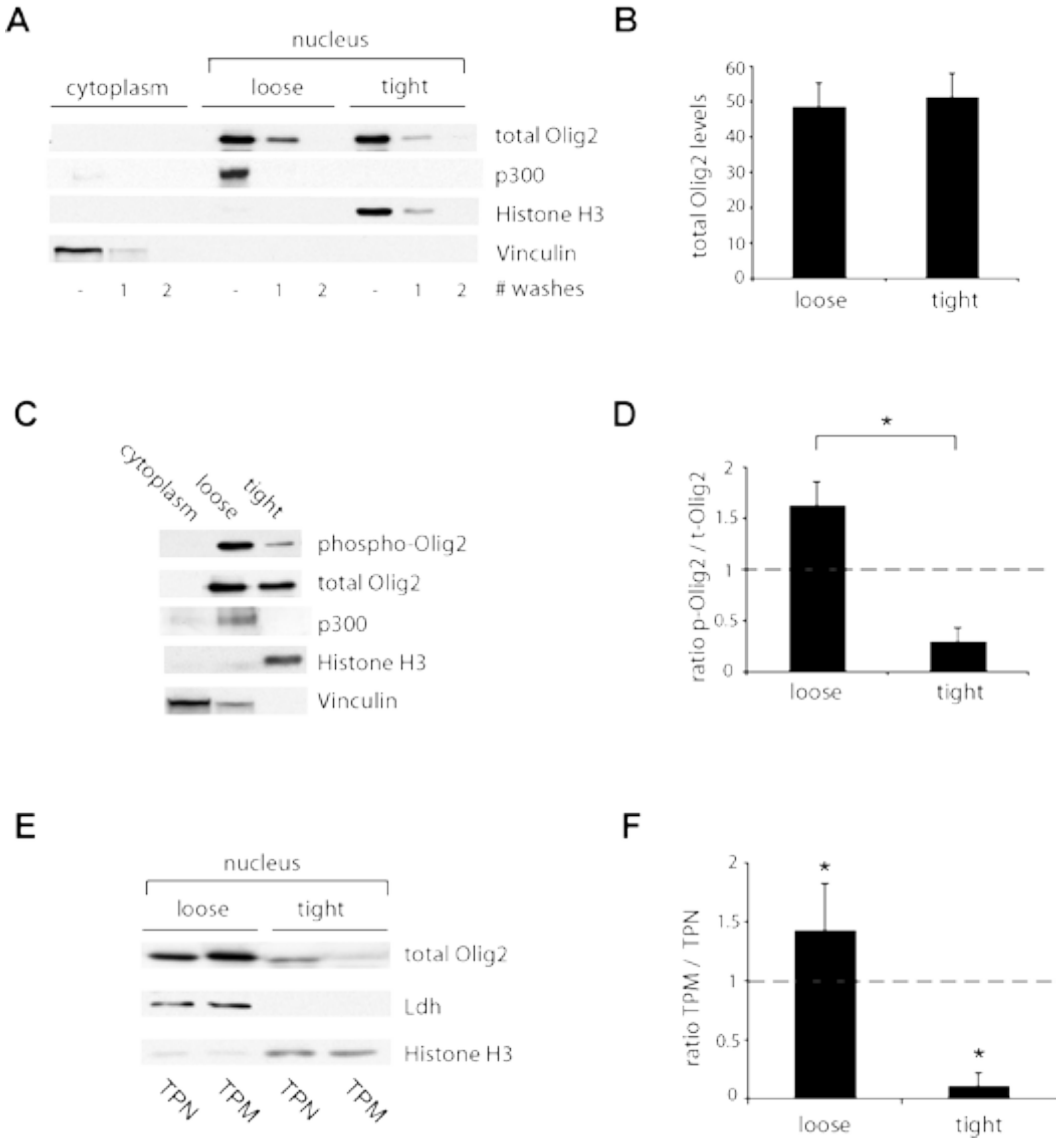

FIGURE 6. **Olig2 phosphorylation regulates intranuclear localization. (A)** *Olig2* WT mouse neural progenitor cells were plated at 10 cells / μL, and collected under proliferating conditions. Cells were lysed in hypotonic buffer to collect cytoplasmic fraction. Nuclear proteins were separated into loose and tight chromatin-bound fractions using medium salt buffer and micrococcal nuclease. After collecting each fraction, the pellet was washed twice to wash out all residual proteins. Immunoblots were probed with antibodies against p300 (loose fraction), histone 3 (tight fraction) and vinculin (cytoplasmic fraction), to assess fraction purity. Olig2 is evenly distributed over loose and tight nuclear compartments. Distribution of total Olig2 protein is quantified in **(B)**. **(C)** Western blot analysis with phosphorylation state-specific antibody shows that phosphorylated Olig2 is most abundant in the

cells in hypotonic buffer to separate cytosol from nuclei. Nuclear proteins were further resolved into loose and chromatin-bound fractions by fractionation with high salt buffer and micrococcal nuclease.

As indicated in Figs. 6A and 6B, total Olig2 is evenly distributed over both intranuclear protein fractions. However, immunoblotting with the phosphorylation state-specific antibody to the triple serine motif shows that phosphorylated Olig2 is preferentially localized to the loose nuclear fraction (Figs. 6C and 6D). Impact of the phosphorylation motif on intranuclear localization of Olig2 was confirmed independently by transducing *Olig2*-null neural progenitor cells with *Olig2* TPN or TPM. As indicated in Figs. 6E and 6F, Olig2 TPM localizes preferentially to the loose compartment, whereas Olig2 TPN associates mainly with the condensed chromatin fraction.

Phosphorylated Olig2 and non-phosphorylated Olig2 have differential access to compartment-specific co-regulator proteins

An emerging theme in the biology of bHLH transcription factors is that these proteins per se do not actually regulate transcription. Rather dimers or heterodimers of bHLH proteins serve as "scaffolding" upon which to assemble a multimeric complex of transcription co-regulator proteins. Transcription co-regulators serve many functions but broadly speaking can be assigned into three groups—1) those that are components of the basal transcriptional machinery 2) those that modify the structure of chromatin and 3) other types of transcription factors. An example of the latter mechanism was reported by Ma *et al*. who showed that a double serine phosphorylation motif (Ser231, Ser234) in the carboxy terminal domain of Ngn2 regulates a physical interaction between Ngn2 and Lim homeodomain transcription factors via their NLI adaptor proteins (Ma et al., 2008).

loose chromatin fraction. Most Olig2 protein in tight fraction is unphosphorylated. This is quantified in **(D)**. **(E)** Subnuclear fractions were generated from *Olig2*-null mouse neural progenitor cells transduced with retrovirus encoding TPN or TPM Olig2 construct. Olig2 TPN is primarily located in the tight fraction, whereas Olig2 TPM is preferentially localized in the loose fraction. See **(F)** for quantification. Data represented are average of three independent experiments. LDH, lactate dehydrogenase (loading control). Error bar, SD. Unpaired t test, two-tailed, * = $p<0.05$.

To generate a list of potential Olig2 co-regulators, we transduced *Olig2*-null mouse neural progenitor cell with a doubly tagged (FLAG and HA) *Olig2* WT construct (Nakatani and Ogryzko, 2003), Using tandem affinity purification, we obtained highly purified preparations of Olig2 and associated proteins (Fig. 7A and Supplemental Table). Importantly, this material was prepared from cell nuclei that had been processed to include protein from both the loose and tight chromatin fractions.

Mass spectrometry analysis revealed presence of multiple transcriptional co-regulators in the Olig2 preparations (Fig. 7B). Immunoblotting studies showed that, with the exception of Olig2 itself and the closely related Olig1, most of these potential co-regulator proteins were localized to the soluble fraction (data not shown). However, one notable exception was nuclear factor 1 (Nfia/b/x), a member of the CCAAT-box family of transcription factors. Nfi controls the onset of gliogenesis during development and quiescence in adult neural stem cells (Deneen et al., 2006; Martynoga et al., 2013). As shown in Fig. 7C, Nfi is localized exclusively to the condensed chromatin fraction, whereas Hdac1 is preferentially localized in the loose compartment. We performed co-immunoprecipitation experiments with HA or control IgG and confirmed that Olig2 in the loose fraction binds to Hdac1, whereas Olig2 in the chromatin fraction interacts with Nfi (Fig. 7D). Importantly, the Hdac1 : Olig2 interaction is dependent on DNA binding, even though the interaction occurs in the loose compartment (Fig. 7E). In addition, Olig2 TPM has more access to Hdac1 compared to Olig2 TPN, and this is reflected in protein pull-down experiments (Fig. 7F). Summarized, we show here that key Olig2 co-regulator proteins are differentially sequestered to loose and tight chromatin wherein, as a consequence, they enjoy differential access to phosphorylated and non-phosphorylated Olig2.

Phosphorylated Olig2 colocalizes with p53 and Hdac1

Hdac1 is a known deacetylating enzyme for p53 *in vitro* and *in vivo* (Ito et al., 2002; Juan et al., 2000; Luo et al., 2000). As demonstrated in Fig. 8A, acetylated p53 protein localizes with Hdac1 and Olig2 in wild-type mouse neural progenitor cells (Fig. 8A). Also, these three proteins have binding sites on the promoter of a p53 target gene, *p21* (Fig. 8B, inset). This would allow for phos-

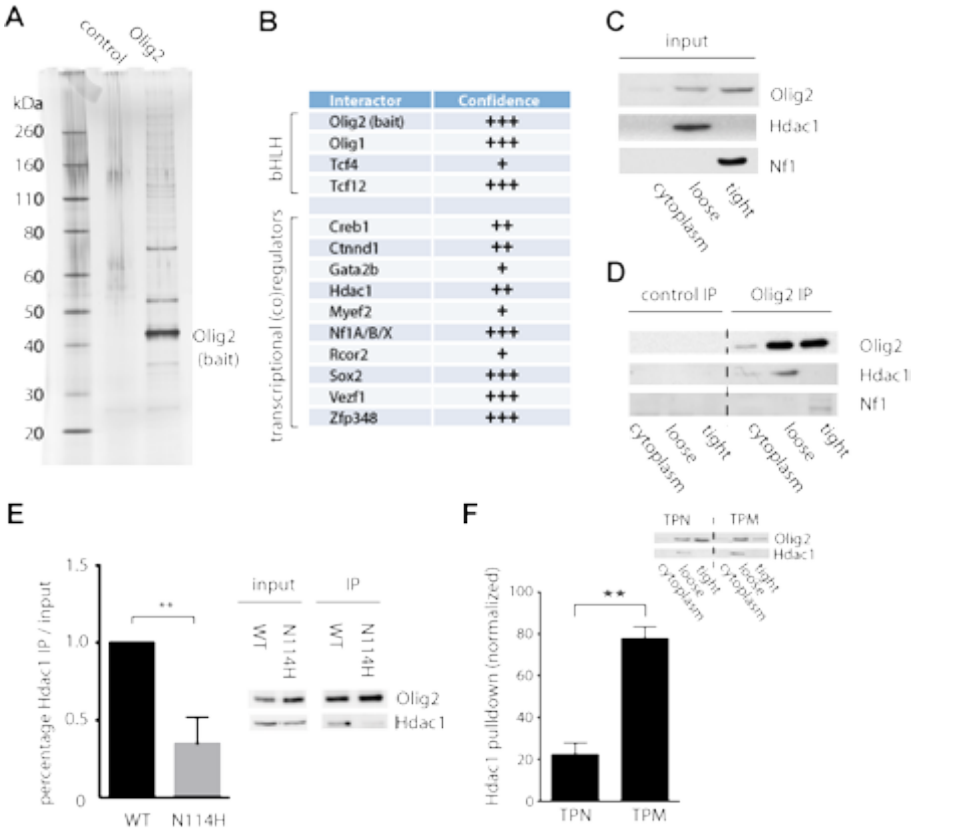

FIGURE 7. **Olig2 triple phosphorylation controls access to co-regulator proteins. (A)** *Olig2*-null mouse neural progenitor cells were transduced with an *Olig2* FLAG HA construct. Cell lysates were collected under proliferating conditions and subjected to FLAG pull-down followed by HA pull-down. Silver stain shows Olig2 and its protein co-regulator complex separated on 4–12% SDS PAGE gel. **(B)** Olig2 protein complex was analysed by LC-MS/MS and a subset of Olig2 interactors are shown. +++ = detected in 3 out of 3 repeats, ++ = detected in 2 out of 3 repeats, + = detected in 1 out of 3 repeats. **(C)** Mouse neural progenitor cells were collected and subnuclear fractions were generated using medium salt conditions and micrococcal nuclease treatment. Hdac1 is mainly present in the loose compartment, as demonstrated by immunoblot. Nuclear factor 1 (Nf1) is preferentially localized in the tight pool. **(D)** *Olig2*-null mouse neural progenitor cells were transduced with WT Olig2-v5. Antibody pull-down followed by Western blotting for Hdac1 shows that Olig2 interacts with Hdac1 in loose compartment. Olig2 interacts with NF1 in the tight fraction. Control = control IgG. **(E)** *Olig2*-null mouse neural progenitor cells were transduced with WT *Olig2*-v5 or Δ*Olig2*. Antibody pull-down was performed with total Olig2 antibody. Pull-down efficiency was determined as ratio IP / input of three independent repeats. Inset shows representative image of IP followed by Western blotting for Hdac1 antibody. Unpaired t test, two-tailed, ** = $p<0.01$. **(F)** *Olig2*-null mouse neural progenitor cells were transduced with WT Olig2-TPN or TPM. Antibody pull-down was performed with total Olig2 antibody. Bar graph shows quantification of Hdac1 pull-down in loose fraction only. Inset shows representative image of Olig2 IP followed by Western blotting for Hdac1 antibody. Unpaired t test, two-tailed, ** = $p<0.01$.

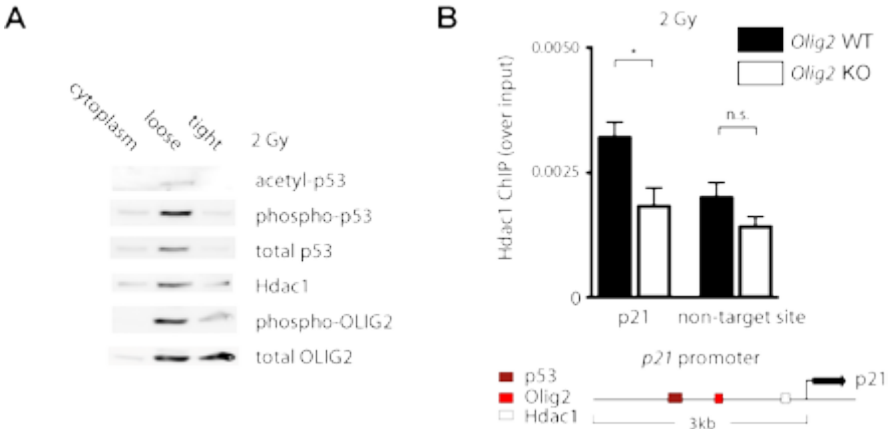

FIGURE 8. **Phosphorylated Olig2 colocalizes with Hdac1 and p53. (A)** Mouse neural progenitor cells were collected and subnuclear fractions were generated. Immunoblot for acetylated p53 (Lys379), phopshorylated p53 (Ser15) and total p53 shows that p53, Hdac1 and phosphorylated Olig2 colocalize before (data not shown) and after 2 gray irradiation treatment. **(B)** *Olig2* WT and *Olig2*-null cells were processed for ChIP with Hdac1 antibody. Immunoprecipitated DNA was analyzed with primers spanning the Hdac1 binding site on the p21 promoter region. Error bar, SD. Unpaired t test, two-tailed, * = $p<0.05$. Inset is a schematic overview of the mouse p21 promoter containing binding sites for Olig2, p53 and Hdac1.

phorylated Olig2 to recruit Hdac1 and bring it into close proximity to p53. As such, phosphorylated Olig2 might indirectly affect p53 acetylation levels, as observed in previous studies (Mehta et al., 2011; Sun et al., 2011). Importantly, *Olig2*-null mouse neural progenitor cells indeed have less Hdac1 loaded onto the *p21* promoter element compared to *Olig2* WT cells (Fig. 8B).

Discussion

In previous work we have shown that in neural progenitor cells, the bHLH transcription factor Olig2 functions as a developmentally regulated suppressor of p53 (Mehta et al., 2011; Sun et al., 2011). Anti-p53 functions of Olig2 are exerted by modulating the phosphorylation state of an N-terminal triple serine motif. In studies summarized here, we address an important unresolved question. How does the phosphorylation state of the triple serine motif modulate biological responses to Olig2? Our initial efforts to address this question revealed some-

thing of a paradox: On one hand, the pro-mitogenic, anti-p53 functions of Olig2 clearly require it to function as a transcription factor by binding to canonical E-box promoter/enhancer elements. On the other hand however, the phosphorylation state of the amino terminal motif has no apparent impact on target gene binding. This apparent paradox may be resolved by the observation that phosphorylation impacts the intranuclear localization of Olig2. These observations collectively raise a series of additional interesting and unresolved questions.

Phosphorylation state of Olig2 and DNA binding

Previously, we have shown that the phosphorylation state of Olig2 opposes p53 functions (Mehta et al., 2011; Sun et al., 2011). In this study, we demonstrate that neural progenitor cells expressing a DNA binding mutant of Olig2 cannot oppose p53 functions (Fig. 2). What is the connection between the triple phosphorylation motif and DNA binding in Olig2? As shown here, Olig2 phosphorylation results in a change in intranuclear localization of Olig2 protein. Particularly, unphosphorylated Olig2 binds targets in the condensed chromatin fraction, whereas phosphorylated Olig2 is associated with the loose binding fraction (Fig. 6). However, there are approximately one hundred amino acids between the triple phosphorylation motif and the basic domain. How does a phosphorylation motif that far away from the DNA targeting domain affect DNA binding? We might speculate that the N-terminal folds over towards the bHLH domain to contribute to DNA binding. Negatively charged phosphates in close vicinity of an E-box sequence on the DNA likely results in repulsion between the protein and the—negatively charged—DNA (Brownlie et al., 1997; Mitsui et al., 1993; Neufeld et al., 2000). Conversely, an unphosphorylated serine motif will have increased affinity for DNA. Thus, upon triple phosphorylation, the N-terminal of Olig2 might be released from the DNA because of the repulsive force. Subsequently, the N-terminal will become available for partner protein recruitment, such as Hdac1. Alternatively, tight DNA binding by unphosphorylated Olig2 might locally condense the DNA and make it inaccessible for binding of other transcription factors and co-regulators. This would obstruct Hdac1 from accessing the promoter regions occupied by unphosphorylated Olig2. Upon phosphorylation, Olig2 binds DNA more loosely and coregulators might be able

to access their DNA binding sites. Our experimental data support the latter model, because the Olig2 : Hdac1 interaction is dependent on DNA binding (Fig. 7E).

Lessons learned from Olig2 ChIP-seq data

To determine the effect of Olig2 phosphorylation on target gene binding, we performed ChIP-seq analysis of Olig2 WT, TPN and TPM in cycling neural progenitor cells. Previously, Olig2 WT ChIPseq experiments have been carried out in motor neuron progenitor cells and oligodendrocyte progenitor cells (OPCs) (Mazzoni et al.; Yu et al., 2013). We characterized the Olig2 preferred E-box as CAGCTG, corresponding to previous findings (see Fig. S3) (De Masi et al., 2011; Mazzoni et al.; Yu et al., 2013). In addition, we have identified CAT as an E-box halfsite recognized by Olig2, but mostly in presence of the CAG halfsite (i.e. only CAGATG and CATCTG but not CATATG). This halfsite has not been detected by Olig2 ChIP-seq in OPCs, and this suggests that Olig2 functions with a different bHLH dimerization partner in OPCs compared to neural progenitor cells.

Olig2 has traditionally been known as transcriptional repressor because of its function in the developing CNS (Lee et al., 2005; Novitch et al., 2001). Specifically, by repressing *Hb9* gene expression, the replication-competent state of motor neuron progenitors is sustained in the developing spinal cord (Lee et al., 2005). Importantly, by combining our ChIPseq study with RNA sequencing, we do not see a bias for direct target genes that are transcriptionally repressed. Thus, we state that Olig2 can function as transcriptional repressor, as well as a transcriptional activator in neural progenitor cells. In addition, we have identified certain co-regulator proteins that are transcriptional activators (e.g. Creb1) and repressors (e.g. Myef2 and Ncor2).

Olig2 co-regulator complex

Many transcription factors contain at least two domains; the DNA binding domain and a dimerization domain for protein:protein interactions. The choice of dimerization partner depends on developmental stage and tissue type. Proteins that belong to the bHLH family typically bind ID proteins or E proteins that respectively inhibit or activate their function. Here, we have identified sever-

al bHLH proteins as potential dimerization partner for Olig2 in mouse neural progenitor cells, namely Tcf4, Tcf12 (both E proteins) and Olig1 (Fig. 7). Also, we have identified several homeodomain proteins (Adnp, Hdx, Zeb2/Sip1, Pbx1 and Prox1) that interact with Olig2 (see Supplemental Table). Homeodomain (HD) proteins frequently interact with bHLH proteins to regulate tissue-specific development (Babu et al., 2008; Makarenkova et al., 2009; Poulin et al., 2000). Interestingly, an HD protein that is a well-established interactor of Olig2, Nkx2.2, did not show up in our pull-downs. However, Nkx2.2 is involved in specification of V3 interneurons and maturation of oligodendrocytes, and does not have a known function in proliferation of neural progenitor cells (Briscoe et al., 1999; Sun et al., 2003). Even though most other known interactors of Olig2 are based on COS7 cell overexpression experiments, we have confirmed Olig1 and Nfi as bonafide Olig2 interactors in cycling neural progenitor cells (Deneen et al., 2006; Li et al., 2007). Of note, it is unlikely that HD or bHLH proteins are directly affected by triple serine phosphorylation because both these proteins bind directly to the bHLH motif in Olig2 (Li et al., 2007; Sun et al., 2003).

Regulation of p53 functions by acetylation

Upon genotoxic damage, p53 is phosphorylated and subsequently acetylated to stabilize DNA binding. The acetylation state of p53 is controlled by acetylating enzymes, such as p300/CBP, and deacetylating enzymes, for instance Hdac1. Hdac1 has been shown to deacetylate p53 directly, both *in vitro* and *in vivo* (Ito et al., 2002; Juan et al., 2000; Luo et al.). We propose a mechanism by which phosphorylated Olig2 presents Hdac1 to p53 and thus inhibits p53 function. We show that Hdac1, p53 and Olig2 all colocalize in the loosely bound fraction (Fig. 8A). Importantly, in Olig2 KO neural progenitor cells (with high p53 acetylation status) less Hdac1 is loaded onto the p21 promoter, compared to Olig2 WT cells (with low p53 acetylation status), after 2 gray irradiation (Fig. 8B).

Olig2 co-regulator proteins as therapeutic targets?

Human tumor microarrays in combination with mouse modeling studies of human glioma indicate that a small molecule inhibitor of Olig2 might serve as

a targeted therapeutic for a wide range of pediatric and adult gliomas. (Ligon et al., 2004; Ligon et al., 2007). However, an anti-tumor therapy that generally targets all Olig2 activity in the brain (e.g., shRNA) might have severe off-target effects in non-tumor cells, such as oligodendrocytes. Moreover, transcription factors have been unattractive targets for drug development because their complex interactions with DNA and co-regulator proteins.

In contrast to transcription factors, protein kinases lend themselves readily to the development of small molecule inhibitors. Previous studies have indicated that the functions of Olig2 critical for glioma growth are distinguished by several phosphorylation sites (Huillard et al., 2010; Li et al., 2011; Setoguchi and Kondo, 2004; Sun et al., 2011). Current research in our lab is focused on the identification of the kinase(s) that phosphorylate Olig2 on Serine 10,13 and 14.

Alternatively, protein co-regulators that are crucial for Olig2 function might be another avenue to specifically target Olig2-dependent tumor growth. Especially, co-regulator proteins that are specific to Olig2 TPM but do not interact with Olig2 TPN would be attractive candidates. Although most of the discussed Olig2-interacting proteins are transcription factors themselves, several cofactors and enzymes have been identified in the Olig2 protein complex (Supplemental Table). Eventually, specific small molecule inhibitors of Olig2 co-regulator proteins could have practical overtones for patients with glioma, and provide a targeted therapy with minimized side effects in non-tumor cells.

Methods

Animal procedures, tissue harvest and cell culture

Animal husbandry was performed according to DFCI guidelines under IACUC-approved protocols. The strains used have been described previously (Lu et al., 2002). Neural progenitor cells were isolated from lateral ganglionic eminence (LGE) of E13.5 embryos from time-pregnant mice using techniques previously described (Qian et al., 1998). Cells were maintained as neurosphere cultures in poly(2-hydroxyethyl methacrylate) (Sigma) coated plates in DMEM and F12 supplemented with B27 (Invitrogen) and N2 (Invitrogen), in presence of 20ng ml-1 Egf (Millipore) and 20ng ml-1 bFgf (Millipore) (Ligon et al., 2007; Sun et al., 2011). Neural progenitor cell lines transduced with retroviruses con-

taining various constructs of Olig2 were maintained in media as described above, in addition of 2 ug ml-1 blasticidin.

Retroviral Vectors and Virus Production

Olig2 constructs containing triple phosphorylation motif variants and DNA binding mutations were generated using QuikChange Site-Directed Mutagenesis (Stratagene) (Sun et al., 2011). Full-length mouse *Olig2*, its various mutants, or EGFP was cloned into the PWZL-BLAST retroviral vector as previously described (Sun et al., 2011 2011). Retroviruses were generated in 293T cells by transfection with packaging plasmids encoding VSVG, gag-pol, and the retroviral vector (PWZL) encoding *Olig2* construct of interest.

Secondary neurosphere assay

Olig2-null neural progenitor cells were transduced with retroviruses containing various mutants of *Olig2* under neurosphere culture conditions. Transduced cells were selected with blasticidin for 7 days. Primary transduced neurospheres were dissociated into single cells and replated at 10 cells ml-1 in 6-well plates for secondary neurosphere formation assays. Total viable cells were counted with hemocytometer using 0.2% trypan blue exclusion. The neurosphere images were taken using a 2x objective on a Nikon Eclipse TE200.

Immunoblotting

Immunoblotting was performed according to standard protocols using rabbit polyclonal anti-Olig2 antibody (1:100,000), monoclonal mouse anti-Olig2 antibody (1:2,000) (Arnett et al., 2004), phospho Olig2 antibody (Sun et al., 2011), and antibodies directed against p21 (BD Pharmingen), acetyl-p53 (Lys379, 2570, Cell Signaling Technology), phospho-p53 (Ser15, 9284, Cell Signaling Technology), total p53 (2524, Cell Signaling Technology), Olig1 (our laboratory), Histone H3 (Ab10799, Abcam), p300 (05-257, Millipore), Ldh (Abcam), Hdac1 (2062, Cell Signaling Technology), Nf1 (Ab72602, Abcam) and vinculin (V9131, Sigma-Aldrich).

Chromatin immunoprecipitation

Mouse neural progenitor cells transduced with various mutants of Olig2 were plated at a density of 10 cells ml-1 and cultured on laminin-coated 6-well plates (Pollard et al., 2009). Cells were crosslinked with 1% formaldehyde for 10 min at RT and reaction was quenched with 125 mM glycine for 5 min at RT. Cells were harvested in ice-cold PBS and sonicated in 300 ml SDS lysis buffer. For immunoprecipitation, 50 ul protein A dynabeads (Invitrogen) were incubated with Olig2 or IgG antibody for at least 4 hours at 4°C. Precleared chromatin and antibody-bound beads were incubated overnight at 4°C. Beads were washed six times in RIPA wash buffer and twice in TE. After overnight reverse crosslinking at 65°C in reverse crosslinking buffer (200 mM NaCl, 1% SDS, and 0.1 M $NaHCO_3$), immunoprecipitated DNA was submitted to PCR cleanup (QIAGEN) and eluted in ddH2O. Chromatin-immunoprecipitated DNA was analyzed with quantitative PCR in real-time PCR system (Applied Biosystems), using SYBR green mix. Presented data are delta CT values normalized for WT promoter occupancy.

Gene	Forward	Reverse
Egfr	GTGGTCCCAATTTCCTGCTG	ATGGAGCTCATGGACCTCATTG
Fgfr3	TAGACCCCCACCGAAGTCAA	GACTGTCTACCAGCACGCTT
Wnt5a	TCTCGCTCTGTTCTCTCTGGA	CTTGAGCGGTTGATGGACAG
p21 (Olig2)	AGGTCAGCTAAATCCGAGGAGGAA	TCCTGCTTTGGAGAAGCTGTGAGT
Tgfb2	CTCCTGCAGCTCTGTTGTGA	TTTATTTCTTTGCTTGCTTGCTTT
Epha2	ATCCCATTCACCCCACACAC	GTCACCAGGCTTTCAGCTCT
p21 (Hdac1)	GCTGCGTGACAAGAGAATAGC	GTCGAGCTGCCTCCTTATAG
p21 (p53)	GGTCCCTTGGATTTCCTTTC	CTTCAATTCCAGGGCTGAAC

Quantitative PCR

For q-PCR analys, RNA was isolated using Trizol and RNeasy Mini kit (Qiagen). At least 1 ug of RNA was used for CDNA synthesis with Superscript III reverse transcriptase (Invitrogen). Taqman assays were performed for target genes and controls (beta-actin and ubiquitin C) on 100x diluted CDNA template.

ChIP library construction and sequencing

Library construction and sequencing on immunopurified DNA fragments and control (input) samples were performed according to standard guidelines of Bejing Genomics Institute on HiSeq 2000 (Illumina).

ChIP-seq analysis

Sequence reads were aligned to mouse genome (mm9) using TopHat with default settings (min anchor 8, splice mismatches 0, min report intron 50, max report intron 500000, min isoform fraction 0.15, max multihits 20, segment length 19, segment mismatches 2, min closure exon 100, min closure intron 50, max closure intron 5000, min coverage intron 50, max coverage intron 20000, min segment intron 50, max segment intron 500000) with the exception of segment length ½ average read length of cleaned data. Peak calling was performed using MACS2 (Model-based Analysis of Chipseq) using default parameters (Feng et al., 2012 and Tao Liu, personal communication). Annotated peaks were then assigned to genes within 30.000 bases of transcription start sites using Peak2gene tool in Cistrome. Motif analysis was performed in 600bp windows with a p-value cutoff of 0.001 on top 5000 peaks for WT, TPN and TPM ChIPseq samples using SeqPos motif tool in cistrome (He et al., 2010).

RNA-seq library preparation and sequencing

RNA was isolated from ~10 million cells using Trizol followed by RNeasy Mini kit (Qiagen). Samples were subjected to hybridization with Locked Nucleic Acid probes specific for abundant ribosomal RNA molecules. Unwanted rRNA was separated using RiboMinus Magnetic beads. The RiboMinus-enriched RNA sample was then used for cDNA library preparation using GenomePlex Complete WGA Kit (Sigma). Each cDNA library was sequenced at the Dana Farber Center for Cancer Computational Biology on an Illumina Genome Analyzer II following manufacturer's protocol.

RNA-seq analysis

Raw 50bp paired-end sequence data were quality controlled with FastQC using Galaxy platform. Sequence reads were groomed and trimmed to increase per base sequence quality by Trim sequences tool and Filter by quality tool using a cut off for quality score of above 30. Sequences were mapped on to NCBI37/mm9 using Tophat 1.4.1 (http://tophat.cbcb.umd.edu/index.shtml) with segment length = 19 and the same settings as indicated above for ChIP seq analysis (Langmead et al., 2009). Mappable data were then processed by RNA-seq analysis program Cufflinks using the Cistrome platform (Liu et al., 2011; Trapnell et al., 2010). Assuming the total transcriptional activity is comparable between different datasets, the obtained data (data units in RPKM, reads per kilobase exon model per million mapped reads) were analyzed using Cuffdiff to find significant changes in transcript expression (settings: Perform quartile normalization and bias correction, FDR=0.05). The output file 'gene differential expression testing' was used to sort for significant differentially expressed genes.

Electrophoretic mobility shift assay

Olig2 protein was purified from cos7 cells by immunoprecipitation with v5 antibody (Sigma) and v5 peptide (Sigma) elution, followed by immunoprecipitation with Ni-NTA beads (Qiagen) and elution in 200mM imidazole. Purified Olig2 protein was quantified by silver stain against known concentrations of BSA protein. Oligonucleotides used for EMSA are: AGCTAATTTCCCAGATGGGCCAA and AGCTTTGGCCCATCTGGGAAATT (*Hb9*), AGCTAGAAGACAGCTGTTGGAAG and AGCTCTTCCAACAGCTGTCTTCT (*Mycn*). Oligonucleotides were annealed in annealing buffer (10mM Tris HCl pH7.5, 50mM NaCl, 1mM EDTA) using a thermocycler for 5 min at 95°C, and allowed to cool down for approximately 1 hour. Annealed probe was labeled with [α-^{32}p] 6000 Ci mmol-^{1} dCTP (PerkinElmer) using Klenow (New England Biolabs). Radioactive DNA probe was incubated with 2 ng Olig2 protein in binding buffer (20mM Tris-HCl pH7.5, 5mM MgCl2, 0.1% NP40, 0.5mM DTT, 10% glycerol) for 30 min at 4°C. Protein:DNA complex was analyzed on 4% non-denaturing poly-acrylamide gel electrophoresis (PAGE) for 30 min at 4°C.

Subcellular fractionation

Primary mouse neural progenitor cells were centrifuged at 1000 rpm to collect cell pellets. Cell pellets were treated with 5x pcv hypotonic buffer (10mM Hepes pH 7.9, 1.5mM MgCl2, 10mM KCl) and centrifuged at 6000 rpm to collect nuclei. Supernatant was treated with 0.11 volume 10x cytoplasmic extract buffer (0.3M Hepes, 1.4M KCl, 0.03M MgCl2). Cell nuclei were incubated in mild salt buffer (20mM Hepes pH7.9, 10% glycerol, 1.5mM MgCl2, 0.2mM EDTA, 150mM KCl) for 10 min on ice and rotated for 10 min at 4°C. Soluble nuclear protein fraction was collected by centrifugation at 10.000 g. Chromatin-bound proteins were extracted by incubating with 4 units mL^{-1} micrococcal nuclease (Sigma) in MNase buffer (20mM Tris-HCl pH7.5, 100mM KCl, 3mM MgCl2, 1mM CaCl2) for 10 min on ice. Reaction was quenched by addition of 2mM EDTA in buffer B (50mM Tris-HCl pH7.5, 0.05% NP40, 100mM KCl, 10% glycerol), followed by centrifugation at max speed for 10 min to separate chromatin-bound proteins from insoluble fraction. All buffers were supplemented with EDTA-free protease inhibitors (Roche), 1mM $Navo_4$, 5mM NaF, 1mM $Na_4P_2O_7$, 25mM beta-glycerophosphate and 0.5mM PMSF.

Immunoprecipitation

Olig2-null mouse neural progenitor cells were transduced retrovirus encoding v5-tagged *Olig2* constructs. Subcellular fractions were generated as described above and each fraction was incubated with v5 (Sigma) or Myc (Sigma) antibodies overnight rotating at 4°C. Antibody-bound fractions were washed four times in buffer B (see above) over bio-spin column (Biorad) and incubated with 0.5 mg ml^{-1} v5 peptide for 30 min at 4 °C. Immunopurified fractions were collected by centrifugation at 8000 rpm for 1 min at 4 degree and analyzed by standard SDS-PAGE followed by immunoblotting.

Tandem affinity purification

Subcellular fractions from *Olig2*-null mouse neural progenitor cells transduced with FLAG and HA-tagged *Olig2* were prepared as described above. Tandem affinity purification was performed by M2 FLAG affinity gel-based purification

and 0.5 mg ml-1 3x FLAG peptide (Sigma) elution in buffer B (see above), followed by HA affinity gel capture (Santa Cruz Biotechnology). Finally, protein complexes were eluted in 0.5 mg ml-1 HA peptide (Covance) in elution buffer (50mM Tris-HCl pH7.5, 0.01% NP40, 100mM KCl, 10% glycerol) and 10% of eluted fraction was separated on SDS 4–12% bis tris polyacrylamide gradient gels (Invitrogen) and visualized by silver stain with Silver Quest staining kit (Invitrogen) (Nakatani and Ogryzko, 2003). Purified protein complexes were analyzed by mass spectrometry LC/MS-MS as described elsewhere (Adelmant et al., 2012).

Immunofluorescence

Mouse neural progenitor cells transduced with retrovirus encoding various *Olig2* constructs were plated on poly-L-ornithine coated coverslips in 24-well plate at 20 cell ul-1 per well. After 72 h, cells were fixed with 4% paraformaldehyde. Coverslips were incubated with 5% normal goat serum (NGS) and 0.2 % Tween. Primary antibody solutions were applied for 1 hour at RT, followed by secondary antibody staining for 30 min at RT, and shortly exposed to DAPI for nuclear staining. Coverslips were mounted on slides with fluoromount and analyzed with a Zeiss Axio Observer.Z1

Statistical analysis

For each experiment, data were collected from at least three biological repeats and analyzed by One-way ANOVA with Posthoc Tukey test or Student's t-test, as indicated. SD, standard deviation; SEM, standard error of the mean; *, $p<0.05$; **, $P<0.01$; ***, $P<0.001$

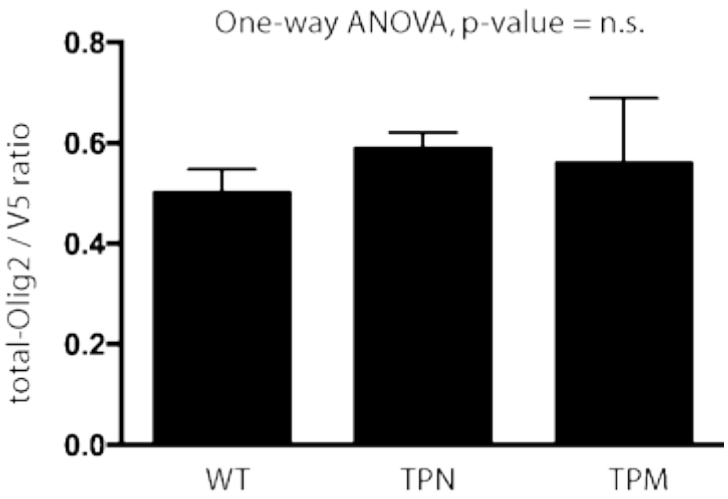

SUPPLEMENTAL FIGURE S1. **Total Olig2 antibody has equal affinity for Olig2 WT, TPN and TPM.** COS7 cells were transduced with retroviral expression vectors for *Olig2* WT, TPN or TPM in combination with a carboxy terminal V5 tag. Cell lysates were collected and prepared for SDS-PAGE size fractionation followed by Western blotting with either V5 or total Olig2 antibody. Quantitative analysis shows no preference of total Olig2 antibody for either of the three variants.

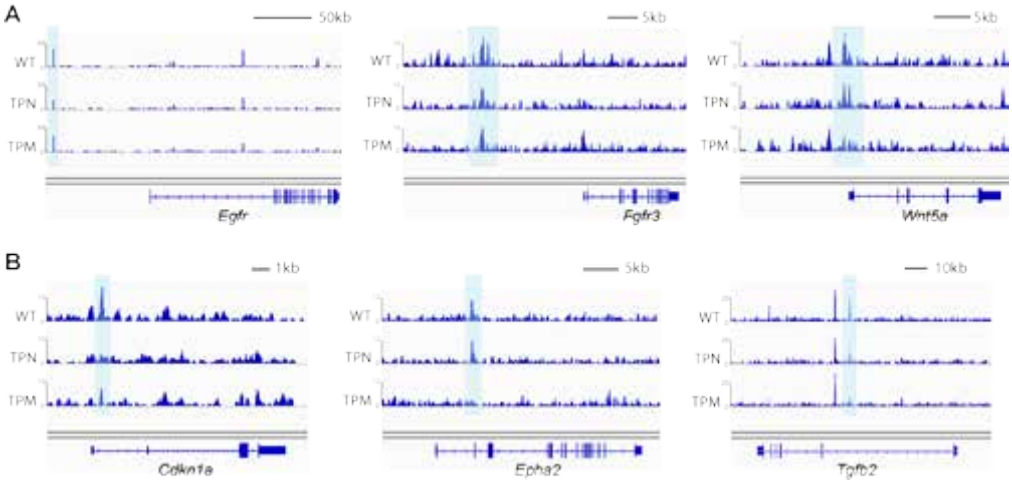

SUPPLEMENTAL FIGURE S2. **ChIPseq data in IGV**. Integrated Genome Viewer (IGV) images of genes that are differentially regulated by TPM/TPN but show no difference in occupancy by TPM/TPN. MACS2-identified peaks are shaded in blue.

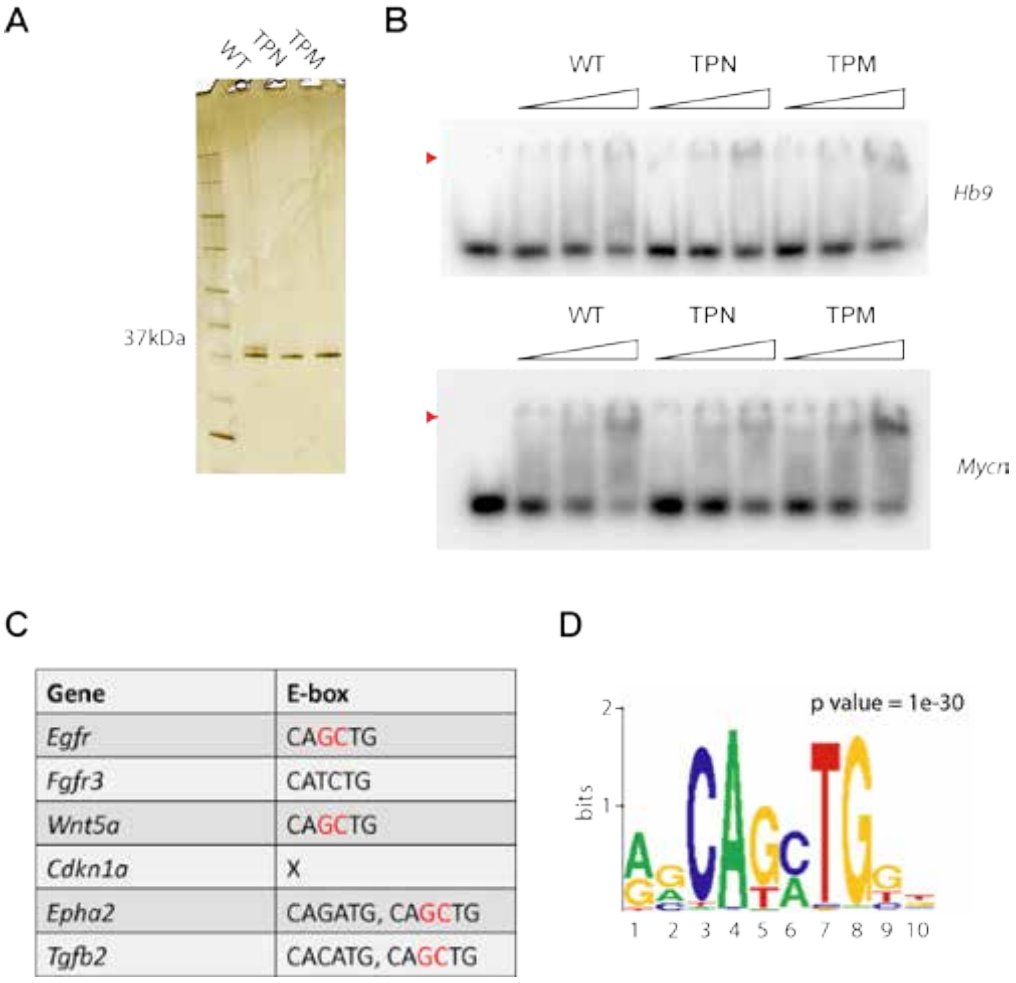

Gene	E-box
Egfr	CAGCTG
Fgfr3	CATCTG
Wnt5a	CAGCTG
Cdkn1a	X
Epha2	CAGATG, CAGCTG
Tgfb2	CACATG, CAGCTG

SUPPLEMENTAL FIGURE S3. **Gel mobility shift assay with purified Olig2 protein**. **(A)** Olig2 protein was overexpressed in COS7 and tandemly purified by means of V5 and Ni-NTA column pull-down. Purified protein was size separated on SDS-PAGE gel and visualized with silver stain. **(B)** Increasing concentrations of Olig2 WT, TPN or TPM purified protein was incubated with radioactive DNA probe *Hb9* or *Mycn*. Red arrowhead, protein : DNA complex. **(C)** E-box element in the 6 target genes that are differentially expressed in TPM / TPN. **(D)** Motif analysis of ChIP-seq data reveals CAGCTG as most prominent E-box in Olig2-binding sites in cycling mouse neural progenitor cells (see Methods section)

	1	2	3	Total	Total #peptides
Olig2	12	18	18	3	48
Ddx5	11	10	11	3	32
Olig1	4	10	11	3	25
Top2a	7	8	3	3	18
Trim28	4	7	1	3	12
Tardbp	4	2	4	3	10
Khsrp	3	1	5	3	9
Prmt5	1	3	4	3	8
Rbbp4	2	4	2	3	8
Mta2	1	2	3	3	6
Mybbp1a	3	2	1	3	6
Nfib	2	2	1	3	5
Adnp	1	1	2	3	4
Hmga2	1	2	1	3	4
Creb1	1	1	1	3	3
Trps1		6	3	2	9
Tmpo	3	5		2	8
Smarca5	3	4		2	7
Hdx		5	1	2	6
Rbm39	2		3	2	5
Hip1	3	1		2	4
Mcm3	2	2		2	4
Nfia		1	3	2	4
Ruvbl1	2	1		2	3
Sox2	1	2		2	3
Chd4	1	2		2	3
Hdac1	1	2		2	3
Tcf12	1	2		2	3

SUPPLEMENTAL TABLE. **Overview of Olig2 pull-down mass spectrometry data.** Proteins involved in 'regulation of transcription' were selected from the complete list of interacting proteins using Database for Annotation, Visualization and Integrated Discovery (DAVID) website.

Continues on pages xx–xxx

	1	2	3	Total	Total #peptides
Khdrbs1	1		1	2	2
Psip1	1	1		2	2
Wdr77		1	1	2	2
Cand1	1	1		2	2
Ilf2	1		1	2	2
Mbd1	1	1		2	2
Nacc1		1	1	2	2
Kdm1a		1	1	2	2
Mta1		1	1	2	2
Rbm15			5	1	5
Zfp319			3	1	3
Hdac2			2	1	2
Mcm5	2			1	2
Nr2f1	2			1	2
Ybx1		2		1	2
Gm5196		2		1	2
Sall3		2		1	2
Snd1	2			1	2
Tcf4		2		1	2
Zfp26			2	1	2
Xrn2			1	1	1
Ctcf			1	1	1
Gatad2b		1		1	1
Fiz1			1	1	1
Rcor2		1		1	1
Rbm15b			1	1	1
Ruvbl2		1		1	1
Smarcd3	1			1	1
Baz1b			1	1	1
Cask	1			1	1
Ctnnd1		1		1	1
Carm1	1			1	1

	1	2	3	Total	Total #peptides
Dmrtc2			1	1	1
Gtf2i		1		1	1
Ilf3	1			1	1
Mecp2			1	1	1
Mcm7		1		1	1
Nono			1	1	1
Mapk1	1			1	1
Nfix			1	1	1
Nfatc1		1		1	1
Nsd1			1	1	1
Prdx2		1		1	1
Pbx1			1	1	1
Pogz	1			1	1
Tceb2			1	1	1
Cnot1		1		1	1
Gm6917			1	1	1
Pdcd11			1	1	1
Prox1			1	1	1
Purb			1	1	1
Rnf2			1	1	1
Sall2			1	1	1
Ssbp2			1	1	1
Sf1			1	1	1
Tcf7			1	1	1
Tsg101			1	1	1
Uhrf1		1		1	1
Zeb2			1	1	1
Zfp512	1			1	1
Zfp748		1		1	1
Zmym2			1	1	1

SUPPLEMENTAL TABLE. *Continued from page pages xxx.*

4 Targeting bHLH transcription factor Olig2 using stabilized alpha-helical peptidomimetics

Dimphna H. Meijer,* Amanda Lee Edwards,*
Remco Molenaar, Valeria Bevilaqua, Michael Kane,
John Alberta, Federico Bernal, Yoshihiro Nakatani,
Charles Stiles and Loren D. Walensky

Abstract

Basic helix-loop-helix (bHLH) transcription factor Olig2 regulates proliferation of neural progenitor cells during central nervous system development. This anti-neurogenic / pro-mitotic function of Olig2 is recapitulated in tumor progenitor cells derived from human glioma tissue. Importantly, Olig2 meets the requirements for a suitable therapeutic target to inhibit brain tumor growth, because it is essential for brain tumor growth, specific to the central nervous system and dispensable for mature brain function.

Generally speaking, bHLH transcription factors like Olig2 require dimerization to carry out their downstream functions. Here, we tested a set of stabilized alpha-helical (SAH) mimetics for their ability to interfere with Olig2 dimerization and thus Olig2 function. Hydrocarbon stapling successfully produced a number of alpha-helical peptides mimicking a single helix or the entire HLH domain of Olig2. However, none of the SAH OLIGOpeptides specifically and potently disrupted Olig2 dimerization and subsequent DNA binding. We conclude that the HLH domain is required, but perhaps not sufficient for Olig2 dimerization. Possibly, the Olig2 C-terminal region gives supporting structure to the HLH domain, consequently stabilizing Olig2's dimeric complex.

Introduction

During development of the central nervous system, bHLH transcription factor *Olig2* is expressed in neural progenitor cells, regulating self-renewal as well as differentiation into neurons and oligodendrocytes (Ligon et al., 2007; Lu et al.,

2002; Zhou and Anderson, 2002). In the postnatal brain, *Olig2* expression is maintained in transit-amplifying cells of the subventricular zone, NG2-positive glia and mature oligodendrocytes (Lu et al., 2000; Menn et al., 2006; Zhou et al., 2000). In addition to its developmental functions, *Olig2* is expressed in 100% of diffuse human gliomas, where it identifies a subset of highly tumorigenic cells that are resistant to radiation and chemotherapy (Ligon et al., 2004; Lu et al., 2001; Marie et al., 2001; Ohnishi et al., 2003). Beyond simply marking glioma progenitor cells, Olig2 is required for brain tumor growth in a genetically relevant mouse model of human gliomas (Appolloni et al., 2012; Bao et al., 2008; Barrett et al., 2012; Ligon et al., 2007; Mehta et al., 2011). The pro-mitotic role of Olig2 is partly attained through its N-terminal triple serine motif that — when phosphorylated—opposes p53 functions, both in normal neural progenitor cells and their malignant equivalents (Mehta et al., 2011; Sun et al., 2011).

Olig2 serves as a promising drug target in the search for effective brain tumor medicine for three reasons. Firstly, *Olig2*, and its close relative *Olig1*, are expressed exclusively in the central nervous system (Lu et al., 2000; Takebayashi et al., 2000; Zhou et al., 2000). Secondly, although Olig2 has an essential role during CNS development, it seems largely dispensable for mature CNS function (Chen et al., 2008). Finally, Olig2 is required for tumor formation in a mouse model for glioma, as well as for growth of intracranially injected human primary tumor cells (Ligon et al., 2007; Mehta et al., 2011).

Unfortunately, transcription factors have historically been cast aside as therapeutic targets due to the difficulty of targeting their complex protein-protein and protein-DNA interaction surfaces. Recently, progress has been made in interfering with both these interaction types. For instance, zinc finger nucleases have been used to target specific DNA binding sequences, while small molecules and short peptides have been designed to disrupt specific transcription factor protein-protein binding interfaces (Follis et al., 2008; Nickols et al., 2007; Shi et al.).

Regarding bHLH transcription factors, nature has already provided a solution for disruption of their function. The Id proteins, which have a HLH domain but lack a basic region and thus cannot bind to DNA, serve as natural dominant negatives through the formation of nonfunctional heterodimers (Benezra et al., 1990). Several approaches have been taken to artificially reproduce this type of in-

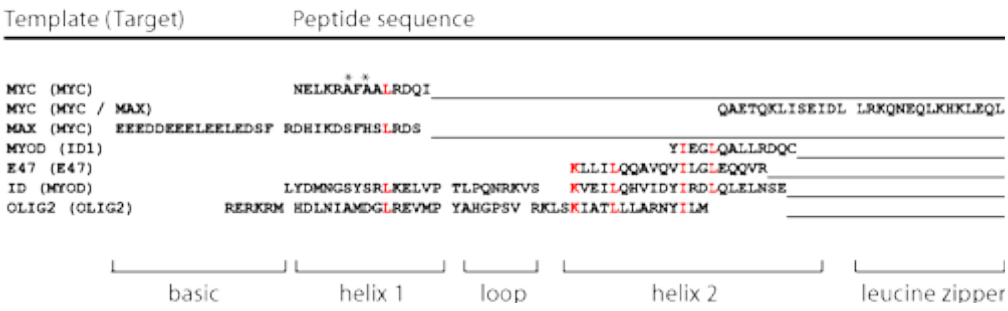

TABLE 1. **Overview of alpha-helical mimetics designed to target bHLH proteins** (see text for references). The helix 1 Myc peptidomimetic contains two amino acid substitutions (marked with "*") compared to the native Myc sequence. Notably, it has been reported that an inverted sequence of the same peptide, attached to an internalization sequence, can inhibit growth of an HCT-116 colon carcinoma cell line at 10μM dose (Pescarolo et al., 2001). Three single amino acid mutations in the inverted peptide sequence (Glu2Ala, Asp11Ala and Gln13Ala) show even more than 100% growth inhibition (i.e. cell death) in such cell-based assay (Nieddu et al., 2005).

teraction through the generation of HLH domain peptidomimetics (see Table 1). For instance, a peptide spanning the HLH domain of Id was able to inhibit DNA binding of a myogenic bHLH protein, MyoD, and its dimerization partner E47, in a gel mobility shift assay (Fairman et al., 1993). Conversely, a peptide modeled on the helix 2 of MyoD was able to bind Id1 *in vitro*, and negatively affect cell viability in a panel of cancer cell lines (Chen et al., 2010). In a follow-up study, the authors designed N-terminal and C-terminal deletion constructs of their MyoD peptide to optimize inhibition of cell growth (Yang et al., 2011). Unfortunately, the previously published effect of the peptide on human breast cancer cell growth (~80% inhibition) is much less dramatic (~20%) in this follow-up paper. Using a similar approach, peptides designed against helix 2 of the bHLH protein E47, were shown to disrupt E47 homodimerization *in vitro* at low micromolar doses, as shown by gel mobility shift assays, size-exclusion gel chromatography, protein crosslinking and analytical ultracentrifugation (Ghosh and Chmielewski, 1998; Ghosh et al., 1999).

Several groups have utilized peptidomimetics to probe the interaction between the bHLH leucine zipper protein Myc and its dimerization partner Max. Peptides designed against helix 1 or the leucine zipper domain of the Myc : Max heterodimer have shown variable efficacy in cellular systems (Draeger and Mullen, 1994; Giorello et al., 1998; Krylov et al., 1997; Nieddu et al., 2005;

Pescarolo et al., 2001). Notably, the leucine zipper region is the predominant contributor to successful binding of the Myc/Max peptides to their bHLH counterparts (D'Agnano et al., 2007; Savino et al., 2011; Soucek et al., 1998; Soucek et al., 2002).

In the studies described above, two principal difficulties have been noted. First, while the HLH domain consists of two alpha-helical regions, the HLH peptidomimetics had little secondary structure, thus unsuccessfully mimicking the native binding interface (Draeger and Mullen, 1994; Ghosh and Chmielewski, 1998). Second, unmodified short peptides usually have limited proteolytic stability in a cellular environment (D'Agnano et al., 2007). To address these difficulties, we have utilized a hydrocarbon crosslinking technique, in which *i,i+4* residues of the peptide sequence are replaced with non-natural amino acids bearing terminal olefins that are covalently linked together by ruthenium-catalyzed olefin metathesis (Chang, 1998). The process of covalent linking is referred to as "stapling". This stapling frequently restores the native alpha-helicity of the peptide, as well as increasing proteolytic stability and cell penetrance (Walensky et al., 2004). Today, stapled peptides are used for a variety of purposes, including mechanistic studies and therapeutic applications (For examples, see Moellering et al., 2009, Bernal et al., 2010 and Edwards et al., 2013).

Using a similar approach, stabilized alpha helices (SAHS) of Olig2 bHLH domains were synthesized for this study. Specifically, we generated panels of SAH Olig2 peptides for helix 1, helix 2, and full-length bHLH (all referred to as "OLIGOpeptides") to comprehensively test a variety of peptide lengths, compositions, and charges. These SAH OLIGOpeptides were then evaluated for their ability to disrupt Olig2 dimerization and DNA binding in gel mobility shift assays.

We succeeded in creating alpha-helical peptides that mimic the predicted alpha-helical region of Olig2's bHLH domain, but further study is required for efficient disruption of Olig2 dimerization, and thus Olig2 function.

Results

Olig2 dimerization is required for DNA binding

Most, if not all, bHLH transcription factors require dimerization to form a stable complex with an E-box-containing DNA region. A helicomimetic could poten-

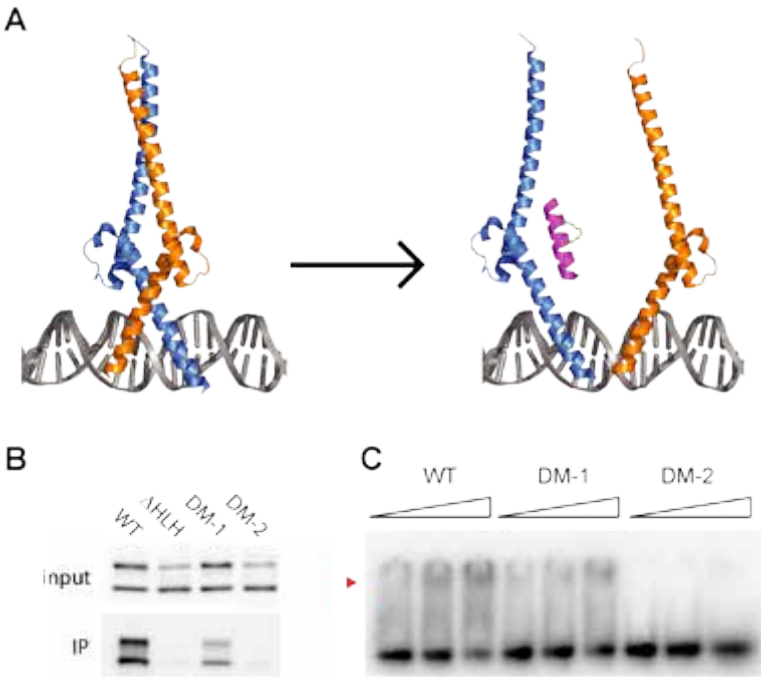

FIGURE 1. **Rationale for using "stapled peptide" chemistry to inhibit Olig2 dimerization (A)** Schematic representation of an alpha-helical mimetic disrupting bHLH homodimerization. Crystal structures shown are E47 and NeuroD1 onto the insulin promoter E-box sequence. A stapled alpha-helical peptide could disrupt a bHLH dimer, thus preventing downstream transcription. **(B)** We generated dimerization mutants of Olig2 by single or double amino acid mutations in the HLH domain (S147A and S147A, T151A, referred to as DM-1 and DM-2). Constructs encoding V5-tagged Olig2 WT, an HLH deletion construct, DM-1 or DM-2 were transfected into COS7 cells, together with HA-tagged Olig2 WT. Cell lysates were harvested and incubated with an HA-specific antibody to immunoprecipitate Olig2 dimers. HA-bound fractions were separated on a 10% SDS-PAGE gel, followed by V5 immunoblotting. **(C)** Olig2 WT, DM-1 or DM-2 was purified from COS7 cells and incubated with radioactive DNA probe containing E-box element CAGCTG from the *Mycn* promoter. The top band correlates to protein : DNA complex (red arrowhead), while the bottom band corresponds to free DNA probe.

tially separate a bHLH dimer into two monomers and block downstream effects (Fig. 1A). To test whether a monomeric variant of Olig2 is indeed unable to form a stable complex on an E-box element, we mutated two amino acids in the HLH domain to abolish dimerization. As shown in Fig. 1B and 1C, a dimerization mutant (DM-2) of Olig2 is unable to dimerize and, consequently, cannot shift an E-box in a gel mobility shift assay.

Synthesis and functional characterization of single helix OLIGopeptides

To investigate the capacity of short peptidomimetics to inhibit Olig2 dimerization, we designed a panel of peptides corresponding to the first or second helical region in the HLH domain of Olig2 (SAH OLIGopeptides). These peptides varied in staple position and sequence coverage of the helical domains (Fig. 2A and 2B, top). Circular dichroism analysis determined a range of alpha-helicities amongst the peptides, from 23% to 100% alpha-helical (Fig. 2A and B, bottom). In comparison, unstapled peptides of either the first or second helix sequence were unstructured in solution (Fig. 2C).

The SAH OLIGopeptides were screened for their ability to alter formation of an Olig2 : DNA complex, by electrophoretic mobility shift assays (EMSA). In these experiments, purified recombinant Olig2 protein was pre-incubated with varying concentrations of OLIGopeptides, and the mixtures were then added to radiolabeled DNA probe containing a canonical E-box sequence. While all SAH OLIGopeptides showed some interference with shift, our control peptides (unstapled and scrambled) also showed this effect (representative examples are shown in Fig. 3. For complete single helix screen, see Fig. S1). We therefore concluded that short alpha-helical OLIGopeptides were insufficient for disrupting the Olig2 dimer : DNA interface.

Synthesis and functional characterization of double helix OLIGopeptides

We next generated Olig2 peptidomimetics that encompassed a larger portion of the HLH dimerization domain, in an effort to maximize binding potential. Peptides were synthesized that incorporated the C-terminal portion of the basic DNA-binding region as well as helix 1, the loop, and helix 2 of Olig2. Since these peptides were designed to mimic two helices, with helix-breaking prolines in the intervening loop, hydrocarbon staples were inserted into both helical regions to induce alpha-helicity, creating double stabilized alpha-helical (dSAH) OLIGopeptides. Additionally, the non-natural amino acids were placed two alpha-helical turns apart (*i*,*i*+7), rather than one (*i*,*i*+4), to stabilize a longer region of the peptide. To evaluate successful induction of alpha-helicity in the double helix OLIGopeptides, circular dichroism was performed (Fig. 4A). While

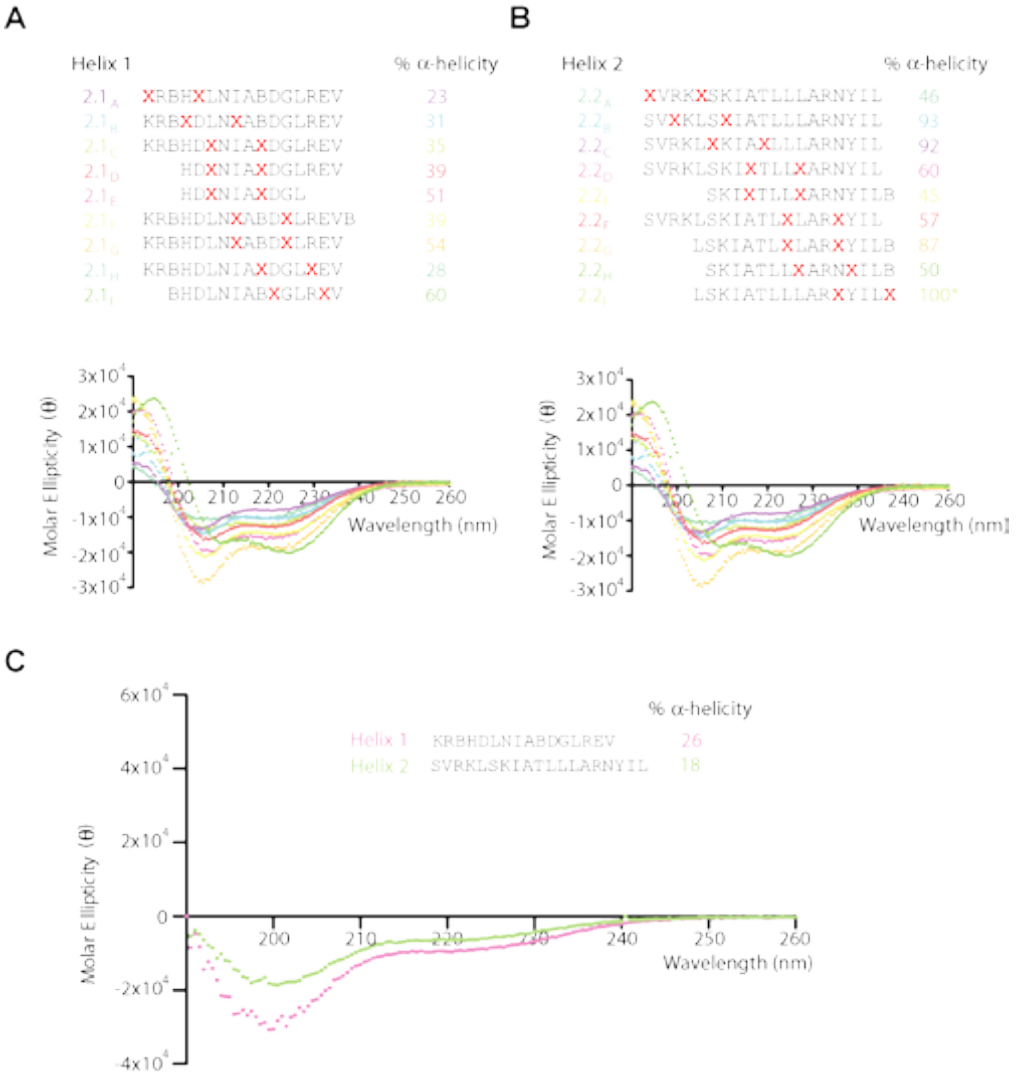

FIGURE 2. **SAH OLIGopeptides with varying lengths and staple positions show a range of alpha-helicities**. We generated a set of Olig2 alpha-helical mimetics based on the (**A**) first or (**B**) second helix in the HLH domain of Olig2. In order to reinforce the helicity of these sequences, non-natural amino acids were inserted into the peptides one alpha-helical turn apart (*i,i+4)* and chemically linked together using ruthenium-catalyzed olefin metathesis. The peptides demonstrate a wide range of alpha-helicities as reflected in the percent alpha-helical content and circular dichroism spectra. (**C**) Native native, unstapled OLIGOpeptides are relatively unstructured in solution, as demonstrated by circular dichroism. *, exceeds the calculated ideal alpha-helicity of an undecapeptide standard. X = S_5 non-natural amino acid

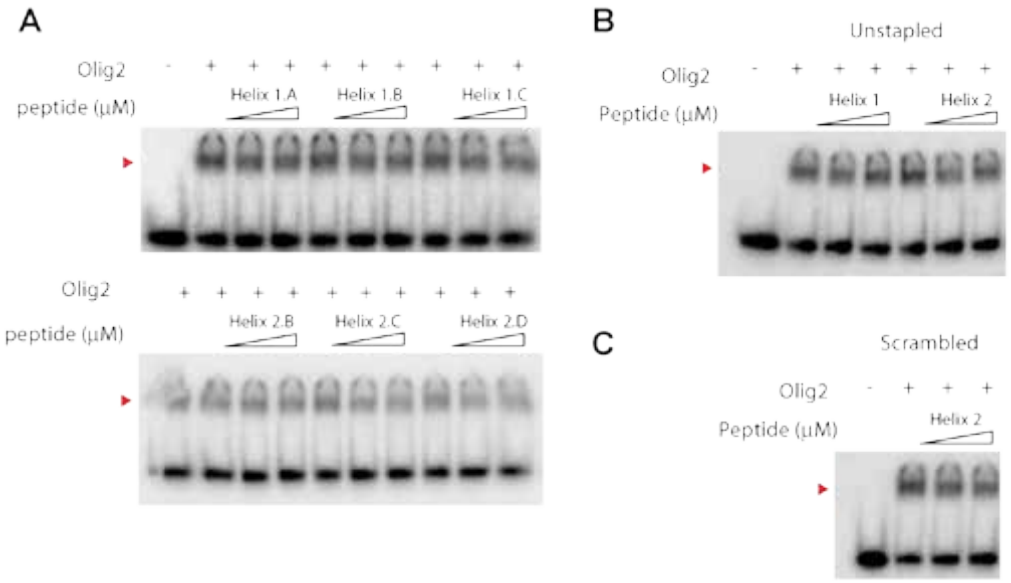

FIGURE 3. **No inhibition of Olig2 dimerization by single helix OLIGOpeptides**. **(A)** Olig2 protein was pre-incubated with 0μM, 0.15μM or 1.5μM SAH OLIGOpeptides, before allowing complex formation with radioactive DNA probe containing a *Mycn* promoter E-box. Complexes and free DNA were separated by electrophoresis. Three representative peptides are shown for helix 1 **(**top) and helix 2 **(**bottom). **(B)** We generated unstapled Olig2 mimetic control peptides, spanning the first or second helix of the bHLH domain. We tested unstapled peptides in gel mobility shift assay at concentrations of 0μM, 0.15μM or 1.5μM. **(C)** Gel mobility shift assay using a randomly scrambled control peptide based upon the second helix of the Olig2 bHLH domain. Red arrowheads indicate shifted protein : DNA complex

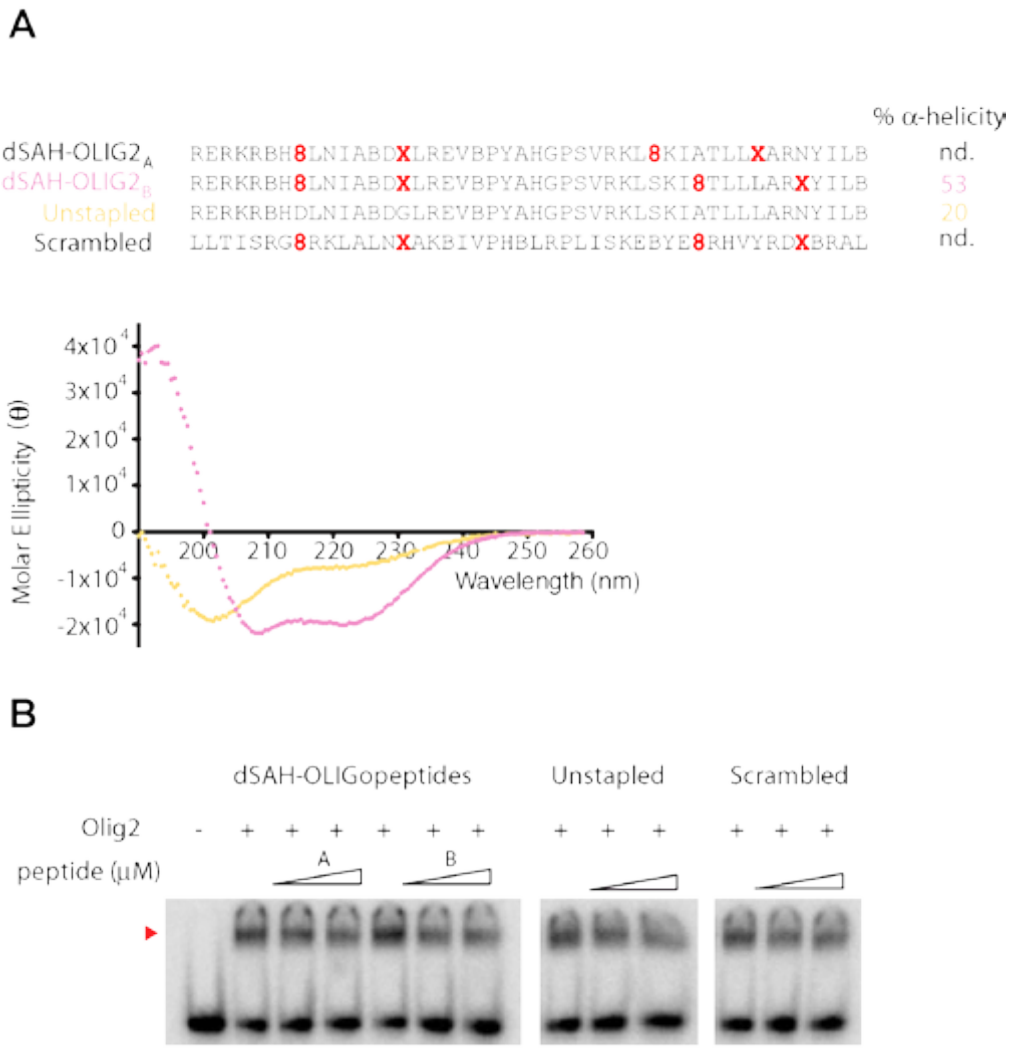

FIGURE 4. **No inhibition of Olig2 dimerization by double helix OLIGopeptides. (A)** Double stapled alpha-helical peptides (dSAH) were generated using two i,i+7 staples spanning the first or second helix of Olig2 HLH domain. We tested the alpha-helicity of dSAH Olig2.B and an unstapled control peptide by circular dichroism. X = S5 non-natural amino acid, R8 = non-natural amino acid, Nd. = non determined **(B)** Olig2 protein was pre-incubated with 0μM, 0.15μM or 1.5μM dSAH OLIGopeptides or control peptides, before allowing complex formation with radioactive DNA probe containing a *Mycn* promoter E-box. Red arrowheads indicate shifted protein : DNA complex

an unstapled peptide was unstructured, dsAH Olig2B was over 50% alpha-helical, confirming the efficacy of *i,i+7* stapling in restoring alpha-helicity.

As shown in Fig. 4B, dsAH Olig2 peptides, and their controls, show minimal effect on Olig2 : DNA affinity in gel mobility shift assay. These data suggest that neither short, single helix peptides nor longer, double helix peptides of the Olig2 bHLH domain can bind and disrupt full-length Olig2 dimerization and DNA binding.

C-terminal region of Olig2 is critical for bHLH dimer stability

To determine whether any additional domains in Olig2 are required for dimerization, we tested Olig2 deletion constructs for their ability to form dimers. We generated a v5-tagged and HA-tagged variant of a set of Olig2 deletion constructs. As expected, WT and a Δbasic variant are able to dimerize, whereas ΔHLH has no dimerization capacity (Fig. 5A and B, lane 1–3). Surprisingly, the

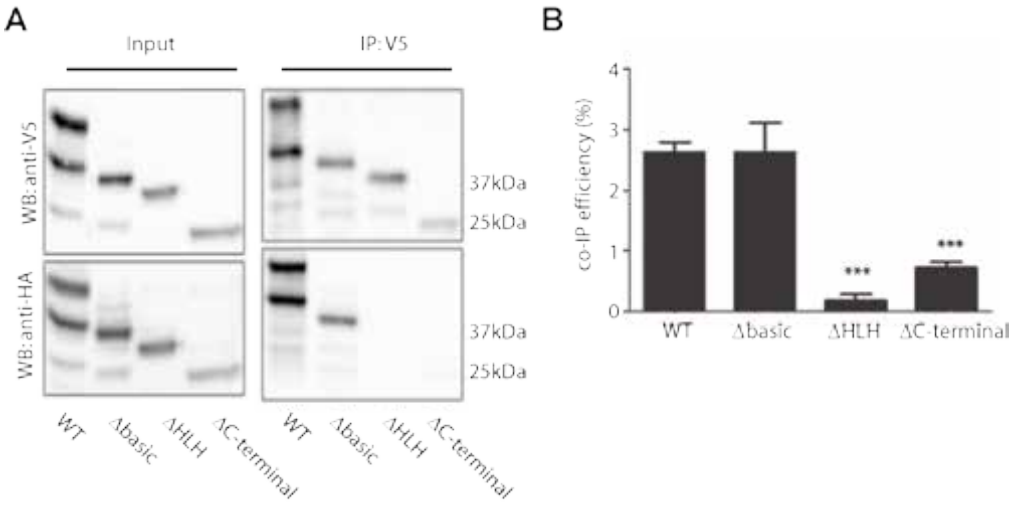

FIGURE 5. **Olig2 dimerization requires C-terminal domain. (A)** We generated various HA and V5-tagged constructs by deleting the C-terminal (amino acids 209-323), basic (amino acids 109-121) or HLH (amino acids 121-175) domains of Olig2. COS7 cells were transfected with V5 and HA protein pairs (i.e. WT-V5 and WT-HA, etc.). Cell lysates were harvested and incubated with an HA-specific antibody to immunoprecipitate Olig2 dimers. HA-bound fractions were separated on a 10% SDS-PAGE gel, followed by V5 immunoblotting. Data are quantified in **(B).** *** , $p < 0.001$

C-terminal deletion constructs showed greatly reduced dimerization efficiency (Fig. 5A and B, lane 4). We did not observe any change in dimer formation for the N-terminal deletion constructs (data not shown). These data suggest an important function for the C-terminal of Olig2 in stable Olig2 : Olig2 dimer formation.

Discussion

The bHLH transcription factor Olig2 drives cells towards replication or differentiation, depending on the cell type and stage of development (Ligon et al.; Lu et al., 2002; Zhou and Anderson, 2002). Reflective of its developmental roles, Olig2 is necessary for brain tumor growth, in a genetically relevant mouse model for glioblastoma multiforme and in primary human tumor cells (Appolloni et al., 2012; Bao et al., 2008; Barrett et al., 2012; Ligon et al., 2007; Mehta et al., 2011). Accordingly, there is significant interest in therapeutic intervention of Olig2 function. As a bHLH transcription factor, Olig2 must dimerize to stably bind E-box elements on the DNA, recruit necessary co-factors, and exert its transcriptional effects. This dimerization is driven through the interaction of two adjacent alpha-helices. Here, we described our approaches to disrupt Olig2 dimerization with stabilized alpha-helical peptides that mimic Olig2's own dimerization domain. We have encountered several challenges (listed below), all converging on the same topic of how to "drug the undruggable".

Is Olig2 active as a homodimer or does it preferentially dimerize with E proteins?

In this study, we have shown our attempts to interfere with Olig2 homodimerization using gel mobility shift assays. However, tissue-specific bHLH transcription factors, such as Olig2, are predicted to dimerize with broadly expressed E proteins to regulate transcription. Although *in vitro* protein pull-down assays have identified E12 and E47 as dimerization partners for Olig2 (Lee et al., 2005; Li et al., 2007; Samanta and Kessler, 2004), we have not been able to demonstrate Olig2 : E12/E47 interaction in neural progenitor cells (data not shown). Our preliminary data indicate that two other members of the same

E-protein family, Tcf4 and Tcf12, might serve as bona-fide Olig2 interactors. Both Tcf4 and Tcf12 were identified by mass spectrometry after tandem affinity Olig2 pull-downs in mouse neural progenitor cells. If Olig2 prefers heterodimerization with an E-protein rather than homodimerization, we might benefit by designing, synthesizing and testing a new set of stapled peptidomimetics, based on the HLH region of Tcf4 and Tcf12.

Post-translational modifications in the bHLH domain

We and others have identified several phosphorylation sites in Olig2 that are important for proliferation and differentiation functions (Huillard et al., 2010; Li et al., 2011; Setoguchi and Kondo, 2004; Sun et al., 2011). Specifically, Li et al. have demonstrated that a phosphorylated serine in the second helix of Olig2 is important for motor neuron formation. Interestingly, they show that mutating this serine into alanine (Ser147Ala) results in a change of dimerization partner. Phosphorylated Olig2 prefers to dimerize with itself or Olig1, whereas Ser147Ala mutant shows more affinity for another bHLH transcription factor, Neurogenin2 (Ngn2). Thus far, we did not detect Ser147 phosphorylation in cycling mouse neural progenitor cells or Olig2-transfected COS7 cells. Hopefully, closer scrutiny of Olig2's phosphorylation profile in neural progenitor cells and their gliomagenic counterparts will confirm the phosphorylation status of the serine at position Ser147. If phosphorylated, we should reconsider using recombinant Olig2 protein (unphosphorylated due to expression in *Escherichia Coli*) in our experiments. Likewise, if Ser147 is unphosphorylated in cycling progenitor cells, we could switch from inhibiting Olig2 homodimerization to inhibiting heterodimerization with other bHLH proteins, such as Ngn2 or E proteins (see above), to improve our experimental design.

C-terminal function in dimerization

As shown in Fig. 5, the C-terminal portion of Olig2 contributes to dimer formation. Preliminary experiments in our lab show that C-terminal deletions of Olig2 affect the ability to overexpress these constructs in COS7 cells (data not shown). This could indicate that the C-terminus is important for stabilization

of Olig2 protein. Alternatively, the C-terminus might create an additional dimerization interface (compare with the leucine zipper domain in Myc : Max). A closer look at the C-terminus reveals the presence of a CxCxxC motif (also present in Olig1) and fourteen highly conserved histidines (all but one specific to Olig2). Together, this suggests metal-binding properties of the C-terminal, potentially important for protein folding and stability (Rousselot-Pailley et al., 2006; Yu et al., 2013).

Our attempts to disrupt bHLH dimerization using small peptides were not the first. Indeed, several groups have generated bHLH peptidomimetics to hinder formation of the requisite dimer (see table 1). Such attempts have had limited success at disruption *in vitro*, with even less success at prolonged effect *in vivo*. Therapeutic success with stabilized peptides has thus far occurred when the target is a helix-in-groove interface, allowing for numerous energetically favorable interactions (Moellering et al., 2009; Stewart et al., 2010; Walensky et al., 2004). Future attempts to target Olig function may require structural studies, such as x-ray crystallography, to further support rational design of Olig2 antagonists.

Methods

Coimmunoprecipitation

COS7 cells were transfected with Olig2 WT and Olig2 mutant constructs. Cells were lysed in hypotonic lysis buffer (50mM Tris-HCl pH7.5, 0.2% NP-40, 5mM EDTA) followed by high salt buffer (final concentrations: 10mM Hepes, 12.5% glycerol, 0.2mM EDTA, 420mM $NaCl_2$). Cell lysates were cleared by centrifugation and incubated with v5 agarose beads overnight. Beads were washed three times with low salt buffer (50mM Tris-HCl pH7.5, 0.1%NP-40, 100mM KCl and 10% glycerol), followed by a high salt buffer wash (300mM KCl). All buffers were supplemented with EDTA-free protease inhibitors (Roche), 1mM $Navo_4$, 5mM NaF, 1mM $Na_4P_2O_7$, 25mM beta-glycerophosphate and 0.5mM PMSF

Electrophoretic mobility shift assay

Olig2 WT and Olig2 mutants were transiently transfected into COS7 cells. Following cellular lysis, protein was purified by immunoprecipiation with v5

antibody (Sigma) and v5 peptide (Sigma) elution, followed by immunoprecipitation with Ni-NTA beads (Qiagen) and elution in high imidazole buffer (50mM Tris-HCl, pH 7.5, 200mM imidazole 150mM KCl, 5mM $MgCl_2$, 0.1% NP40 and 10% percent glycerol). Purified protein was quantified by silver stain using known concentrations of BSA protein as standard. Oligonucleotides used are the *Hb9* and *Mycn* E-box-containing promoters with the following DNA sequences: *Hb9*: AGCTAATTTCCCAGATGGGCCAA and AGCTTTGGCCCATCTGGGAAATT; *Mycn*: AGCTAGAAGACAGCTGTTGGAAG and AGCTCTTCCAACAGCTGTCTTCT. In addition, mutant sequences were also generated: *Hb9* mutant: AGCTAATTTCCTAGACTGGCCAA and AGCTTTGGCCAGTCTAGGAAATT; *Mycn* mutant: AGCTAGAAGATAGCCTTTGGAAG and AGCTCTTCCAAAGGCTATCTTCT. Oligonucleotides were annealed in annealing buffer (10mM Tris-HCl pH7.5, 50mM NaCl, 1mM EDTA) using a thermocycler for 5 min at 95°C, and allowed to cool down for approximately 1 hour. Annealed probe was labeled with [α-^{32}P] 6000 Ci mmol-^{1} dCTP (PerkinElmer) using Klenow (New England Biolabs). Radioactive DNA probe was incubated with 2 ng of Olig2 protein in binding buffer (20mM Tris-HCl pH7.5, 5mM $MgCl_2$, 0.1% NP40, 0.5mM DTT and 10% glycerol) and increasing concentrations of SAH OLIGOpeptides for 30 min at 4°C. Protein:DNA complex was analyzed using 4% non-denaturing poly-acrylamide gel electrophoresis (PAGE) for 30 min at 4°C. Following drying of the gel, radioactive signal was detected using a Typhoon 9400 (GE Healthcare Life Sciences).

Recombinant Olig2 production.

GB1-Olig2-His was expressed in Escherichia coli BL21 (DE3) from the pGEV2 vector and induced with 1mM isopropylthio-β-galactoside for 4 hours at 30°C. Bacterial pellets were resuspended on ice in Buffer A (50mM Tris-HCl, pH 7.5, 150mM KCl, 5mM $MgCl_2$, 10% glycerol, 0.1% NP40, and protease inhibitors), lysed by high pressure using a microfluidizer, and ultracentrifuged in a SW28 rotor at 27,000 rpm for 1 hour at 4°C. Cleared lysate was purified by affinity chromatography using nickel-NTA agarose beads (Qiagen), followed by sequential washes with Buffer A containing 5, 10, and 15mM imidazole. GB1-Olig2-His was eluted with Buffer B (50mM Tris, pH 7.5, 150mM KCl, 5mM $MgCl_2$, 250mM imidazole), concentrated, and buffer-exchanged to Buffer C (50mM

Tris, pH 7.5, 150mM KCl, 5mM $MgCl_2$) using 10kDa cutoff centrifugal filter unit (Millipore) to remove the imidazole. GB1-Olig2-His protein was further purified by gel filtration FPLC and ultimately stored in Buffer A.

Stapled peptide synthesis and characterization.

Stapled peptides were synthesized, derivatized, purified to >95% homogeneity (assessed by LC/MS), quantified by amino acid analysis, and subjected to circular dichroism (Aviv Biomedical spectrophotometer) in water as previously described (Bird et al., 2008; Bird et al., 2011). Single helix peptides used (S)-N-Fmoc-2-(4'-pentylenyl)alanine [S5] as both of the non-natural amino acids, while double helix peptides used (R)-N-Fmoc-2-(7'-octenyl)alanine [R8] for one of the non-natural amino acids in a staple pair and S5 for the second. Methionine (M) is substituted for norleucine (B) in stapled peptide sequences.

SUPPLEMENTAL FIGURE S1. **Full panel of SAH OLIGopeptides EMSA screen.** Purified GB1-Olig2 was incubated with radiolabeled *Mycn* E-box sequence in the presence of increasing concentrations of SAH OLIGopeptides. Complexes and free DNA were separated by gel electrophoresis. The top band correlates to protein : DNA complex (red arrowhead), while the bottom band corresponds to free DNA probe.

SAH-OLIGopeptides helix 1

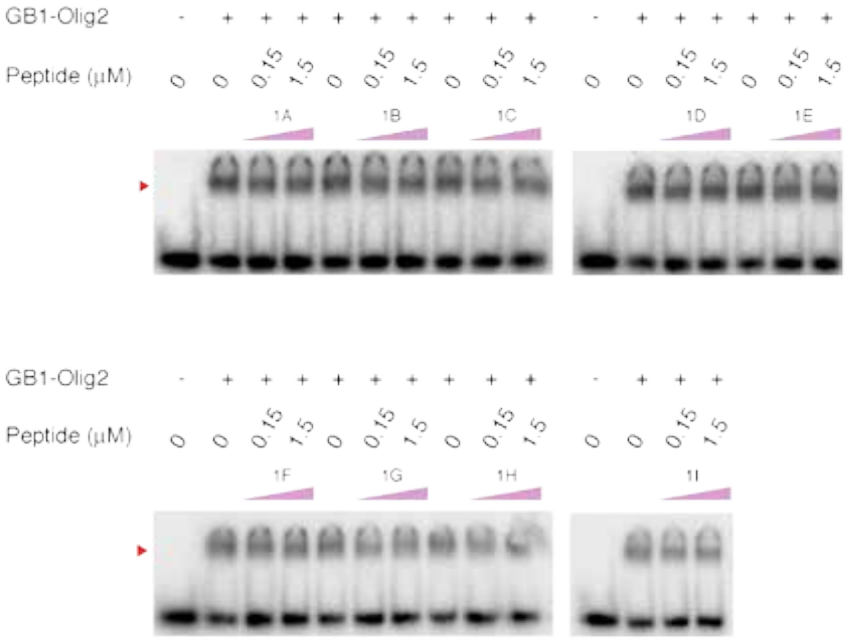

SAH-OLIGopeptides helix 2

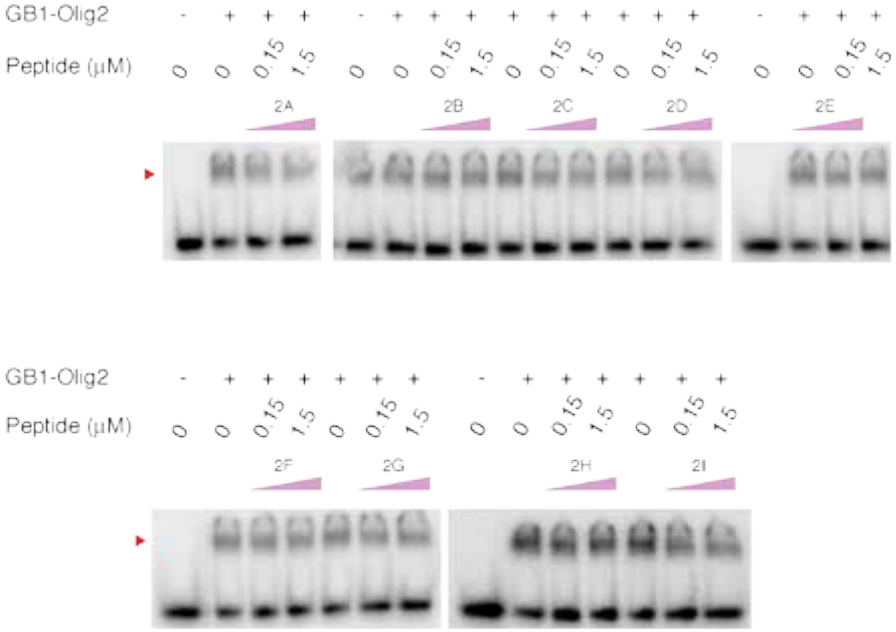

5 Discussion and future directions

Olig1 and Olig2 in the developing CNS

A pair of bHLH transcription factors

The object of this dissertation has been to study the structure—function relationships of the Olig proteins. I set off reviewing Olig1 and Olig2 on a structural and functional level, comparing co-regulator proteins, genetic targets and post-translational modifications (Chapter 1). The amino acid sequences of Olig1 and Olig2 are highly similar within the bHLH domain. Outside of this domain, differences between the two proteins become quite evident. Notably, the N- and C-terminal of Olig1 are about two third the size of the corresponding domains in Olig2. As such, it is not surprising that the set of co-regulator proteins, genetic targets, and post-translational modifications are largely unique for each protein. The main exception to this divergence is an overlapping set of bHLH proteins as potential dimerization partners for both Olig1 and Olig2. On a functional level, primarily Olig2 is important for the specification of certain neural cell types such as motor neurons and oligodendrocytes, whereas Olig1 has only a minor task in neural subtype specification. Moreover, Olig2 by itself has a distinctive role in neural progenitor cell proliferation, with a clinically significant link to brain tumors. Similarly, Olig1—but not Olig2—has been associated with neurodegenerative diseases (such as multiple sclerosis), where it functions in repair of demyelinating lesions.

Why would the close paralogues *Olig1* and *Olig2* have such dissimilar functions? A closer look at the evolution of the *Olig* genes can help us understand this apparent contradiction. Well-conserved synteny of *Olig1* and *Olig2* (for instance on chromosome 21 in humans) suggests that *Olig1* and *Olig2* originated from a common ancestral *Olig* gene (Bronchain et al., 2007). Generally speaking, gene duplication results in rapid genetic specification after a short period of genetic redundancy (Huminiecki and Wolfe). Such genetic diversion can occur through differences in spatiotemporal expression patterns or changes in amino acid sequence. Duplicated genes that have subfunctionalized through different

expression patterns are likely to retain their genetic redundancy (Cadigan et al., 1994; Huang et al., 2008; Kellerer et al., 2006; Molin et al., 2000; Stolt et al., 2004; Yasunami et al., 1996). For instance, expression of the highly similar E proteins is strictly regulated during CNS development, and bHLH proteins such as NeuroD2 can dimerize with each of the E proteins *in vitro* (Ravanpay and Olson, 2008). Consequently, dimeric partner choice *in vivo* depends on E protein availability rather than E protein identity (Ravanpay and Olson, 2008; Zhuang et al.). On the contrary, gene duplicates that have subfunctionalized through amino acid sequence change are likely to lose their redundancy (Bochkis et al., 2012; Conant and Wagner, 2003). The largely overlapping expression patterns of *Olig1* and *Olig2*, together with their structural differences, suggest that *Olig* gene duplication has occurred through amino acid sequence change only and that their functions are mostly non-redundant. Moreover, we predict that forcing nuclear expression of *Olig1* cannot replace *Olig2* function in mouse neural progenitor cells (or other functional assays, see *Proposal for Olig1/2 functional studies*). Interestingly, *Olig3* shows completely non-overlapping expression patterns with *Olig1* and *Olig2* in the central nervous system (Liu et al., 2008; Muller et al.). The structural resemblance between Olig2 and Olig3 protein suggests that Olig3 retained its redundancy and mainly subfunctionalized through different spatial expression patterns.

From a therapeutical point of view, subfunctionalization of the *Olig* genes confers an advantage with regard to the design of small molecule modulators of Olig1 and Olig2 protein. Theoretically, an inhibitor of Olig2 function could slow down brain tumor growth without interfering with Olig1's functions in myelin repair. Likewise, an activator of Olig1 could help the repair of demyelinating lesions, without stimulating unwanted (i.e. cancerous) proliferation of neural progenitor cells. Thus far, no postnatal functions have been ascribed to Olig3, such that off-target effects of either Olig1 or Olig2 small molecules on Olig3 protein are not expected.

Olig2 phosphorylation in proliferating neural progenitor cells

A unique post-translational modification for Olig2 is an N-terminal triple phosphorylation motif. We identified three serines at position Ser10, Ser13 and Ser14

that are phosphorylated in proliferating neural stem cells, and their gliomagenic counterparts (Chapter 2). This motif is developmentally regulated, as differentiation of neural progenitor cells results in a decrease of phosphorylation at these three serines. Furthermore, in a mouse model for glioma, intracranially injected tumor cells that express phosphomutant Olig2 show impaired tumor growth, whereas a phosphomimetic version of Olig2 results in normal or even expedited tumor cell growth. Moreover, on a mechanistic level, we showed that Olig2 phosphorylation challenges the p53 signaling pathway by directly opposing p53 acetylation.

How is Olig2 phosphorylation regulated? The presence of three serines in the phosphorylation motif suggests that multiple kinases orchestrate phosphorylation of this site. The first kinase might create a docking site for the next one, thus acting in sequential fashion. Kinase prediction programs for the N-terminal of Olig2 show that indeed several priming kinases could recognize Ser10, such as Gsk3 and Ck2. In cycling neural progenitor cells, Olig2 triple phosphorylation decreases upon Egf and Fgf withdrawal. Thus, another requirement for an Olig2 kinase is responsiveness to Egfr and Fgfr downstream signaling. Accordingly, predicted kinases that are members of the Erk family deserve careful examination (Doetsch et al., 2002; Learish et al.; Ma et al., 2009; Tropepe et al., 1997). Such experiments are ongoing at time of writing.

What is the mechanism of Olig2 phosphorylation? The addition of phospho groups to the three serines in the N-terminal of Olig2 results in a negatively charged tail of the protein. Such an "acidic tip" could either affect coregulator recruitment or induce a conformational change (and regulate protein : protein interactions indirectly). As discussed below, we investigated the molecular mechanism of Olig2 phosphorylation in detail in Chapter 3.

Molecular mechanism of Olig2 phosphorylation

In Chapter 3, we studied the Olig2 : p53 oppositional relationship, with focus on the role of Olig2 triple phosphorylation. As demonstrated in Chapter 2, phosphorylated Olig2 represses p53 acetylation. To exclude the possibility that Olig2's anti-p53 response is non-transcriptional (e.g. by sequestering acetylating enzymes), we show that Olig2 requires conventional DNA binding to sup-

press p53 acetylation. Secondly, we show by chromatin immunoprecipitation, that Olig2 phosphorylation does not affect selection of direct genetic targets. Importantly, we observed that the triple serine motif on Olig2 causes an intranuclear localization change, where phosphorylated Olig2 is loosely associated with the chromatin, and unphosphorylated Olig2 tightly chromatin-bound. This intranuclear localization switch changes Olig2's access to co-regulator proteins. We hypothesize that the intranuclear localization change allows phosphorylated Olig2 to present a deacetylating enzyme, Hdac1, directly to p53, thus facilitating p53 deacetylation and subsequent inactivation.

How does Olig2 phosphorylation change intranuclear localization? As mentioned earlier, phosphorylation of the three serines results in a negatively charged N-terminal. DNA binding by a transcription factor is mostly regulated by electrostatic (charge-based) interactions between negatively charged DNA and a slightly basic DNA-binding domain. Thus, a negatively charged motif could decrease the affinity of a transcription factor for DNA by electrostatic repulsion, even if this domain is outside the DNA-binding domain. As such, the amino terminal phosphorylation motif in Olig2 might control loose or tight DNA binding, and subsequently affect intranuclear localization.

Olig2 is not the only bHLH protein that regulates its affinity for DNA by phosphorylation sites outside of the DNA binding domain. For instance, multiple phosphorylated residues at the C-terminal end of MyoD interfere with DNA binding of the MyoD homodimer (Mitsui et al., 1993). Likewise, phosphorylation of two serines (S2 and S11) in the N-terminal of Max disrupts the interaction between the Max homodimer and an E-box element (Berberich and Cole, 1992; Brownlie et al., 1997; Koskinen et al.). Structural analysis confirmed that both these serines are in close proximity of the DNA binding region (Brownlie et al., 1997). In addition, several phosphorylation motifs in the N-terminus of E47 are shown to affect DNA binding and subsequent transcriptional activity (Neufeld et al., 2000; Sloan et al., 1996).

We wonder whether Olig2 phosphorylation decreases DNA affinity in order to prevent the formation of a stable Olig2 homodimer : DNA complex. Instead, Olig2 could form multiple heterodimers with other bHLH proteins, such as E proteins. This would increase the number of functional transcriptional complexes, and thus allow more fine-tuned regulation of Olig2 function.

A strategy for targeting Olig2

A DNA-binding mutant of Olig2 does not maintain the neural progenitor cell proliferation advantage and radiation resistance as conferred by wild-type Olig2 (as demonstrated in Chapter 3). Thus, we predicted that disruption of the Olig2 : DNA complex could slow the growth of malignant tumor progenitor cells in a similar fashion. We showed that interfering with Olig2 dimerization results in an inability to bind to an E-box containing DNA element (Chapter 4). Concordantly, we generated a set of peptidomimetics, modeled after the bHLH domain of Olig2, to screen for inhibitors of Olig2 dimerization, with the ultimate goal of impeding brain tumor growth. Hydrocarbon stapling successfully produced a number of stable Olig2 peptidomimetics. Unfortunately, none of the OLIGOpeptides specifically and potentially disrupted Olig2 dimerization and subsequent DNA binding. Thus far, therapeutic success with stabilized peptides involve helix-in-groove interfaces with numerous energetically favorably interactions (Moellering et al., 2009; Stewart et al., 2010; Walensky et al., 2004). In contrast to a helix-in-groove interaction, the bHLH dimer follows a loose handshake-like pattern in which the two alpha-helices are coiled around each other in parallel orientation. Accordingly, we hypothesized that the bHLH domain by itself is not sufficient for DNA binding, and set off to identify other regions in Olig2 that are important for dimerization and subsequent DNA binding. We identified the C-terminus as an important contributor to a dimeric Olig2 complex. In addition, the E-box element could serve as an essential DNA scaffold to stabilize the Olig2 dimer. In light of these considerations, we might include the C-terminal region and/or the DNA binding domain of Olig2 in our further attempts to disrupt the dimeric Olig2 : DNA complex.

Functional association of Olig1 and Olig2?

The non-overlapping functions of Olig1 and Olig2, reflected in different sets of co-regulator proteins, direct target genes and post-translational modifications are extensively reviewed in Chapter 1. A remaining question is whether there is additional cooperation between Olig1 and Olig2—beyond their partial redundancy in neural specification. For instance, is there a role for Olig1 in tumor formation? What is the function of Olig2 in mature Oligodendrocytes? More-

over, interplay rather than redundancy between Olig1 and Olig2 is suggested by protein-protein interaction experiments. For example, we show that full-length Olig2 not only dimerizes with itself, but also heterodimerizes with Olig1, as demonstrated by yeast two-hybrid trapping (Fig. 1A).

Also, in mouse neural progenitor cells, Olig2 forms a dimeric complex with Olig1 (Fig. 1B). Interestingly, although Olig1 is mostly cytosolic in these cells, nuclear Olig1 is one of the stronger Olig2 interactors and can been used as positive control for identification of Olig2 co-regulator proteins (data not shown). The interaction between Olig1 and Olig2 is furthermore demonstrated in a gel mobility shift assay, where increasing concentrations of Olig1 stabilize Olig2 binding to an E-box element (Fig. 1C and D).

It remains a question whether Olig1 / Olig2 dimers are transcriptionally active, or if Olig1 fulfills a role traditionally ascribed to Id proteins; e.g. inhibiting or sequestering Olig2 protein. In support of this hypothesis it seems worthy to point out that Olig1 itself demonstrates minimal affinity for an E-box containing DNA probe (Fig. 1C, lane 2).

How does Olig1/2 structure account for Olig1/2 function?

Both the non-overlapping and overlapping roles of Olig1 and Olig2 raise a fundamental question: What are the differences between Olig1 and Olig2 that account for their divergent functions during development and in disease? Here, I propose to expand on current structure-function studies of Olig1 and Olig2 in a two-fold approach. First, insight into the three dimensional structure of Olig1 and Olig2 by x-ray crystallography might help us understand contribution of various protein regions, extending beyond the well-characterized bHLH motif. Second, an *in vivo* readout for Olig1/2 function is suggested so as to test the contribution of these additional protein parts using a (sub)domain replacement strategy, referred to as "domain swapping".

Proposal for Olig1 and Olig2 structural studies

Thus far, most published bHLH protein structures involve the bHLH dimer only (Ahmadpour et al., 2012; Ellenberger et al.; Ferre-D'Amare et al.; Ferre-D'Amare

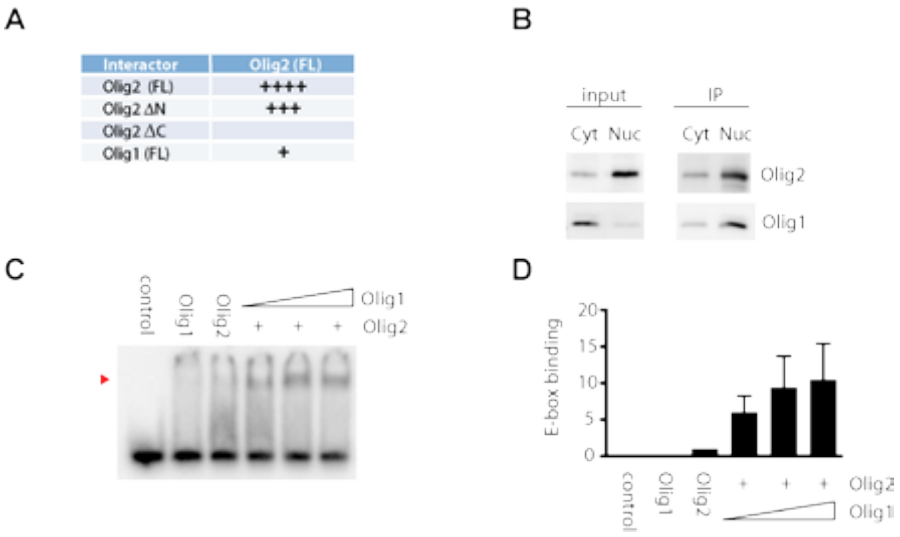

FIGURE 1. **Olig1 and Olig2 are dimerization partners (A)** Full-length human *Olig1*, *Olig2* and *Olig2* deletion constructs were cloned into yeast two-hybrid vectors containing activating domains (AD) or DNA-binding domain. Full-length Olig2-AD was paired with all others. Strength of the interaction is based on colony formation efficiency. Although Olig1 and Olig2 are able to dimerize, Olig2 seems to prefer homodimerization. FL, full-length; ΔN, deletion of amino acids 1-109; ΔC, deletion of amino acids 209-323. **(B)** To demonstrate Olig1 : Olig2 interaction in a relevant cell type, *Olig2*-null mouse neural progenitor cell were transduced with *Olig2*-v5. Cells were harvested under proliferating conditions and subcellular fractions were prepared. After overnight incubation with v5 antibody, Olig2 complexes were separated on SDS-PAGE gel. Olig1 : Olig2 dimer formation was analyzed by immunoblot using an antibody specific for Olig1. Cyt = cytoplasm, Nuc = nuclear fraction **(C)** Purified Olig2 (2ng) from COS7 cells was pre-incubated with increasing concentrations of Olig1 protein (2, 5 and 10ng) before allowing complex formation with radiolabeled E-box element from *Mycn* promoter. Olig1 protein only does not show any E-box affinity (10ng, second lane). Olig2 protein only shows minimal E-box binding (2 ng, third lane). Protein : DNA complexes were separated by SDS-PAGE. The shifted band correlates to protein : DNA complex, while the bottom band corresponds to free DNA. See **(D)** for quantification.

et al., 1993; Huang et al., 2012; Longo et al., 2008; Ma et al., 1994; Shimizu et al., 1997; Wong et al., 2012). From these studies, it is now known that the conserved basic region binds to the major groove of DNA at a CANNTG E-box fragment. In particular, a conserved glutamic acid (E9) binds to the CA nucleotides of the E-box, while other residues dictate specificity for E-box recognition (De Masi et al.; Longo et al.). Especially, a non-conserved residue at position 13 is predicted to interact with the fourth base in the E-box sequence. Olig2 (as well as a Atonal / Math, NeuroD1 and Tfap) has a methionine at position 13, and is predicted

to bind to a CAG or CAT half-site E-box sequence (De Masi et al., 2011). From our own work (see Chapter 3) and prediction programs, the residues at three amino acids from the conserved glutamic acid (in Olig2, N6 and R12) are also crucial for direct contact with the DNA. Notably, some reports show that the interconnecting loop between the two alpha-helices is an additional component required for DNA binding (Bouard et al., 2013; El Ghouzzi et al., 2001; Ma et al., 2007; Xu et al., 2010). This might be of special interest for Olig research, because Olig1 has an atypical loop region compared to Olig2 and most other bHLH proteins.

The second structural region of the bHLH dimer consists of a four-helix bundle, of which each pair of parallel alpha-helices are connected with a loop. Highly conserved hydrophobic residues form the core of the binding interface. Conversely, less conserved, non-hydrophobic amino acids in the helices might determine dimerization specificity, as is the case for MyoD (Shirakata et al., 1993). Phosphorylation of certain serines or threonines within the alpha-helical domains also affects dimerization specificity (Firulli et al., 2003; Firulli et al., 2005; Li et al., 2011; Lluis et al., 2005). Interestingly, Olig1 and Olig2 differ in the first amino acid of the first helix, where Olig1 contains a glutamine and Olig2 a histidine (His122). Also, the last two amino acids of the second helix are different between Olig1 and Olig2 (Gly,Ser for Olig1, and Thr163, Asn163 for Olig2). Five other amino acid changes between Olig1 and Olig2 in the two alpha-helices are conserved substitutions. Unfortunately, general rules for selecting the appropriate bHLH partner are thus far unknown.

Published bHLH structures, as described above, can be used to our advantage to predict the ternary complex of Olig1 and Olig2 bHLH dimers. The structural details can then be solved by molecular replacement, using for instance NeuroD1: E47 as search model (Longo et al., 2008). However, the major differences between Olig1 and Olig2 sequences are seen in the N- and C-terminal regions, outside of the bHLH domain. Thus, we would like to solve the full-length Olig1 and Olig2 protein structure. Only a few structures of full-length bHLH proteins have been described in literature (Brownlie et al., 1997; Ishii et al., 2012). One of the challenges of solving whole protein structures, especially in regard to Olig2, is low solubility of the full-length protein. For this purpose, we developed a construct of Olig2 that could be expressed in a bacterial system by means of a solubility tag (Fig. 2A–C).

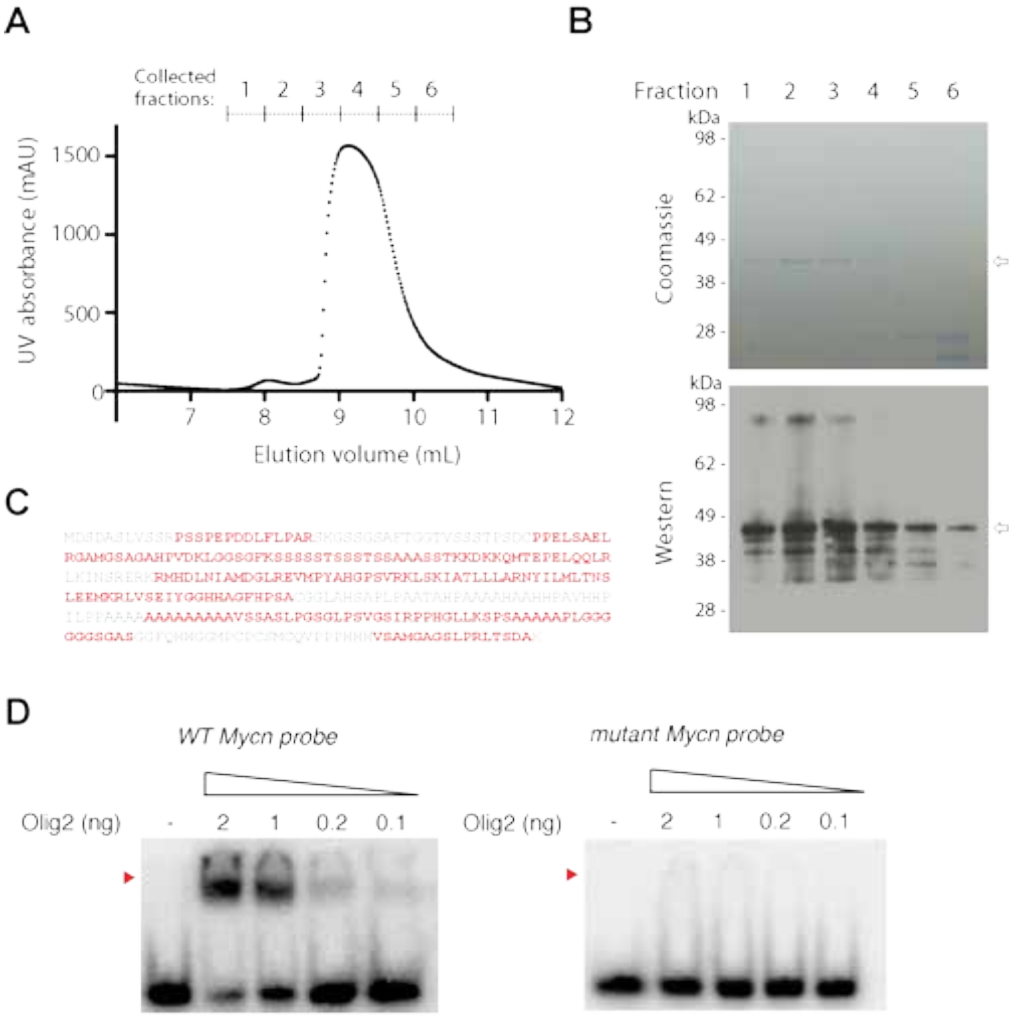

FIGURE 2. **Olig2 recombinant protein production (A)** *Olig2* tagged with the B1 immunoglobulin binding domain of streptococcal protein G (GB-1) and polyhistidine (His) for solubility and purification purposes was overexpressed in Escherichia coli BL21 (DE3). Size exclusion chromatography of cobalt agarose purified Olig2 shows one peak, corresponding to approximately Olig2 dimer size. **(B)** Coomassie staining (top) and western blot analysis (bottom) of collected SEC peaks confirm relative purity and presence of Olig2, as indicated with open arrow. **(C)** Further confirmation of the identity of the isolated protein was performed by mass spectrometry analysis. Identified peptide fragments of Olig2 are in red. **(D)** Purified recombinant Olig2 was tested in gel mobility shift assay, using a *Mycn* probe containing E-box element CAGCTG (left). The upper band corresponds to Olig2 : DNA complex (red arrowhead), while the lower band corresponds to free DNA. This binding is sequence specific, as incubation with a mutant *Mycn* (TAGCCT) results in no shift (right).

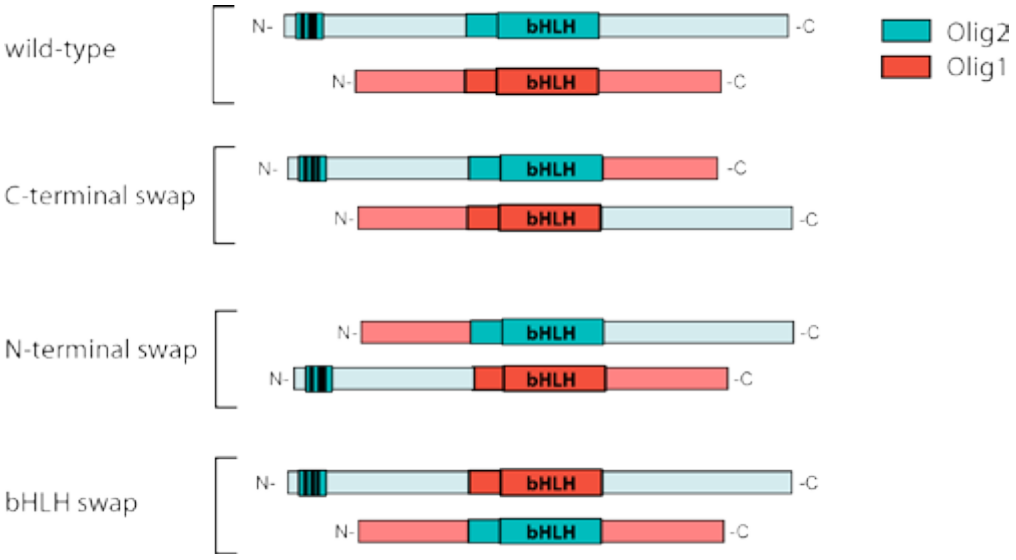

FIGURE 3. **Domain swap approach to test Olig1 and Olig2 function.** Overview of domain swap constructs. Note that all constructs are based on murine Olig1 and Olig2. Red, Olig1; Blue, Olig2.

We were able to overexpress *Olig2* and purify the protein for evaluation in gel mobility shift assays (Fig. 2D). We generated a similar construct containing *Olig1* cDNA. We are currently optimizing our purification steps to obtain micrograms of pure Olig1 and Olig2 protein. These proteins can then be used to generate crystals for x-ray diffraction analysis.

By obtaining the crystal structure of Olig1 and Olig2 homodimers, and Olig1/2 heterodimers, we hope to understand where the differences between Olig1 and Olig2 at the level of amino acid sequence contribute to different ternary structures. Especially, we hope to visualize the difference between the divergent N- and C-terminal domains of Olig1 and Olig2. However, merely solving the structure of the Olig transcription factors will not be sufficient for functional understanding. Structural biology should be combined with *in vivo* analysis of molecular composition, to analyze how changes in structure affects function. For such *in vivo* analysis, whether it is zebrafish behavior, chick electroporation, or mouse genetics, a "domain swap" construct library could be used. Strictly speaking, the only domain present in Olig proteins is the bHLH domain. However, here I refer to the N- and C-terminal regions outside of the bHLH

domain—and even smaller motifs therein—as domains. Olig1 domains can be replaced with domains of Olig2, a concept referred to as domain swapping. The advantage of domain swapping is that it allows for comparison of small and large regions of Olig1/2, while maintaining the size and overall structural nature of the protein. In our lab, we have generated Olig1/2 domain swaps constructs of the N-terminal, bHLH and C-terminal domain (see Fig. 3). Based on future ternary structure data, more domain swap combinations should be constructed and tested.

Structural information about Olig2 homo- or heterodimers could already support further refinement of Olig2 stapled alpha-helical peptides (Chapter 4). However, identification of new protein-binding interfaces and pockets *together* with functional understanding in a biologically relevant system might be the instrumental step forward towards designing an entirely new generation of Olig2 antagonists.

Concluding remarks

This dissertation has focused on the role of Olig2, and its close relative Olig1, during development of the central nervous system. Although the *Olig* genes were originally identified as pro-neural trancription factors important for specification of motor neurons and oligodendrocytes, more recent work has identified an anti-neural/pro-mitotic role for Olig2. Here, we have shown, both biologically and mechanistically, that a triple phosphorylation motif on the N-terminus of Olig2 is required for its pro-mitotic functions, but is dispensable for neural cell type specification. As exemplified by Olig2, post-translational modifications extend the complexity of transcription factor networks that orchestrate correct timing and location of neurogenesis. Hopefully, we are one step closer to understand the intricate molecular framework that organizes mammalian nervous system development.

Summary (in Dutch)

Binnenin elke lichaamscel ligt onze genetische informatie opgeslagen in een vierletterige code. Deze code noemen wij DNA en kan worden opgedeeld in meer dan twintigduizend verschillende informatiefragmenten, genen genoemd. Een gen codeert weer voor een eiwit, de daadwerkelijke bouwsteen van het menselijk lichaam. Zo zijn er bijvoorbeeld eiwitten die fungeren als pompjes, kanalen of sensoren. Het proces waarbij een gen wordt afgelezen en eiwitten worden aangemaakt, wordt transcriptie genoemd. Daarbij zijn zogenaamde transcriptiefactoren betrokken, eiwitten die zich aan DNA binden en een belangrijke rol spelen in het transcriptieproces.

Olig1 en Olig2 zijn twee transcriptiefactoren die belangrijk zijn voor de ontwikkeling van de hersenen. Grofweg zou je kunnen zeggen dat de hersenen bestaan uit drie celtypen, te weten neuronen, astrocyten en oligodendrocyten. Eerder werk van wetenschappers in Californië, Japan en van onze onderzoeksgroep heeft uitgewezen dat zonder Olig1 en Olig2 geen oligodendrocyten gevormd kunnen worden (vandaar de naam Olig). Ook zijn de Olig-eiwitten nodig voor het vormen van een bepaald type neuronen, zoals bijvoorbeeld neuronen die de spieren aansturen, motor neuronen genoemd. Ten slotte heeft Olig2 nog een extra functie. Olig2 stimuleert namelijk de groei van hersencellen vóórdat deze cellen zich specificeren tot neuron, astrocyt of oligodendrocyt. Zulke cellen worden hersenvoorlopercellen (HVCS) genoemd.

Naast hun rol in de gezonde ontwikkeling van de hersenen, zijn Olig1 en Olig2 ook betrokken bij bepaalde ziekteprocessen. Zo is Olig1 noodzakelijk voor het herstel van zenuwschade. Zenuwschade ontstaat bijvoorbeeld in de hersenen van patiënten met multiple sclerose. Olig2 daarentegen is voornamelijk betrokken bij de groei van een bepaald type hersentumoren, namelijk glioma's. Diffuse glioma's, met als kenmerk veel infiltratie van tumorcellen in het gezonde hersenweefsel, bevatten alle Olig2-eiwit. Bovendien is uit verschillend onderzoek gebleken dat in de hersentumorcellen van een muis geen tumor gevormd kan worden zonder Olig2. Ook menselijke tumorcellen van

een kwaadaardige hersentumor, zoals glioblastoma multiforme (GBM) zijn afhankelijk van Olig2 voor hun groei.

Dit proefschrift begint met een korte inleiding en een vooruitblik op mijn promotie-onderzoek. In hoofdstuk 1 geef ik een overzicht van de basic helix-loop-helix (bHLH)-transcriptiefactoren Olig1 en Olig2. Ik vergelijk Olig1 en Olig2 op verschillende punten, zoals eiwitstructuur, eiwit-eiwitverbindingen en eiwit-DNA verbindingen. Hoewel Olig1 en Olig2 vanuit een structureel oogpunt veel op elkaar lijken, hebben ze toch uiteenlopende functies tijdens de ontwikkeling van de hersenen. Zo zorgt Olig2 ervoor dat oligodendrocyten aangemaakt kunnen worden, terwijl Olig1 verantwoordelijk is voor de eindafwerking van deze cellen.

In hoofdstuk 2 ga ik verder in op de rol van Olig2 in HVCS en het kwaadaardige equivalent hiervan, hersentumorvoorlopercellen (HTVCS). Eiwitten, zoals de transcriptiefactoren Olig1 en Olig2, zijn opgebouwd uit verschillende aminozuren. Nu hebben wij in onze onderzoeksgroep drie aminozuren in Olig2 geïdentificeerd die een extra fosfaatgroep kunnen dragen. Deze drie aminozuren, serines genaamd, bevinden zich in het eerste segment van het eiwit, ook wel aminoterminus genoemd. Als deze serines hun extra fosfaatgroepen dragen, dan fungeert Olig2 pas echt goed als groeistimulator van HVCS. Zonder deze fosfaatgroepen op de drie aminozuren kan Olig2 niet de groei van HVCS, en ook niet van HTVCS, aanzwengelen. Dit fosfaattrio is specifiek voor de rol van Olig2 in de groei van HVCS en HTVCS, en heeft geen effect op andere functies van Olig2, zoals de aanmaak van oligodendrocyten en motorneuronen. Wij hebben dat aangetoond met celkweekexperimenten en in een muizenmodel voor GBM, bovengenoemde kwaadaardige hersentumorsoort. Hoe komt het fosfaattrio nu op de serines in de aminoterminus van Olig2 terecht? Kinases zijn de enzymen die een fosfaatgroep op een aminozuur kunnen zetten, een proces dat fosforylering wordt genoemd, Wij weten helaas nog niet welk kinase verantwoordelijk is voor de fosforylering in Olig2. Kinases zijn makkelijk te remmen met specifieke antagonisten, dus op lange termijn zou het identificeren van de Olig2 kinase (s) kunnen leiden tot een medicijn dat de groei van hersentumoren remt.

In hoofdstuk 3 onderzoek ik het moleculaire mechanisme waarbij het fosfaattrio in Olig2 zorgt voor celgroei van HVCS en HVTCS. Het fosfaattrio in Olig2 verhindert de werking van een andere transcriptiefactor genaamd p53. Dit p53 eiwit kan de groei van verschillende celtypen, waaronder HVCS, remmen en zou dus een belemmering kunnen vormen voor de ontwikkeling van de hersenen. Nu heeft onderzoek aangetoond dat p53 een zogenaamde acetylgroep nodig heeft om geactiveerd te worden. In dit hoofdstuk toon ik aan dat gefosforyleerd Olig2 de acetylgroep van p53 weg kan halen, mits Olig2 zich aan DNA heeft gebonden. Ik veronderstel vervolgens dat gefosforyleerd Olig2 in staat is om de acetylgroep bij p53 te verwijderen met behulp van een derde speler op het toneel, Hdac1 (ookwel histone deacetylase 1). Hdac1 is een enzym dat acetyl-groepen afbijt van eiwitten, zoals de transcriptiefactor p53. Mijn hypothese is dat gefosforyleerd Olig2 een brug slaat tussen Hdac1 en p53. Het samenspel tussen Olig2 en Hdac1 vindt alleen maar plaats wanneer Olig2 zich aan DNA bindt. Het lijkt dus alsof DNA als platform fungeert waarop Olig2, p53 en Hdac1 samenkomen. In HVTCS fungeert het fosfaattrio in Olig2 eveneens als remmer van p53 acetylering. In dit geval wordt niet de groei van gezonde hersencellen (HVCS) gestimuleerd zoals in bovengeschetst scenario, maar de groei van kwaadaardige cellen (HVTCS).

In hoofdstuk 4 ben ik begonnen met het ontwikkelen van een nieuw soort remmer voor de werking van Olig2, in samenwerking met enkele chemici van Dana Farber Cancer Institute / Harvard Medical School. De zogenaamde 'stapled peptide' aanpak bestaat uit het maken van kleine stukjes eiwit (peptiden) die qua vorm en uiterlijk lijken op Olig2. Omdat zulke peptiden makkelijk uit elkaar vallen, proberen we ze met behulp van een chemisch 'nietje' bij elkaar te houden. Zulke peptiden zouden dan met Olig2 kunnen concurreren om eiwitverbindingen die essentieel zijn voor de werking van Olig2. Zo zou de werking van Olig2 geremd kunnen worden. We hebben een methode opgezet waarbij we een reeks van zulke peptiden testen in hun potentie om de werking van Olig2 tegen te gaan. Tot nu toe hebben we nog geen peptide gevonden dat de werking van Olig2 remt. Dit onderzoek is nog in volle gang.

In het laatste hoofdstuk beschrijf ik tenslotte eiwitstructuren van andere bHLH-transcriptiefactoren. De eiwitstructuur van Olig1 en Olig2 is nog niet

bekend. Ik omschrijf de experimenten waarmee we de eiwitstructuur zouden kunnen uitzoeken. Ten slotte beargumenteer ik waarom kennis van Olig2-eiwitstructuur noodzakelijk is voor de ontwikkeling van een nieuwe generatie groeiremmers voor hersentumortherapie.

Bibliography

Adelmant, G., Calkins, A.S., Garg, B.K., Card, J.D., Askenazi, M., Miron, A., Sobhian, B., Zhang, Y., Nakatani, Y., Silver, P.A., *et al.* (2012). DNA ends alter the molecular composition and localization of Ku multicomponent complexes. Mol Cell Proteomics 11, 411–421.

Ahmadpour, F., Ghirlando, R., De Jong, A.T., Gloyd, M., Shin, J.A., and Guarne, A. (2012). Crystal structure of the minimalist Max-E47 protein chimera. PLOS One 7, e32136.

Alberta, J.A., and Segal, R.A. (2001). Generation and utilization of phosphorylation state-specific antibodies to investigate signaling pathways. Curr Protoc Neurosci Chapter 3, Unit 3 14.

Aoki, M., Yamashita, T., and Tohyama, M. (2004). EphA receptors direct the differentiation of mammalian neural precursor cells through a mitogen-activated protein kinase-dependent pathway. The Journal of biological chemistry 279, 32643–32650.

Appolloni, I., Calzolari, F., Barilari, M., Terrile, M., Daga, A., and Malatesta, P. (2012). Antagonistic modulation of gliomagenesis by Pax6 and Olig2 in Pdgf-induced oligodendroglioma. Int J Cancer.

Arnett, H.A., Fancy, S.P., Alberta, J.A., Zhao, C., Plant, S.R., Kaing, S., Raine, C.S., Rowitch, D.H., Franklin, R.J., and Stiles, C.D. (2004). bHLH transcription factor Olig1 is required to repair demyelinated lesions in the CNS. Science 306, 2111–2115.

Babu, D.A., Chakrabarti, S.K., Garmey, J.C., and Mirmira, R.G. (2008). Pdx1 and Beta2/NeuroD1 participate in a transcriptional complex that mediates short-range DNA looping at the insulin gene. The Journal of biological chemistry 283, 8164–8172.

Bachoo, R.M., Maher, E.A., Ligon, K.L., Sharpless, N.E., Chan, S.S., You, M.J., Tang, Y., DeFrances, J., Stover, E., Weissleder, R., *et al.* (2002). Epidermal growth factor receptor and Ink4a/Arf: convergent mechanisms governing terminal differentiation and transformation along the neural stem cell to astrocyte axis. Cancer Cell 1, 269–277.

Bao, S., Wu, Q., Li, Z., Sathornsumetee, S., Wang, H., McLendon, R.E., Hjelmeland, A.B., and Rich, J.N. (2008). Targeting cancer stem cells through L1CAM suppresses glioma growth. Cancer Res 68, 6043–6048.

Barlev, N.A., Liu, L., Chehab, N.H., Mansfield, K., Harris, K.G., Halazonetis, T.D., and Berger, S.L. (2001). Acetylation of p53 activates transcription through recruitment of coactivators/histone acetyltransferases. Mol Cell 8, 1243–1254.

Barrett, L.E., Granot, Z., Coker, C., Iavarone, A., Hambardzumyan, D., Holland, E.C., Nam, H.S., and Benezra, R. (2012). Self-renewal does not predict tumor growth potential in mouse models of high-grade glioma. Cancer Cell 21, 11–24.

Beatus, P., and Lendahl, U. (1998). Notch and neurogenesis. Journal of neuroscience research 54, 125–136.

Beckett, D. (2001). Regulated assembly of transcription factors and control of transcription initiation. J Mol Biol 314, 335–352.

Belichenko, P.V., Masliah, E., Kleschevnikov, A.M., Villar, A.J., Epstein, C.J., Salehi, A., and Mobley, W.C. (2004). Synaptic structural abnormalities in the Ts65Dn mouse model of Down Syndrome. J Comp Neurol 480, 281–298.

Benezra, R., Davis, R.L., Lockshon, D., Turner, D.L., and Weintraub, H. (1990). The protein Id: a negative regulator of helix-loop-helix DNA binding proteins. Cell 61, 49–59.

Berberich, S., Hyde-DeRuyscher, N., Espenshade, P., and Cole, M. (1992). Max encodes a sequence-specific DNA-binding protein and is not regulated by serum growth factors. Oncogene 7, 775–779.

Bernal, F., Wade, M., Godes, M., Davis, T.N., Whitehead, D.G., Kung, A.L., Wahl, G.M., and Walensky, L.D. (2010). A stapled p53 helix overcomes HDMX-mediated suppression of p53. Cancer Cell 18, 411–422.

Billiards, S.S., Haynes, R.L., Folkerth, R.D., Borenstein, N.S., Trachtenberg, F.L., Rowitch, D.H., Ligon, K.L., Volpe, J.J., and Kinney, H.C. (2008). Myelin abnormalities without oligodendrocyte loss in periventricular leukomalacia. Brain Pathol 18, 153–163.

Bird, G.H., Bernal, F., Pitter, K., and Walensky, L.D. (2008). Synthesis and biophysical characterization of stabilized alpha-helices of Bcl-2 domains. Methods Enzymol 446, 369–386.

Bird, G.H., Crannell, W.C., and Walensky, L.D. (2011). Chemical synthesis of hydrocarbon-stapled peptides for protein interaction research and therapeutic targeting. Curr Protoc Chem Biol 3, 99–117.

Bochkis, I.M., Schug, J., Ye, D.Z., Kurinna, S., Stratton, S.A., Barton, M.C., and Kaestner, K.H. (2012). Genome-wide location analysis reveals distinct transcriptional circuitry by paralogous regulators Foxa1 and Foxa2. PLOS genetics 8, e1002770.

Bouard, C., Terreux, R., Hope, J., Chemelle, J.A., Puisieux, A., Ansieau, S., and Payen, L. (2013). Interhelical loops within the bHLH domain are determinant in maintaining Twist1-DNA complexes. J Biomol Struct Dyn.

Bouvier, C., Bartoli, C., Aguirre-Cruz, L., Virard, I., Colin, C., Fernandez, C., Gouvernet, J., and Figarella-Branger, D. (2003). Shared oligodendrocyte lineage gene expression in gliomas and oligodendrocyte progenitor cells. J Neurosurg 99, 344–350.

Briscoe, J., Sussel, L., Serup, P., Hartigan-O'Connor, D., Jessell, T.M., Rubenstein, J.L., and Ericson, J. (1999). Homeobox gene Nkx2.2 and specification of neuronal identity by graded Sonic hedgehog signalling. Nature 398, 622–627.

Bronchain, O.J., Pollet, N., Ymlahi-Ouazzani, Q., Dhorne-Pollet, S., Helbling, J.C., Lecarpentier, J.E., Percheron, K., and Wegnez, M. (2007). The olig family: phylogenetic analysis and early gene expression in Xenopus tropicalis. Dev Genes Evol 217, 485–497.

Brownlie, P., Ceska, T., Lamers, M., Romier, C., Stier, G., Teo, H., and Suck, D. (1997). The crystal structure of an intact human Max-DNA complex: new insights into mechanisms of transcriptional control. Structure 5, 509–520.

Buffo, A., Rite, I., Tripathi, P., Lepier, A., Colak, D., Horn, A.P., Mori, T., and Gotz, M. (2008). Origin

and progeny of reactive gliosis: A source of multipotent cells in the injured brain. Proc Natl Acad Sci U S A 105, 3581–3586.

Buffo, A., Vosko, M.R., Erturk, D., Hamann, G.F., Jucker, M., Rowitch, D., and Gotz, M. (2005). Expression pattern of the transcription factor Olig2 in response to brain injuries: implications for neuronal repair. Proc Natl Acad Sci U S A 102, 18183–18188.

Cadigan, K.M., Grossniklaus, U., and Gehring, W.J. (1994). Functional redundancy: the respective roles of the two sloppy paired genes in Drosophila segmentation. Proceedings of the National Academy of Sciences of the United States of America 91, 6324–6328.

Cahoy, J.D., Emery, B., Kaushal, A., Foo, L.C., Zamanian, J.L., Christopherson, K.S., Xing, Y., Lubischer, J.L., Krieg, P.A., Krupenko, S.A., *et al.* (2008). A transcriptome database for astrocytes, neurons, and oligodendrocytes: a new resource for understanding brain development and function. J Neurosci 28, 264–278.

Cai, J., Chen, Y., Cai, W.H., Hurlock, E.C., Wu, H., Kernie, S.G., Parada, L.F., and Lu, Q.R. (2007). A crucial role for Olig2 in white matter astrocyte development. Development 134, 1887–1899.

Cai, J., Qi, Y., Hu, X., Tan, M., Liu, Z., Zhang, J., Li, Q., Sander, M., and Qiu, M. (2005). Generation of oligodendrocyte precursor cells from mouse dorsal spinal cord independent of Nkx6 regulation and Shh signaling. Neuron 45, 41–53.

Cameron-Curry, P., and Le Douarin, N.M. (1995). Oligodendrocyte precursors originate from both the dorsal and the ventral parts of the spinal cord. Neuron 15, 1299–1310.

Cassiani-Ingoni, R., Coksaygan, T., Xue, H., Reichert-Scrivner, S.A., Wiendl, H., Rao, M.S., and Magnus, T. (2006). Cytoplasmic translocation of Olig2 in adult glial progenitors marks the generation of reactive astrocytes following autoimmune inflammation. Exp Neurol 201, 349–358.

Chakrabarti, L., Best, T.K., Cramer, N.P., Carney, R.S., Isaac, J.T., Galdzicki, Z., and Haydar, T.F. (2010). Olig1 and Olig2 triplication causes developmental brain defects in Down syndrome. Nat Neurosci 13, 927–934.

Chang, A., Tourtellotte, W.W., Rudick, R., and Trapp, B.D. (2002). Premyelinating oligodendrocytes in chronic lesions of multiple sclerosis. N Engl J Med 346, 165–173.

Chang, R.G.S. (1998). Recent Advances in Olefin Metathesis and Its Application in Organic Synthesis Tetrahedron, pp. 4413–4450.

Charcot, J.M. (1868). Histologie de la sclerose en plaques. Gazette des hopitaux Paris 41, 554–555.

Chen, C.H., Kuo, S.C., Huang, L.J., Hsu, M.H., and Lung, F.D. (2010). Affinity of synthetic peptide fragments of MyoD for Id1 protein and their biological effects in several cancer cells. J Pept Sci 16, 231–241.

Chen, C.T., Gottlieb, D.I., and Cohen, B.A. (2008a). Ultraconserved elements in the Olig2 promoter. PLOS One 3, e3946.

Chen, J.A., Huang, Y.P., Mazzoni, E.O., Tan, G.C., Zavadil, J., and Wichterle, H. (2011). Mir-17-3p controls spinal neural progenitor patterning by regulating Olig2/Irx3 cross-repressive loop. Neuron 69, 721–735.

Chen, Y., Miles, D.K., Hoang, T., Shi, J., Hurlock, E., Kernie, S.G., and Lu, Q.R. (2008b). The basic helix-loop-helix transcription factor Olig2 is critical for reactive astrocyte proliferation after cortical injury. J Neurosci 28, 10983–10989.

Coleman, M.L., Marshall, C.J., and Olson, M.F. (2003). Ras promotes p21(Waf1/Cip1) protein stability via a cyclin D1-imposed block in proteasome-mediated degradation. Embo J 22, 2036–2046.

Conant, G.C., and Wagner, A. (2003). Asymmetric sequence divergence of duplicate genes. Genome research 13, 2052–2058.

D'Agnano, I., Valentini, A., Gatti, G., Chersi, A., and Felsani, A. (2007). Oligopeptides impairing the Myc-Max heterodimerization inhibit lung cancer cell proliferation by reducing Myc transcriptional activity. J Cell Physiol 210, 72–80.

De Masi, F., Grove, C.A., Vedenko, A., Alibes, A., Gisselbrecht, S.S., Serrano, L., Bulyk, M.L., and Walhout, A.J. (2011). Using a structural and logics systems approach to infer bHLH-DNA binding specificity determinants. Nucleic acids research 39, 4553–4563.

Deneen, B., Ho, R., Lukaszewicz, A., Hochstim, C.J., Gronostajski, R.M., and Anderson, D.J. (2006). The transcription factor Nfia controls the onset of gliogenesis in the developing spinal cord. Neuron 52, 953–968.

Doetsch, F., Petreanu, L., Caille, I., Garcia-Verdugo, J.M., and Alvarez-Buylla, A. (2002). Egf converts transit-amplifying neurogenic precursors in the adult brain into multipotent stem cells. Neuron 36, 1021–1034.

Dornan, D., Shimizu, H., Perkins, N.D., and Hupp, T.R. (2003). DNA-dependent acetylation of p53 by the transcription coactivator p300. The Journal of biological chemistry 278, 13431–13441.

Draeger, L.J., and Mullen, G.P. (1994). Interaction of the bHLH-zip domain of c-Myc with H1-type peptides. Characterization of helicity in the H1 peptides by NMR. The Journal of biological chemistry 269, 1785–1793.

Edlund, T., and Jessell, T.M. (1999). Progression from extrinsic to intrinsic signaling in cell fate specification: a view from the nervous system. Cell 96, 211–224.

Edwards, A.L., Gavathiotis, E., LaBelle, J.L., Braun, C.R., Opoku-Nsiah, K.A., Bird, G.H., and Walensky, L.D. (2013). Multimodal interaction with Bcl-2 family proteins underlies the proapoptotic activity of PUMA BH3. Chemistry & biology 20, 888–902.

El Ghouzzi, V., Legeai-Mallet, L., Benoist-Lasselin, C., Lajeunie, E., Renier, D., Munnich, A., and Bonaventure, J. (2001). Mutations in the basic domain and the loop-helix II junction of Twist abolish DNA binding in Saethre-Chotzen syndrome. FEBS Lett 492, 112–118.

el-Husseini Ael, D., and Bredt, D.S. (2002). Protein palmitoylation: a regulator of neuronal development and function. Nature reviews Neuroscience 3, 791–802.

Ellenberger, T., Fass, D., Arnaud, M., and Harrison, S.C. (1994). Crystal structure of transcription factor E47: E-box recognition by a basic region helix-loop-helix dimer. Genes & development 8, 970–980.

Fairman, R., Beran-Steed, R.K., Anthony-Cahill, S.J., Lear, J.D., Stafford, W.F., 3rd, DeGrado, W.F., Benfield, P.A., and Brenner, S.L. (1993). Multiple oligomeric states regulate the DNA binding of

helix-loop-helix peptides. Proceedings of the National Academy of Sciences of the United States of America 90, 10429–10433.

Fancy, S.P., Harrington, E.P., Yuen, T.J., Silbereis, J.C., Zhao, C., Baranzini, S.E., Bruce, C.C., Otero, J.J., Huang, E.J., Nusse, R., *et al.* (2011). Axin2 as regulatory and therapeutic target in newborn brain injury and remyelination. Nat Neurosci.

Fancy, S.P., Zhao, C., and Franklin, R.J. (2004). Increased expression of Nkx2.2 and Olig2 identifies reactive oligodendrocyte progenitor cells responding to demyelination in the adult CNS. Mol Cell Neurosci 27, 247–254.

Featherstone, M. (2002). Coactivators in transcription initiation: here are your orders. Current opinion in genetics & development 12, 149–155.

Feng, J., Liu, T., Qin, B., Zhang, Y., and Liu, X.S. (2012). Identifying ChIP-seq enrichment using MACS. Nat Protoc 7, 1728–1740.

Fernandez, F., and Garner, C.C. (2007). Over-inhibition: a model for developmental intellectual disability. Trends Neurosci 30, 497–503.

Ferre-D'Amare, A.R., Prendergast, G.C., Ziff, E.B., and Burley, S.K. (1993). Recognition by Max of its cognate DNA through a dimeric b/HLH/Z domain. Nature 363, 38–45.

Fogarty, M., Richardson, W.D., and Kessaris, N. (2005). A subset of oligodendrocytes generated from radial glia in the dorsal spinal cord. Development 132, 1951–1959.

Follis, A.V., Hammoudeh, D.I., Wang, H., Prochownik, E.V., and Metallo, S.J. (2008). Structural rationale for the coupled binding and unfolding of the c-Myc oncoprotein by small molecules. Chemistry & biology 15, 1149–1155.

Frazer, K.A., Sheehan, J.B., Stokowski, R.P., Chen, X., Hosseini, R., Cheng, J.F., Fodor, S.P., Cox, D.R., and Patil, N. (2001). Evolutionarily conserved sequences on human chromosome 21. Genome Res 11, 1651–1659.

Fu, H., Cai, J., Clevers, H., Fast, E., Gray, S., Greenberg, R., Jain, M.K., Ma, Q., Qiu, M., Rowitch, D.H., *et al.* (2009). A genome-wide screen for spatially restricted expression patterns identifies transcription factors that regulate glial development. The Journal of neuroscience : the official journal of the Society for Neuroscience 29, 11399–11408.

Fukuda, S., Kondo, T., Takebayashi, H., and Taga, T. (2004). Negative regulatory effect of an oligodendrocytic bHLH factor Olig2 on the astrocytic differentiation pathway. Cell Death Differ 11, 196–202.

Furusho, M., Ono, K., Takebayashi, H., Masahira, N., Kagawa, T., Ikeda, K., and Ikenaka, K. (2006). Involvement of the Olig2 transcription factor in cholinergic neuron development of the basal forebrain. Dev Biol 293, 348–357.

Gabay, L., Lowell, S., Rubin, L.L., and Anderson, D.J. (2003). Deregulation of dorsoventral patterning by Fgf confers trilineage differentiation capacity on CNS stem cells in vitro. Neuron 40, 485–499.

Georgieva, L., Moskvina, V., Peirce, T., Norton, N., Bray, N.J., Jones, L., Holmans, P., Macgregor, S., Zammit, S., Wilkinson, J., *et al.* (2006). Convergent evidence that oligodendrocyte lineage transcription factor 2 (Olig2) and interacting genes influence susceptibility to schizophrenia. Proc Natl Acad Sci U S A 103, 12469–12474.

Ghosh, I., and Chmielewski, J. (1998). A beta-sheet peptide inhibitor of E47 dimerization and DNA binding. Chemistry & biology 5, 439–445.

Ghosh, I., Issac, R., and Chmielewski, J. (1999). Structure-function relationship in a beta-sheet peptide inhibitor of E47 dimerization and DNA binding. Bioorg Med Chem 7, 61–66.

Gill, G. (2004). SUMO and ubiquitin in the nucleus: different functions, similar mechanisms? Genes & development 18, 2046–2059.

Giorello, L., Clerico, L., Pescarolo, M.P., Vikhanskaya, F., Salmona, M., Colella, G., Bruno, S., Mancuso, T., Bagnasco, L., Russo, P., and Parodi, S. (1998). Inhibition of cancer cell growth and c-Myc transcriptional activity by a c-Myc helix 1-type peptide fused to an internalization sequence. Cancer research 58, 3654–3659.

Giusti, S., Bogetti, M.E., Bonafina, A., and Fiszer de Plazas, S. (2009). An improved method to obtain a soluble nuclear fraction from embryonic brain tissue. Neurochem Res 34, 2022–2029.

Gong, J., Ammanamanchi, S., Ko, T.C., and Brattain, M.G. (2003). Transforming growth factor beta 1 increases the stability of p21/WAF1/CIP1 protein and inhibits Cdk2 kinase activity in human colon carcinoma FET cells. Cancer research 63, 3340–3346.

Gray, P.A., Fu, H., Luo, P., Zhao, Q., Yu, J., Ferrari, A., Tenzen, T., Yuk, D.I., Tsung, E.F., Cai, Z., *et al.* (2004). Mouse brain organization revealed through direct genome-scale TF expression analysis. Science 306, 2255–2257.

Guo, S.J., Hu, J.G., Zhao, B.M., Shen, L., Wang, R., Zhou, J.S., and Lu, H.Z. (2011). Olig1 and Id4 interactions in living cells visualized by bimolecular fluorescence complementation technique. Mol Biol Rep 38, 4637–4642.

Hay, R.T. (2004). Modifying NEMO. Nat Cell Biol 6, 89–91.

Hay, R.T. (2005). SUMO: a history of modification. Mol Cell 18, 1–12.

He, H.H., Meyer, C.A., Shin, H., Bailey, S.T., Wei, G., Wang, Q., Zhang, Y., Xu, K., Ni, M., Lupien, M., *et al.* (2010). Nucleosome dynamics define transcriptional enhancers. Nat Genet 42, 343–347.

Huang, K., Tang, W., Tang, R., Xu, Z., He, Z., Li, Z., Xu, Y., Li, X., He, G., Feng, G., *et al.* (2008a). Positive association between Olig2 and schizophrenia in the Chinese Han population. Hum Genet 122, 659–660.

Huang, M., Sage, C., Li, H., Xiang, M., Heller, S., and Chen, Z.Y. (2008b). Diverse expression patterns of Lim-homeodomain transcription factors (LIM-HDS) in mammalian inner ear development. Developmental dynamics : an official publication of the American Association of Anatomists 237, 3305–3312.

Huang, N., Chelliah, Y., Shan, Y., Taylor, C.A., Yoo, S.H., Partch, C., Green, C.B., Zhang, H., and Takahashi, J.S. (2012). Crystal structure of the heterodimeric CLOCK:Bmal1 transcriptional activator complex. Science 337, 189–194.

Huang, T.T., Wuerzberger-Davis, S.M., Wu, Z.H., and Miyamoto, S. (2003). Sequential modification of NEMO/IKKgamma by SUMO-1 and ubiquitin mediates NF-kappaB activation by genotoxic stress. Cell 115, 565–576.

Huillard, E., Ziercher, L., Blond, O., Wong, M., Deloulme, J.C., Souchelnytskyi, S., Baudier, J., Cochet, C., and Buchou, T. (2010). Disruption of CK2beta in embryonic neural stem cells compromises proliferation and oligodendrogenesis in the mouse telencephalon. Mol Cell Biol 30, 2737–2749.

Huminiecki, L., and Wolfe, K.H. (2004). Divergence of spatial gene expression profiles following species-specific gene duplications in human and mouse. Genome research 14, 1870–1879.

Ikushima, H., Komuro, A., Isogaya, K., Shinozaki, M., Hellman, U., Miyazawa, K., and Miyazono, K. (2008). An Id-like molecule, Hhm, is a synexpression group-restricted regulator of TGF-beta signalling. Embo J 27, 2955–2965.

Imoto, S., Ohbayashi, N., Ikeda, O., Kamitani, S., Muromoto, R., Sekine, Y., and Matsuda, T. (2008). Sumoylation of Smad3 stimulates its nuclear export during Piasy-mediated suppression of TGF-beta signaling. Biochem Biophys Res Commun 370, 359–365.

Ito, A., Kawaguchi, Y., Lai, C.H., Kovacs, J.J., Higashimoto, Y., Appella, E., and Yao, T.P. (2002). Mdm2-Hdac1-mediated deacetylation of p53 is required for its degradation. Embo J 21, 6236–6245.

Jackson, E.L., Garcia-Verdugo, J.M., Gil-Perotin, S., Roy, M., Quinones-Hinojosa, A., VandenBerg, S., and Alvarez-Buylla, A. (2006). Pdgfr alpha-positive B cells are neural stem cells in the adult SVZ that form glioma-like growths in response to increased Pdgf signaling. Neuron 51, 187–199.

Jan, Y.N., and Jan, L.Y. (1990). Genes required for specifying cell fates in Drosophila embryonic sensory nervous system. Trends in neurosciences 13, 493–498.

Jessell, T.M. (2000). Neuronal specification in the spinal cord: inductive signals and transcriptional codes. Nat Rev Genet 1, 20–29.

Johnson, E.S. (2004). Protein modification by SUMO. Annu Rev Biochem 73, 355–382.

Juan, L.J., Shia, W.J., Chen, M.H., Yang, W.M., Seto, E., Lin, Y.S., and Wu, C.W. (2000). Histone deacetylases specifically down-regulate p53-dependent gene activation. The Journal of biological chemistry 275, 20436–20443.

Justice, N.J., and Jan, Y.N. (2002). Variations on the Notch pathway in neural development. Curr Opin Neurobiol 12, 64–70.

Kaas, J.H. (2005). From mice to men: the evolution of the large, complex human brain. J Biosci 30, 155–165.

Kageyama, R., and Nakanishi, S. (1997). Helix-loop-helix factors in growth and differentiation of the vertebrate nervous system. Current opinion in genetics & development 7, 659–665.

Kamakaka, R.T., and Kadonaga, J.T. (1994). The soluble nuclear fraction, a highly efficient transcription extract from Drosophila embryos. Methods Cell Biol 44, 225–235.

Kellerer, S., Schreiner, S., Stolt, C.C., Scholz, S., Bosl, M.R., and Wegner, M. (2006). Replacement of the Sox10 transcription factor by Sox8 reveals incomplete functional equivalence. Development 133, 2875–2886.

Kippin, T.E., Martens, D.J., and van der Kooy, D. (2005). p21 loss compromises the relative quiescence of forebrain stem cell proliferation leading to exhaustion of their proliferation capacity. Genes & development 19, 756–767.

Kitada, M., and Rowitch, D.H. (2006). Transcription factor co-expression patterns indicate heterogeneity of oligodendroglial subpopulations in adult spinal cord. Glia 54, 35–46.

Komitova, M., Serwanski, D.R., Lu, Q.R., and Nishiyama, A. (2011). NG2 cells are not a major source of reactive astrocytes after neocortical stab wound injury. Glia 59, 800–809.

Koskinen, P.J., Vastrik, I., Makela, T.P., Eisenman, R.N., and Alitalo, K. (1994). Max activity is affected by phosphorylation at two NH2-terminal sites. Cell Growth Differ 5, 313–320.

Krylov, D., Kasai, K., Echlin, D.R., Taparowsky, E.J., Arnheiter, H., and Vinson, C. (1997). A general method to design dominant negatives to B-HLHzip proteins that abolish DNA binding. Proceedings of the National Academy of Sciences of the United States of America 94, 12274–12279.

Kuhlmann, T., Miron, V., Cui, Q., Wegner, C., Antel, J., and Bruck, W. (2008). Differentiation block of oligodendroglial progenitor cells as a cause for remyelination failure in chronic multiple sclerosis. Brain 131, 1749–1758.

Kuspert, M., Hammer, A., Bosl, M.R., and Wegner, M. (2011). Olig2 regulates Sox10 expression in oligodendrocyte precursors through an evolutionary conserved distal enhancer. Nucleic Acids Res 39, 1280–1293.

Langmead, B., Trapnell, C., Pop, M., and Salzberg, S.L. (2009). Ultrafast and memory-efficient alignment of short DNA sequences to the human genome. Genome biology 10, R25.

Langseth, A.J., Munji, R.N., Choe, Y., Huynh, T., Pozniak, C.D., and Pleasure, S.J. (2010). Wnts influence the timing and efficiency of oligodendrocyte precursor cell generation in the telencephalon. J Neurosci 30, 13367–13372.

Learish, R.D., Bruss, M.D., and Haak-Frendscho, M. (2000). Inhibition of mitogen-activated protein kinase kinase blocks proliferation of neural progenitor cells. Brain Res Dev Brain Res 122, 97–109.

Ledent, V., Paquet, O., and Vervoort, M. (2002). Phylogenetic analysis of the human basic helix-loop-helix proteins. Genome Biol 3.

Lee, J.C., Mayer-Proschel, M., and Rao, M.S. (2000). Gliogenesis in the central nervous system. Glia 30, 105–121.

Lee, J.E. (1997). Basic helix-loop-helix genes in neural development. Curr Opin Neurobiol 7, 13–20.

Lee, S.K., Lee, B., Ruiz, E.C., and Pfaff, S.L. (2005). Olig2 and Ngn2 function in opposition to modulate gene expression in motor neuron progenitor cells. Genes Dev 19, 282–294.

Li, H., de Faria, J.P., Andrew, P., Nitarska, J., and Richardson, W.D. (2011). Phosphorylation regulates Olig2 cofactor choice and the motor neuron-oligodendrocyte fate switch. Neuron 69, 918–929.

Li, H., Lu, Y., Smith, H.K., and Richardson, W.D. (2007). Olig1 and Sox10 interact synergistically to drive myelin basic protein transcription in oligodendrocytes. J Neurosci 27, 14375–14382.

Li, M., Luo, J., Brooks, C.L., and Gu, W. (2002). Acetylation of p53 inhibits its ubiquitination by Mdm2. The Journal of biological chemistry 277, 50607–50611.

Ligon, K.L., Alberta, J.A., Kho, A.T., Weiss, J., Kwaan, M.R., Nutt, C.L., Louis, D.N., Stiles, C.D., and Rowitch, D.H. (2004). The oligodendroglial lineage marker Olig2 is universally expressed in diffuse gliomas. J Neuropathol Exp Neurol 63, 499–509.

Ligon, K.L., Huillard, E., Mehta, S., Kesari, S., Liu, H., Alberta, J.A., Bachoo, R.M., Kane, M., Louis, D.N., Depinho, R.A., *et al.* (2007). Olig2-regulated lineage-restricted pathway controls replication competence in neural stem cells and malignant glioma. Neuron 53, 503–517.

Liu, T., Ortiz, J.A., Taing, L., Meyer, C.A., Lee, B., Zhang, Y., Shin, H., Wong, S.S., Ma, J., Lei, Y., *et al.* (2011). Cistrome: an integrative platform for transcriptional regulation studies. Genome biology 12, R83.

Liu, Z., Li, H., Hu, X., Yu, L., Liu, H., Han, R., Colella, R., Mower, G.D., Chen, Y., and Qiu, M. (2008). Control of precerebellar neuron development by Olig3 bHLH transcription factor. J Neurosci 28, 10124–10133.

Longo, A., Guanga, G.P., and Rose, R.B. (2008). Crystal structure of E47-NeuroD1/Beta2 bHLH domain-DNA complex: heterodimer selectivity and DNA recognition. Biochemistry 47, 218–229.

Louis, D.N., Ohgaki, H., Wiestler, O.D., Cavenee, W.K., Burger, P.C., Jouvet, A., Scheithauer, B.W., and Kleihues, P. (2007). The 2007 WHO classification of tumours of the central nervous system. Acta Neuropathol 114, 97–109.

Lu, Q.R., Park, J.K., Noll, E., Chan, J.A., Alberta, J., Yuk, D., Alzamora, M.G., Louis, D.N., Stiles, C.D., Rowitch, D.H., and Black, P.M. (2001). Oligodendrocyte lineage genes (Olig) as molecular markers for human glial brain tumors. Proc Natl Acad Sci U S A 98, 10851–10856.

Lu, Q.R., Sun, T., Zhu, Z., Ma, N., Garcia, M., Stiles, C.D., and Rowitch, D.H. (2002). Common developmental requirement for Olig function indicates a motor neuron/oligodendrocyte connection. Cell 109, 75–86.

Lu, Q.R., Yuk, D., Alberta, J.A., Zhu, Z., Pawlitzky, I., Chan, J., McMahon, A.P., Stiles, C.D., and Rowitch, D.H. (2000). Sonic hedgehog--regulated oligodendrocyte lineage genes encoding bHLH proteins in the mammalian central nervous system. Neuron 25, 317–329.

Lucchinetti, C., Bruck, W., Parisi, J., Scheithauer, B., Rodriguez, M., and Lassmann, H. (1999). A quantitative analysis of oligodendrocytes in multiple sclerosis lesions. A study of 113 cases. Brain 122 (Pt 12), 2279–2295.

Luo, J., Su, F., Chen, D., Shiloh, A., and Gu, W. (2000). Deacetylation of p53 modulates its effect on cell growth and apoptosis. Nature 408, 377–381.

Ma, D.K., Ponnusamy, K., Song, M.R., Ming, G.L., and Song, H. (2009). Molecular genetic analysis of Fgfr1 signalling reveals distinct roles of Mapk and Plcg1 activation for self-renewal of adult neural stem cells. Mol Brain 2, 16.

Ma, L., Sham, Y.Y., Walters, K.J., and Towle, H.C. (2007). A critical role for the loop region of the basic helix-loop-helix/leucine zipper protein Mlx in DNA binding and glucose-regulated transcription. Nucleic acids research 35, 35–44.

Ma, P.C., Rould, M.A., Weintraub, H., and Pabo, C.O. (1994). Crystal structure of MyoD bHLH domain-DNA complex: perspectives on DNA recognition and implications for transcriptional activation. Cell 77, 451–459.

Ma, Y.C., Song, M.R., Park, J.P., Henry Ho, H.Y., Hu, L., Kurtev, M.V., Zieg, J., Ma, Q., Pfaff, S.L., and Greenberg, M.E. (2008). Regulation of motor neuron specification by phosphorylation of neurogenin 2. Neuron 58, 65–77.

Magnus, T., Coksaygan, T., Korn, T., Xue, H., Arumugam, T.V., Mughal, M.R., Eckley, D.M., Tang, S.C., Detolla, L., Rao, M.S., *et al.* (2007). Evidence that nucleocytoplasmic Olig2 translocation mediates brain-injury-induced differentiation of glial precursors to astrocytes. J Neurosci Res 85, 2126–2137.

Makarenkova, H.P., Gonzalez, K.N., Kiosses, W.B., and Meech, R. (2009). Barx2 controls myoblast fusion and promotes MyoD-mediated activation of the smooth muscle alpha-actin gene. The Journal of biological chemistry 284, 14866–14874.

Malatesta, P., Hack, M.A., Hartfuss, E., Kettenmann, H., Klinkert, W., Kirchhoff, F., and Gotz, M. (2003). Neuronal or glial progeny: regional differences in radial glia fate. Neuron 37, 751–764.

Marburg, O. (1906). Die sogenannte akute multiple Sklerose. Jahrb Psychiatre 27, 211–312.

Marie, Y., Sanson, M., Mokhtari, K., Leuraud, P., Kujas, M., Delattre, J.Y., Poirier, J., Zalc, B., and Hoang-Xuan, K. (2001). Olig2 as a specific marker of oligodendroglial tumour cells. Lancet 358, 298–300.

Marshall, C.A., Novitch, B.G., and Goldman, J.E. (2005). Olig2 directs astrocyte and oligodendrocyte formation in postnatal subventricular zone cells. J Neurosci 25, 7289–7298.

Martin, S., Wilkinson, K.A., Nishimune, A., and Henley, J.M. (2007). Emerging extranuclear roles of protein SUMOylation in neuronal function and dysfunction. Nature reviews Neuroscience 8, 948–959.

Martynoga, B., Mateo, J.L., Zhou, B., Andersen, J., Achimastou, A., Urban, N., van den Berg, D., Georgopoulou, D., Hadjur, S., Wittbrodt, J., *et al.* (2013). Epigenomic enhancer annotation reveals a key role for NFIX in neural stem cell quiescence. Genes & development 27, 1769–1786.

Massari, M.E., and Murre, C. (2000). Helix-loop-helix proteins: regulators of transcription in eucaryotic organisms. Molecular and cellular biology 20, 429–440.

Mazzoni, E.O., Mahony, S., Iacovino, M., Morrison, C.A., Mountoufaris, G., Closser, M., Whyte, W.A., Young, R.A., Kyba, M., Gifford, D.K., and Wichterle, H. (2011). Embryonic stem cell-based mapping of developmental transcriptional programs. Nat Methods 8, 1056–1058.

McCracken, S., Longman, D., Marcon, E., Moens, P., Downey, M., Nickerson, J.A., Jessberger, R., Wilde, A., Caceres, J.F., Emili, A., and Blencowe, B.J. (2005). Proteomic analysis of SRm160-containing complexes reveals a conserved association with cohesin. The Journal of biological chemistry 280, 42227–42236.

Mehta, S., Huillard, E., Kesari, S., Maire, C.L., Golebiowski, D., Harrington, E.P., Alberta, J.A., Kane, M.F., Theisen, M., Ligon, K.L., *et al.* (2011). The central nervous system-restricted transcription factor Olig2 opposes p53 responses to genotoxic damage in neural progenitors and malignant glioma. Cancer Cell 19, 359–371.

Meletis, K., Wirta, V., Hede, S.M., Nister, M., Lundeberg, J., and Frisen, J. (2006). p53 suppresses the self-renewal of adult neural stem cells. Development 133, 363–369.

Menn, B., Garcia-Verdugo, J.M., Yaschine, C., Gonzalez-Perez, O., Rowitch, D., and Alvarez-Buylla, A. (2006). Origin of oligodendrocytes in the subventricular zone of the adult brain. J Neurosci 26, 7907–7918.

Mitsui, K., Shirakata, M., and Paterson, B.M. (1993). Phosphorylation inhibits the DNA-binding activity of MyoD homodimers but not MyoD-E12 heterodimers. The Journal of biological chemistry 268, 24415–24420.

Miyoshi, G., Butt, S.J., Takebayashi, H., and Fishell, G. (2007). Physiologically distinct temporal cohorts of cortical interneurons arise from telencephalic Olig2-expressing precursors. J Neurosci 27, 7786–7798.

Mizuguchi, R., Sugimori, M., Takebayashi, H., Kosako, H., Nagao, M., Yoshida, S., Nabeshima, Y., Shimamura, K., and Nakafuku, M. (2001). Combinatorial roles of Olig2 and Neurogenin2 in the coordinated induction of pan-neuronal and subtype-specific properties of motoneurons. Neuron 31, 757–771.

Moellering, R.E., Cornejo, M., Davis, T.N., Del Bianco, C., Aster, J.C., Blacklow, S.C., Kung, A.L., Gilliland, D.G., Verdine, G.L., and Bradner, J.E. (2009). Direct inhibition of the NOTCH transcription factor complex. Nature 462, 182–188.

Molin, L., Mounsey, A., Aslam, S., Bauer, P., Young, J., James, M., Sharma-Oates, A., and Hope, I.A. (2000). Evolutionary conservation of redundancy between a diverged pair of forkhead transcription factor homologues. Development 127, 4825–4835.

Mostoslavsky, G., Kotton, D.N., Fabian, A.J., Gray, J.T., Lee, J.S., and Mulligan, R.C. (2005). Efficiency of transduction of highly purified murine hematopoietic stem cells by lentiviral and oncoretroviral vectors under conditions of minimal in vitro manipulation. Mol Ther 11, 932–940.

Muller, T., Anlag, K., Wildner, H., Britsch, S., Treier, M., and Birchmeier, C. (2005). The bHLH factor Olig3 coordinates the specification of dorsal neurons in the spinal cord. Genes Dev 19, 733–743.

Muroyama, Y., Fujiwara, Y., Orkin, S.H., and Rowitch, D.H. (2005). Specification of astrocytes by bHLH protein SCL in a restricted region of the neural tube. Nature 438, 360–363.

Muskal, S.M., Holbrook, S.R., and Kim, S.H. (1990). Prediction of the disulfide-bonding state of cysteine in proteins. Protein Eng 3, 667–672.

Nakatani, Y., and Ogryzko, V. (2003). Immunoaffinity purification of mammalian protein complexes. Methods Enzymol 370, 430–444.

Neufeld, B., Grosse-Wilde, A., Hoffmeyer, A., Jordan, B.W., Chen, P., Dinev, D., Ludwig, S., and Rapp, U.R. (2000). Serine/Threonine kinases 3pK and Mapk-activated protein kinase 2 interact with the basic helix-loop-helix transcription factor E47 and repress its transcriptional activity. The Journal of biological chemistry 275, 20239–20242.

Nickols, N.G., Jacobs, C.S., Farkas, M.E., and Dervan, P.B. (2007). Modulating hypoxia-inducible transcription by disrupting the Hifi-DNA interface. ACS Chem Biol 2, 561–571.

Nieddu, E., Melchiori, A., Pescarolo, M.P., Bagnasco, L., Biasotti, B., Licheri, B., Malacarne, D., Tortolina, L., Castagnino, N., Pasa, S., *et al.* (2005). Sequence specific peptidomimetic molecules inhibitors of a protein-protein interaction at the helix 1 level of c-Myc. FASEB journal : official publication of the Federation of American Societies for Experimental Biology 19, 632–634.

Niu, J., Mei, F., Wang, L., Liu, S., Tian, Y., Mo, W., Li, H., Lu, Q.R., and Xiao, L. (2012). Phosphorylated olig1 localizes to the cytosol of oligodendrocytes and promotes membrane expansion and maturation. Glia.

Novitch, B.G., Chen, A.I., and Jessell, T.M. (2001). Coordinate regulation of motor neuron subtype identity and pan-neuronal properties by the bHLH repressor Olig2. Neuron 31, 773–789.

Ohnishi, A., Sawa, H., Tsuda, M., Sawamura, Y., Itoh, T., Iwasaki, Y., and Nagashima, K. (2003). Expression of the oligodendroglial lineage-associated markers Olig1 and Olig2 in different types of human gliomas. J Neuropathol Exp Neurol 62, 1052–1059.

Parras, C.M., Galli, R., Britz, O., Soares, S., Galichet, C., Battiste, J., Johnson, J.E., Nakafuku, M., Vescovi, A., and Guillemot, F. (2004). Mash1 specifies neurons and oligodendrocytes in the postnatal brain. Embo J 23, 4495–4505.

Pekny, M., and Nilsson, M. (2005). Astrocyte activation and reactive gliosis. Glia 50, 427–434.

Pescarolo, M.P., Bagnasco, L., Malacarne, D., Melchiori, A., Valente, P., Millo, E., Bruno, S., Basso, S., and Parodi, S. (2001). A retro-inverso peptide homologous to helix 1 of c-Myc is a potent and specific inhibitor of proliferation in different cellular systems. FASEB journal : official publication of the Federation of American Societies for Experimental Biology 15, 31–33.

Petryniak, M.A., Potter, G.B., Rowitch, D.H., and Rubenstein, J.L. (2007). Dlx1 and Dlx2 control neuronal versus oligodendroglial cell fate acquisition in the developing forebrain. Neuron 55, 417–433.

Pollard, S.M., Yoshikawa, K., Clarke, I.D., Danovi, D., Stricker, S., Russell, R., Bayani, J., Head, R., Lee, M., Bernstein, M., *et al.* (2009). Glioma stem cell lines expanded in adherent culture have tumor-specific phenotypes and are suitable for chemical and genetic screens. Cell Stem Cell 4, 568–580.

Poulin, G., Lebel, M., Chamberland, M., Paradis, F.W., and Drouin, J. (2000). Specific protein-protein interaction between basic helix-loop-helix transcription factors and homeoproteins of the Pitx family. Molecular and cellular biology 20, 4826–4837.

Prineas, J.W., and Connell, F. (1979). Remyelination in multiple sclerosis. Ann Neurol 5, 22–31.

Pringle, N.P., and Richardson, W.D. (1993). A singularity of Pdgf alpha-receptor expression in the dorsoventral axis of the neural tube may define the origin of the oligodendrocyte lineage. Development 117, 525–533.

Qian, X., Goderie, S.K., Shen, Q., Stern, J.H., and Temple, S. (1998). Intrinsic programs of patterned cell lineages in isolated vertebrate CNS ventricular zone cells. Development 125, 3143–3152.

Raff, M.C., Miller, R.H., and Noble, M. (1983). A glial progenitor cell that develops in vitro into an astrocyte or an oligodendrocyte depending on culture medium. Nature 303, 390–396.

Rao, M.S., Noble, M., and Mayer-Proschel, M. (1998). A tripotential glial precursor cell is present in the developing spinal cord. Proc Natl Acad Sci U S A 95, 3996–4001.

Ravanpay, A.C., and Olson, J.M. (2008). E protein dosage influences brain development more than family member identity. J Neurosci Res 86, 1472–1481.

Ravasi, T., Suzuki, H., Cannistraci, C.V., Katayama, S., Bajic, V.B., Tan, K., Akalin, A., Schmeier, S., Kanamori-Katayama, M., Bertin, N., *et al.* (2010). An atlas of combinatorial transcriptional regulation in mouse and man. Cell 140, 744–752.

Ross, S.E., Greenberg, M.E., and Stiles, C.D. (2003). Basic helix-loop-helix factors in cortical development. Neuron 39, 13–25.

Roussa, E., Wiehle, M., Dunker, N., Becker-Katins, S., Oehlke, O., and Krieglstein, K. (2006). Transforming growth factor beta is required for differentiation of mouse mesencephalic progenitors into dopaminergic neurons in vitro and in vivo: ectopic induction in dorsal mesencephalon. Stem Cells 24, 2120–2129.

Rousselot-Pailley, P., Seneque, O., Lebrun, C., Crouzy, S., Boturyn, D., Dumy, P., Ferrand, M., and Delangle, P. (2006). Model peptides based on the binding loop of the copper metallochaperone Atx1: selectivity of the consensus sequence MxCxxC for metal ions Hg(II), Cu(I), Cd(II), Pb(II), and Zn(II). Inorg Chem 45, 5510–5520.

Rowitch, D.H., Lu, Q.R., Kessaris, N., and Richardson, W.D. (2002). An 'oligarchy' rules neural development. Trends Neurosci 25, 417–422.

Samanta, J., and Kessler, J.A. (2004). Interactions between Id and Olig proteins mediate the inhibitory effects of BMP4 on oligodendroglial differentiation. Development 131, 4131–4142.

Savino, M., Annibali, D., Carucci, N., Favuzzi, E., Cole, M.D., Evan, G.I., Soucek, L., and Nasi, S. (2011). The action mechanism of the Myc inhibitor termed Omomyc may give clues on how to target Myc for cancer therapy. PLoS One 6, e22284.

Setoguchi, T., and Kondo, T. (2004). Nuclear export of Olig2 in neural stem cells is essential for ciliary neurotrophic factor-induced astrocyte differentiation. J Cell Biol 166, 963–968.

Shi, J., Stover, J.S., Whitby, L.R., Vogt, P.K., and Boger, D.L. (2009). Small molecule inhibitors of Myc/Max dimerization and Myc-induced cell transformation. Bioorg Med Chem Lett 19, 6038–6041.

Shimizu, T., Toumoto, A., Ihara, K., Shimizu, M., Kyogoku, Y., Ogawa, N., Oshima, Y., and Hakoshima, T. (1997). Crystal structure of Pho4 bHLH domain-DNA complex: flanking base recognition. Embo J 16, 4689–4697.

Shirakata, M., Friedman, F.K., Wei, Q., and Paterson, B.M. (1993). Dimerization specificity of myogenic helix-loop-helix DNA-binding factors directed by nonconserved hydrophilic residues. Genes & development 7, 2456–2470.

Sims, R., Hollingworth, P., Moskvina, V., Dowzell, K., O'Donovan, M.C., Powell, J., Lovestone, S., Brayne, C., Rubinsztein, D., Owen, M.J., *et al.* (2009). Evidence that variation in the oligodendrocyte lineage transcription factor 2 (Olig2) gene is associated with psychosis in Alzheimer's disease. Neurosci Lett 461, 54–59.

Singh, S.K., Hawkins, C., Clarke, I.D., Squire, J.A., Bayani, J., Hide, T., Henkelman, R.M., Cusimano, M.D., and Dirks, P.B. (2004). Identification of human brain tumour initiating cells. Nature 432, 396–401.

Sloan, S.R., Shen, C.P., McCarrick-Walmsley, R., and Kadesch, T. (1996). Phosphorylation of E47 as a potential determinant of B-cell-specific activity. Molecular and cellular biology 16, 6900–6908.

Smith, E., and Shilatifard, A. (2010). The chromatin signaling pathway: diverse mechanisms of recruitment of histone-modifying enzymes and varied biological outcomes. Mol Cell 40, 689–701.

Soucek, L., Helmer-Citterich, M., Sacco, A., Jucker, R., Cesareni, G., and Nasi, S. (1998). Design and properties of a Myc derivative that efficiently homodimerizes. Oncogene 17, 2463–2472.

Soucek, L., Jucker, R., Panacchia, L., Ricordy, R., Tato, F., and Nasi, S. (2002). Omomyc, a potential Myc dominant negative, enhances Myc-induced apoptosis. Cancer research 62, 3507–3510.

Stewart, M.L., Fire, E., Keating, A.E., and Walensky, L.D. (2010). The Mcl1 BH3 helix is an exclusive Mcl1 inhibitor and apoptosis sensitizer. Nat Chem Biol 6, 595–601.

Stolt, C.C., Lommes, P., Friedrich, R.P., and Wegner, M. (2004). Transcription factors Sox8 and Sox10 perform non-equivalent roles during oligodendrocyte development despite functional redundancy. Development 131, 2349–2358.

Stolt, C.C., Lommes, P., Sock, E., Chaboissier, M.C., Schedl, A., and Wegner, M. (2003). The Sox9 transcription factor determines glial fate choice in the developing spinal cord. Genes & development 17, 1677–1689.

Stolt, C.C., Rehberg, S., Ader, M., Lommes, P., Riethmacher, D., Schachner, M., Bartsch, U., and Wegner, M. (2002). Terminal differentiation of myelin-forming oligodendrocytes depends on the transcription factor Sox10. Genes & development 16, 165–170.

Sun, T., Dong, H., Wu, L., Kane, M., Rowitch, D.H., and Stiles, C.D. (2003). Cross-repressive interaction of the Olig2 and Nkx2.2 transcription factors in developing neural tube associated with formation of a specific physical complex. J Neurosci 23, 9547–9556.

Sun, T., Echelard, Y., Lu, R., Yuk, D.I., Kaing, S., Stiles, C.D., and Rowitch, D.H. (2001). Olig bHLH proteins interact with homeodomain proteins to regulate cell fate acquisition in progenitors of the ventral neural tube. Curr Biol 11, 1413–1420.

Sun, Y., Meijer, D.H., Alberta, J.A., Mehta, S., Kane, M.F., Tien, A.C., Fu, H., Petryniak, M.A., Potter, G.B., Liu, Z., *et al.* (2011). Phosphorylation state of Olig2 regulates proliferation of neural progenitors. Neuron 69, 906–917.

Takebayashi, H., Yoshida, S., Sugimori, M., Kosako, H., Kominami, R., Nakafuku, M., and Nabeshima, Y. (2000). Dynamic expression of basic helix-loop-helix Olig family members: implication of Olig2 in neuron and oligodendrocyte differentiation and identification of a new member, Olig3. Mech Dev 99, 143–148.

Timsit, S., Martinez, S., Allinquant, B., Peyron, F., Puelles, L., and Zalc, B. (1995). Oligodendrocytes originate in a restricted zone of the embryonic ventral neural tube defined by Dm-20 mRNA expression. J Neurosci 15, 1012–1024.

Torchia, J., Glass, C., and Rosenfeld, M.G. (1998). Co-activators and co-repressors in the integration of transcriptional responses. Curr Opin Cell Biol 10, 373–383.

Trapnell, C., Williams, B.A., Pertea, G., Mortazavi, A., Kwan, G., van Baren, M.J., Salzberg, S.L., Wold, B.J., and Pachter, L. (2010). Transcript assembly and quantification by RNA-Seq reveals unannotated transcripts and isoform switching during cell differentiation. Nat Biotechnol 28, 511–515.

Tripathi, R.B., Rivers, L.E., Young, K.M., Jamen, F., and Richardson, W.D. (2010). NG2 glia generate new oligodendrocytes but few astrocytes in a murine experimental autoimmune encephalomyelitis model of demyelinating disease. J Neurosci 30, 16383–16390.

Tropepe, V., Craig, C.G., Morshead, C.M., and van der Kooy, D. (1997). Transforming growth factor-alpha null and senescent mice show decreased neural progenitor cell proliferation in the

forebrain subependyma. The Journal of neuroscience : the official journal of the Society for Neuroscience 17, 7850–7859.

Tsai, H.H., Li, H., Fuentealba, L.C., Molofsky, A.V., Taveira-Marques, R., Zhuang, H., Tenney, A., Murnen, A.T., Fancy, S.P., Merkle, F., *et al.* (2012). Regional astrocyte allocation regulates CNS synaptogenesis and repair. Science 337, 358–362.

Vallstedt, A., Klos, J.M., and Ericson, J. (2005). Multiple dorsoventral origins of oligodendrocyte generation in the spinal cord and hindbrain. Neuron 45, 55–67.

Verger, A., Perdomo, J., and Crossley, M. (2003). Modification with SUMO. A role in transcriptional regulation. EMBO Rep 4, 137–142.

Verney, C., Pogledic, I., Biran, V., Adle-Biassette, H., Fallet-Bianco, C., and Gressens, P. (2012). Microglial reaction in axonal crossroads is a hallmark of noncystic periventricular white matter injury in very preterm infants. J Neuropathol Exp Neurol 71, 251–264.

Walensky, L.D., Kung, A.L., Escher, I., Malia, T.J., Barbuto, S., Wright, R.D., Wagner, G., Verdine, G.L., and Korsmeyer, S.J. (2004). Activation of apoptosis in vivo by a hydrocarbon-stapled BH3 helix. Science 305, 1466–1470.

Wang, S.Z., Dulin, J., Wu, H., Hurlock, E., Lee, S.E., Jansson, K., and Lu, Q.R. (2006). An oligodendrocyte-specific zinc-finger transcription regulator cooperates with Olig2 to promote oligodendrocyte differentiation. Development 133, 3389–3398.

Warf, B.C., Fok-Seang, J., and Miller, R.H. (1991). Evidence for the ventral origin of oligodendrocyte precursors in the rat spinal cord. J Neurosci 11, 2477–2488.

Weng, Q., Chen, Y., Wang, H., Xu, X., Yang, B., He, Q., Shou, W., Higashi, Y., van den Berghe, V., Seuntjens, E., *et al.* (2012). Dual-mode modulation of smad signaling by smad-interacting protein sip1 is required for myelination in the central nervous system. Neuron 73, 713–728.

Wissmuller, S., Kosian, T., Wolf, M., Finzsch, M., and Wegner, M. (2006). The high-mobility-group domain of Sox proteins interacts with DNA-binding domains of many transcription factors. Nucleic acids research 34, 1735–1744.

Wong, M.V., Jiang, S., Palasingam, P., and Kolatkar, P.R. (2012). A divalent ion is crucial in the structure and dominant-negative function of Id proteins, a class of helix-loop-helix transcription regulators. PLOS One 7, e48591.

Xin, M., Yue, T., Ma, Z., Wu, F.F., Gow, A., and Lu, Q.R. (2005). Myelinogenesis and axonal recognition by oligodendrocytes in brain are uncoupled in Olig1-null mice. J Neurosci 25, 1354–1365.

Xu, J., De Jong, A.T., Chen, G., Chow, H.K., Damaso, C.O., Schwartz Mittelman, A., and Shin, J.A. (2010). Reengineering natural design by rational design and in vivo library selection: the HLH subdomain in bHLHZ proteins is a unique requirement for DNA-binding function. Protein Eng Des Sel 23, 337–346.

Yang, S.Y., Chen, Y., Yang, C.X., Yang, D.L., Kuo, S.C., Huang, L.J., and Lung, F.D. (2011). Structure-activity relationships of a peptidic antagonist of Id1 studied by biosensor method, circular dichroism spectroscopy, and bioassay. J Pept Sci 17, 667–674.

Yasunami, M., Suzuki, K., and Ohkubo, H. (1996). A novel family of TEA domain-containing transcription factors with distinct spatiotemporal expression patterns. Biochem Biophys Res Commun 228, 365–370.

Yu, W.P., Collarini, E.J., Pringle, N.P., and Richardson, W.D. (1994). Embryonic expression of myelin genes: evidence for a focal source of oligodendrocyte precursors in the ventricular zone of the neural tube. Neuron 12, 1353–1362.

Yu, Y., Chen, Y., Kim, B., Wang, H., Zhao, C., He, X., Liu, L., Liu, W., Wu, L.M., Mao, M., *et al.* (2013). Olig2 targets chromatin remodelers to enhancers to initiate oligodendrocyte differentiation. Cell 152, 248–261.

Zawadzka, M., Rivers, L.E., Fancy, S.P., Zhao, C., Tripathi, R., Jamen, F., Young, K., Goncharevich, A., Pohl, H., Rizzi, M., *et al.* (2010). CNS-resident glial progenitor/stem cells produce Schwann cells as well as oligodendrocytes during repair of CNS demyelination. Cell Stem Cell 6, 578–590.

Zhang, Y., Liu, T., Meyer, C.A., Eeckhoute, J., Johnson, D.S., Bernstein, B.E., Nusbaum, C., Myers, R.M., Brown, M., Li, W., and Liu, X.S. (2008). Model-based analysis of ChIP-Seq (MACS). Genome biology 9, R137.

Zhao, J.W., Raha-Chowdhury, R., Fawcett, J.W., and Watts, C. (2009). Astrocytes and oligodendrocytes can be generated from NG2+ progenitors after acute brain injury: intracellular localization of oligodendrocyte transcription factor 2 is associated with their fate choice. Eur J Neurosci 29, 1853–1869.

Zhou, F., Xue, Y., Lu, H., Chen, G., and Yao, X. (2005). A genome-wide analysis of sumoylation-related biological processes and functions in human nucleus. FEBS Lett 579, 3369–3375.

Zhou, Q., and Anderson, D.J. (2002). The bHLH transcription factors Olig2 and Olig1 couple neuronal and glial subtype specification. Cell 109, 61–73.

Zhou, Q., Choi, G., and Anderson, D.J. (2001). The bHLH transcription factor Olig2 promotes oligodendrocyte differentiation in collaboration with Nkx2.2. Neuron 31, 791–807.

Zhou, Q., Wang, S., and Anderson, D.J. (2000). Identification of a novel family of oligodendrocyte lineage-specific basic helix-loop-helix transcription factors. Neuron 25, 331–343.

Zhuang, Y., Barndt, R.J., Pan, L., Kelley, R., and Dai, M. (1998). Functional replacement of the mouse E2A gene with a human Heb cDNA. Molecular and cellular biology 18, 3340–3349.